Doctoral Thesis

博士学位論文

Regulation of Lipid A Immune Function by Amphipathic Compounds for the Development of Vaccine Adjuvant Materials

(ワクチンアジュバントマテリアル開発を目指した

両親媒性化合物によるリピド A 免疫機能の制御)

Tran Duc Khiem

Department of Chemistry
Graduate School of Science
Osaka University

January, 2025

Table of Contents

Abbreviations

APC	Antigen-presenting cells
BCRs	B cell receptors
BSA	Bovine serum albumin
$CHCl_3$	Chloroform
CL	Cardiolipin
DAMP	Damage-associated molecular patterns
DC	Dendritic cells
DHA	Docosahexaenoic acid
DMEM	Dulbecco's modified Eagle's medium
DMSO	Dimethyl sulfoxide
dsRNA	Double-stranded RNA
FBS	Fetal bovine serum
HMGB1	High-mobility group box 1
HMM	Homogenous mixing method
HSPs	Heat-shock proteins
IL	Interleukin
IFN	Interferon
LNP	Lipid nanoparticle
LOS	Lipooligosaccharide
LPB	LPS-binding protein
LPS	Lipopolysaccharide
MD-2	Myeloid differentiation factor 2
MHC	Major histocompatibility complex
NF-κB	Nuclear factor kappa light chain-enhancer of activated B cells

NLRs	Nod-like receptor
PAMP	Pathogen-associated molecular patterns
pNPP	p-nitrophenol phosphate
PRRs	Pattern recognition receptors
RLRs	RIG-I-like receptor
SEAP	Secreted embryonic alkaline phosphatase
SMM	Simple mixing method
^{t}Bu-OH	Tert-butyl alcohol
Tc	T cytotoxic
TCRs	T cell receptors
TGF	Transforming growth factor
Th	T helper
TIR	Toll/IL-1R homology domain
TLRs	Toll-like receptors
TNF	Tumor necrosis factor

Chapter 1: Introduction

Section 1: Immune System

Item 1: Overview of the immune system

The immune system is a defense mechanism employed by the host organism to provide protection against infection. The immune system consists of all the cells, chemicals and processes that act in harmony to protect the host against foreign pathogens, which includes bacteria, fungi, viruses, and toxins etc., as well as endogenous cancer cells [1]. The first line of defense against an intruding pathogen is the anatomic barrier, which consists of the epidermal cells forming the skin surface and the epithelial cells that line the respiratory, gastrointestinal and genitourinary tracts. The skin is both a physical and chemical shield, inducing an acidic environment to prevent the growth of pathogens [2]. Meanwhile, the epithelial cells of mucous membrane secrete mucus that entraps foreign microbes, and carries extension called cilia that move back and forth to remove these microbes from the host mucosa [3]. At the same time, the immune system also possesses the physiological barrier, which are factors such as temperature (high temperature prevents growth of certain bacteria), pH (acidic environment of the stomach, kidney, bladder, etc. inactivate many viruses and bacteria) and chemical mediators that are soluble secretory products of the mucosa (e.g. saliva and tears contains lysozyme that damages cell wall and cell membrane of bacteria) [4].

Beyond the physical and chemical barriers, the immune system is then divided into two categories: innate immunity and adaptive immunity. Both types of immunity are important for the survival of the host, and table 1.1 below summarizes the key differences between them [5][6].

Table 1.1: Summary of innate immunity and adaptive immunity

	Innate immunity	Adaptive immunity
Typical response time	Quick	Delayed
Specificity	Non-specific (antigen-independent), only recognizes general patterns	Highly specific and dependent on unique antigens
Memory	No memory; identical response to the same class of pathogens	Memory; more rapid and efficient response upon re-exposure
Major components	Phagocytes (e.g. macrophages, neutrophils, dendritic cells), NK cells	B cells, T cells, antibodies
Main receptors	Pattern recognition receptors (PRRs)	B-cells receptor (BCR), T-cells receptor (TCR)
Functional role	Immediate defense against pathogens; trigger adaptive immune response	Antigen-specific response in case innate immunity is insufficient; long-term immunity

As shown in table 1.1, innate immunity occurs almost immediately upon encountering pathogens and targets pathogens in a non-specific way, while adaptive immune responses are antigen-specific and require a delayed period between antigen exposure and maximum immune response.

Item 2: Innate immunity

If pathogens successfully escape the anatomical and physiological barriers, they can establish an infection in the host. This triggers the activation of the innate immune system, which generates signals resulting in the release of chemokines and cytokines to rapidly recruit immune cells to the site of infection, initiating an inflammatory response. The innate immune system relies on a variety of specialized cells to mount this defense, including phagocytes (mainly neutrophils and macrophages), dendritic cells, mast cells, natural killer (NK) cells, innate lymphoid cells, eosinophils, and basophils.

Upon exposure to an immune threat, tissue-embedded immune sentinel cells (such as macrophages and dendritic cells) can induce resistance factors that limit the invasion, replication and assembly of pathogens [7]. Inflammatory cytokines and secondary messengers are secreted by these sentinel immune cells to communicate with and recruit other bystanding immune cells within the tissue. After the initial alarm, the next cell type to response against pathogens is phagocytes, which are the macrophages that are already presented in the tissue and the neutrophils that arrive rapidly from the bloodstream [8]. Phagocytes engulf (phagocytose) and destroy pathogens by forming a phagosome that deliver the engulfed pathogen to the cytoplasm and fuse with the lysosomes. Inside the lysosome, bactericidal substances and enzymes kill and digest the pathogens [9].

Innate immunity also includes natural killer (NK) cells, a type of cytotoxic lymphocytes, which play a critical role in identifying and eliminating infected or abnormal cells. NK cells recognize stress proteins on the surface of cells infected with intracellular pathogen, and release perforin and granzyme to initiate apoptotic cell death [10]. NK cells also upregulate cytokines, especially interferon-gamma (IFN-γ) that enhances immune response by activating macrophages and enhances antigen presentation. Mast cells, basophils and eosinophils are granulocytes that function to mediate acute inflammatory reactions associated with allergy and asthma, and function in the destruction of parasites that are too large for phagocytosis [11].

Dendritic cells are phagocytes, but they are considered non-professional phagocytes due to lower phagocytotic capacity and efficiency [8]. Both dendritic cells and macrophages are also antigen-presenting cells (APCs), acting as messengers between innate immunity and adaptive immunity by interacting with T cells. Figure 1.1 below shows the major components and the events that occur during innate immunity.

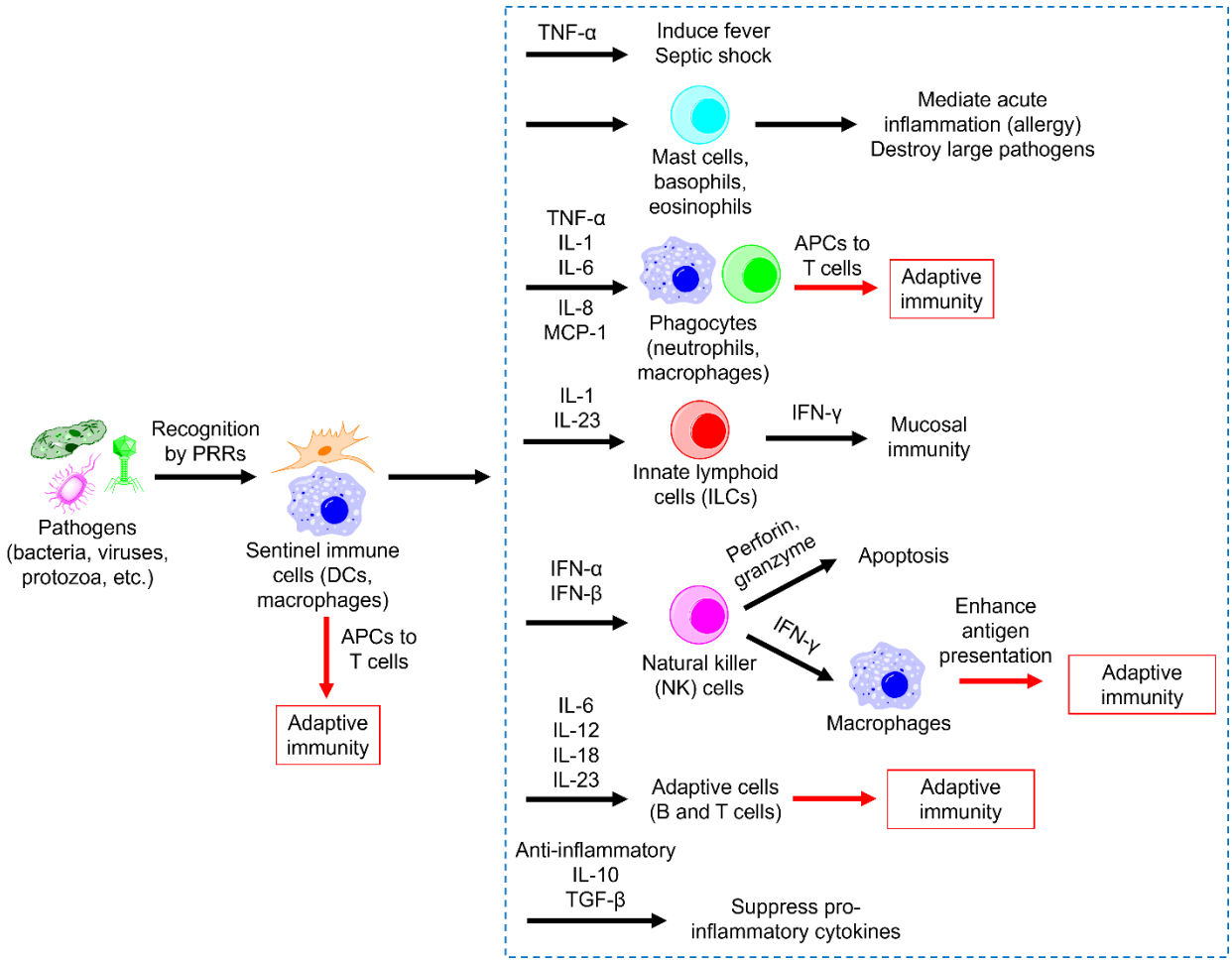

Figure 1.1: Overview of events in innate immunity [20-26]

As shown in figure 1.1, innate immune cells express pattern recognition receptors (PRRs), which recognize pathogens via the detection of small molecular motifs called pathogen-associated molecular patterns (PAMPs). PAMPs are conserved structural features that are shared among microbes of the same class and are essential for the survival and pathogenicity of microbes [12]. Examples of PAMPs include peptidoglycan, lipopolysaccharide (LPS) from Gram-negative bacteria, bacterial flagellin, lipoteichoic acids for Gram-positive bacteria, single-stranded RNA (ssRNA) and double-stranded RNA (dsRNA) for viruses, CpG DNA from bacteria, etc. [13]. Families of PRRs include Toll-like receptors (TLRs) [14], RIG-I-like receptors (RLRs) [15], Nod-like Receptors (NLRs) [16], C-type lectin receptors [17] and scavenger receptors [18].

The recognition of PAMPs by PRRs triggers the activation of innate immune signaling cascade that leads to the upregulation of cytokines (such as chemokines, interferons, interleukins, etc.). These molecules are small proteins that play an essential role in cell signaling by interacting with

cell surface receptors, and regulate the maturation, growth and movement of different immune cell types [19].

Upon PAMPs recognition, the immediate response is the release of pro-inflammatory cytokines such as TNF-α, IL-1 and IL-6. TNF-α and IL-1 (including IL-1α and IL-1β) promotes the recruitment of neutrophil, but they are also responsible for inducing inflammation, fever and septic shock. IL-1, together with IL-23, are also critical for the activation of innate lymphoid cells (ILCs), which leads to the production of IFN-γ and promotes mucosal immunity [20].

IL-6 stimulates the production of acute-phase protein from livers and is involved in the differentiation of adaptive immune cells (B cells and Th17 cells) [21]. If the pathogen is a virus, IFN-α and IFN-β are also released to inhibit viral replication and enhance NK cells activity [22]. Chemokines such as CXCL-8 (IL-8) and CCL2 (MCP-1) are also released and function in the activation of neutrophils and differentiation of monocytes into macrophages at the site of infection [23]. Afterwards, IL-12, IL-18 and IL-23 are released and promote the activation of adaptive immune response, as well as stimulate the production of IFN-γ by NK cells and T cells. IFN-γ helps enhance phagocytosis by macrophage and enhances the adaptive immune response [24][25].

Along with pro-inflammatory cytokines, anti-inflammatory cytokines are also released days after infection. These include IL-10 and TGF-β, which suppress the release of pro-inflammatory cytokines and promote tissue repair [26].

Item 3: Adaptive immunity

As mentioned above, phagocytes are not only involved in innate immunity but also activate adaptive immunity to stimulate an antigen-specific response. Adaptive immunity is mediated by B cells (B lymphocytes) and T cells (T lymphocytes). During phagocytosis, pathogens are engulfed by phagocytes such as macrophages and dendritic cells and the antigens of pathogens are then processed into peptide fragments, called epitopes, through proteolysis and presented on the cell surface to activate T cells [27].

All nucleated cells express proteins called major histocompatibility complex (MHC), and the receptors on T cells (TCRs) only recognize the epitope when they are in complex with MHC on the surface of host cells. All infected host cells display MHC I proteins that present peptide derived from pathogen proteins in the cytoplasm, but APCs also display MHC II that present peptides from engulfed pathogens [28]. Recognition of antigen by TCRs stimulates T cells to differentiate into either cytotoxic T (Tc) cells (CD8+ cells) or T-helper (Th) cells (CD4+ cells). Figure 1.2 highlights the various T cells and their roles in the immune system.

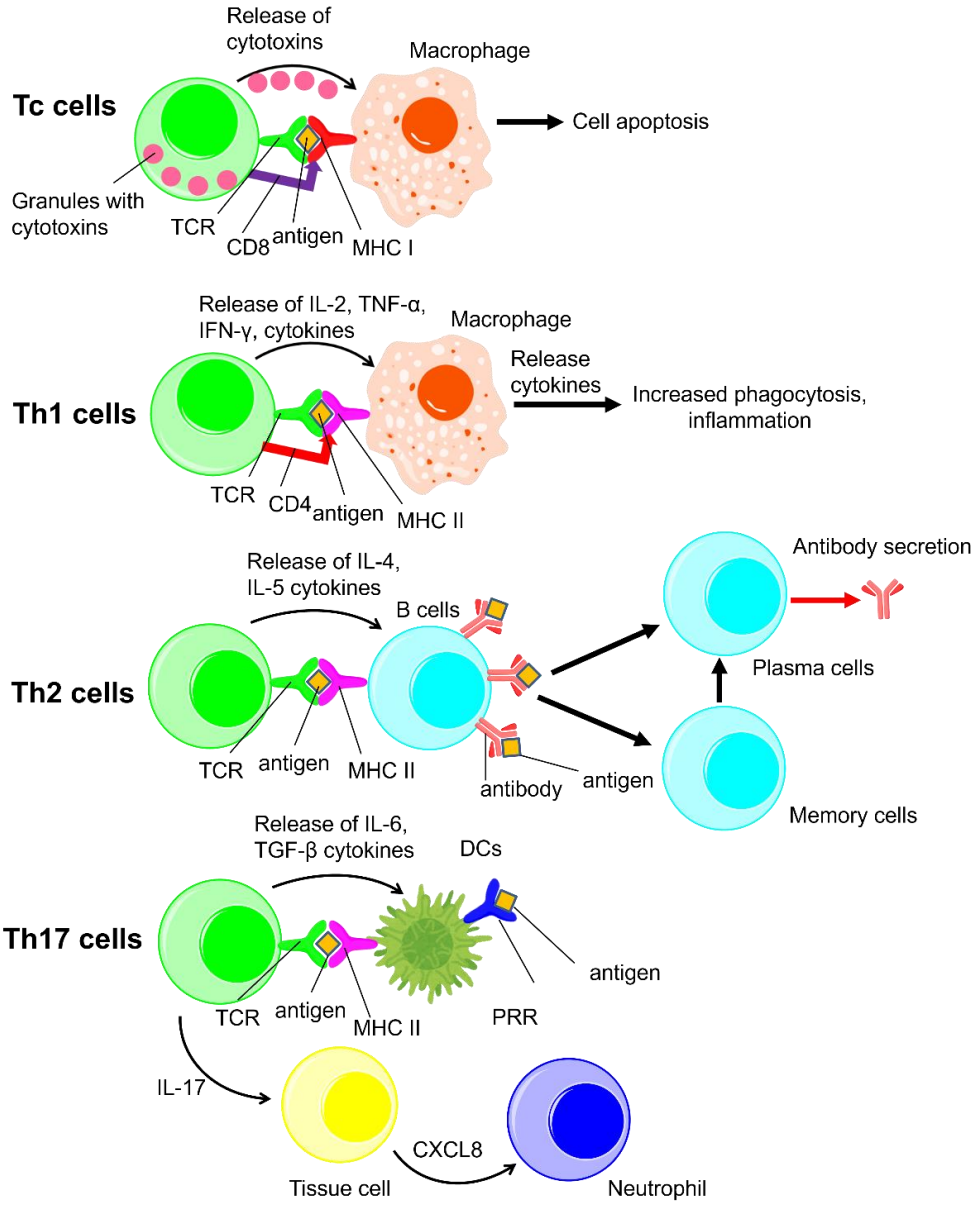

Figure 1.2: Overview of T cells and their roles in adaptive immune response

From figure 1.2, Tc cells recognize foreign antigen embedded in MHC I proteins and directly kill cells that display such antigen by inducing apoptosis using perforins and granzymes [29]. Th cells have no cytotoxic or phagocytic activities, but they are capable of mediating immune response by regulating the activities of other immune cells. Interaction with peptide-MHC II complexes on the surface of APCs causes Th cells to differentiate into different cell types, most commonly Th1, Th2 and Th17 cells.

Th1 cells activate macrophages via cytokines such as IL-2, IFN-γ, and TNF-α to increase phagocytosis and promote inflammation. Th2 cells are important for the process of B cell activation and production of antibody. B cells express B-cells receptors (BCRs), which are

membrane-bound immunoglobulins that serve as receptors for antigens. After endocytosis and proteolysis of antigen, B cells function as APCs by presenting MHC II-antigen complex on their surface and stimulating Th2 cells to release IL-4 and IL-5 cytokines (Figure 1.2), which in turn activate B cells. As a result, B cells differentiate into plasma cells or memory cells [30]. Plasma cells produce and secrete soluble immunoglobulins called antibodies that bind to and inactivate foreign substances as well as promoting phagocytosis, while memory cells provide long term protection against pathogen of specific diseases [31]. Th17 cells are activated by dendritic cells and release IL-17 that attracts neutrophils to the site of infection, amplifying innate immunity response [32] as shown in figure 1.2. Th17 cells play an important role in immune defense against mucosal infection.

Item 4: Recognition of LPS and lipid A by TLR4/MD-2 receptor complex

As illustrated in figure 1.1, pattern recognition receptors (PRRs) are a critical component of the innate immune system, enabling the host to detect and respond to pathogens. PRRs are located on the cell surface, within endosomes and lysosomes, in the cytoplasm, or secreted as soluble receptors. PRRs recognize pathogen-associated molecular patterns (PAMPs), which are conserved molecular motifs derived from pathogens. Toll-like receptors (TLRs) are a major family of PRRs that play a central role in innate immunity. TLRs are type I transmembrane proteins that are evolutionarily conserved between insects and humans, and mammal TLRs are homologous to Toll receptors of *Drosophilia* fruit fly [33]. Each TLR is composed of an extracellular domain for PAMP recognition, a transmembrane domain, and a cytoplasmic Toll/IL-1 receptor (TIR) domain that initiates downstream signaling pathway [34]. In human and mice, 10 and 12 functional TLRs have been identified, respectively, with TLR1-TLR9 conserved between both species [35]. TLRs are classified into two subgroups based on their cellular localization and the PAMPs ligands that they recognize. TLR1, TLR2, TLR4, TLR5, TLR6 and TLR11 are expressed on cell surface and recognize microbial membrane components, such as lipoteichoic acid (TLR2), bacterial flagellin (TLR5), diacyl lipopeptides (TLR6) [13]. In contrast, TLR3, TLR7, TLR8, TLR9 are located in intracellular vesicles (e.g. endoplasmic reticulum, lysosomes) and recognize microbial nucleic acid.

Among these TLRs, it was identified in 1998 that TLR4 is responsible for recognizing immunostimulatory molecules called lipopolysaccharide (LPS) and lipid A that are derived from Gram-negative bacteria [36]. TLR4 consists of a 608-residue extracellular domain and a 187-residue intracellular domain that functions in intracellular signaling cascade [37].

LPS, the major glycoconjugate on the outer membrane of Gram-negative bacteria, is a type of endotoxin and PAMPs. LPS makes up 80% of the cell membrane of *E. coli* and *Salmonella* and is the most common antigen on the surface of most Gram-negative bacteria [38]. LPS is a potent activator of the immune system and can induce high fever, tissue death, organ failure that can lead to septic shock in the host. LPS toxicity is linked to its ability to stimulate the innate immune

response and induce the upregulation of pro-inflammatory cytokines like IL-6 and TNF-α. The structure of LPS is shown in figure 1.3 below, which consists of three covalently linked distinct parts: O-polysaccharide, core oligosaccharide, and a glycolipid moiety called lipid A, which is the active principle of LPS [39].

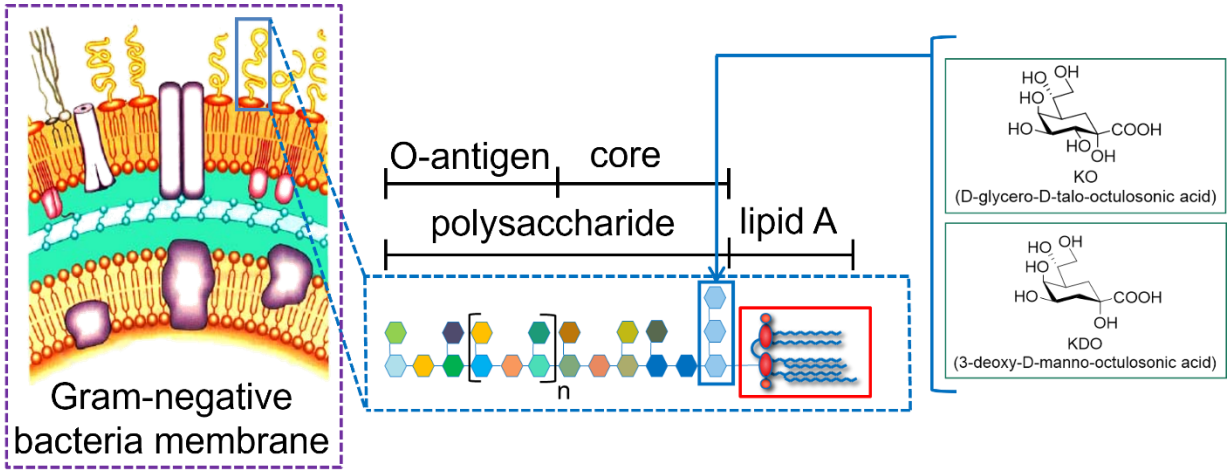

Figure 1.3: Structure of LPS

The core oligosaccharide region is non-repeating and linked to glucosamine of lipid A. Its structure consists of hexoses (glucoses, galactoses, mannoses, etc.), L-glycero-D-manno-heptose (Hep) and 3-deoxy-D-*manno*-octulosonic acid (KDO) residues, although some bacteria have D-glycero-D-talo-octualosonic acid (KO) instead [40]. The O antigen is a repeating oligosaccharide of two to eight sugar molecules and linked to the core oligosaccharide. Lipid A is an amphipathic molecule consisting of covalently linked hydrophilic phosphorylated carbohydrates and lipophilic long chain acyl groups [41]. The total synthesis of *E. coli* lipid A **1** (compound 506) was successfully achieved by Shiba and Kusumoto in 1986 [42]. As shown in figure 1.4, canonical *E. coli* lipid A **1** is composed of an acylated β-1'-6-linked glucosamine disaccharide. The glucosamine disaccharide is phosphorylated at the 1 and 4' position, and acylated at the 2, 3, 2' and 3' positions, plus two secondary acyl chains are also presented in the non-reducing end glucosamine.

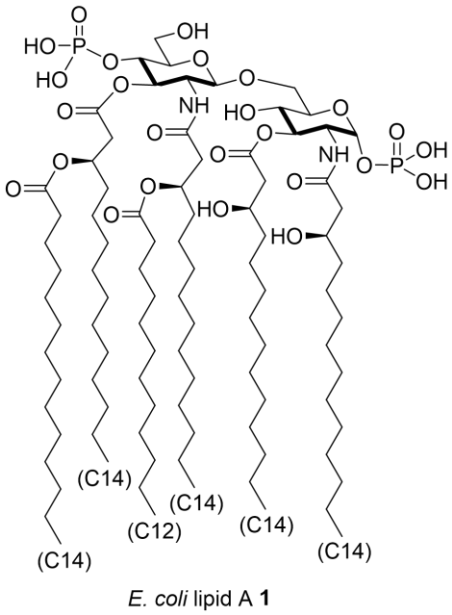

E. coli lipid A **1**

Figure 1.4: Structure of canonical *E. coli* lipid A **1**

Even though TLR4 functions as receptor for LPS and lipid A, TLR4 alone is insufficient for LPS recognition. Myeloid differentiation-factor (MD-2), a protein that lacks

transmembrane and intracellular domain, forms a noncovalent complex with the extracellular domain of TLR4 and is necessary to facilitate the activation of innate immunity by binding directly to LPS [37]. Two other molecules, LPS-binding protein (LBP) and CD14, are also necessary for the presentation of LPS to the TLR4/MD-2 receptor complex. LBP is an acute phase reactant produced in the liver and lungs and binds to the lipid A moiety of LPS. LBP functions as a shuttle protein that transfers LPS from the outer membrane of Gram-negative bacteria to CD14, a glycoprotein that exists in soluble form or as a glycosylphosphatidylinositol-anchored membrane protein [43].

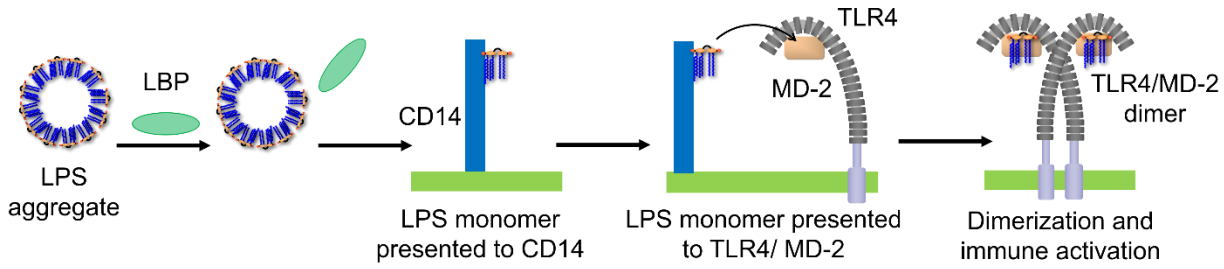

Figure 1.5: Schematic diagram of LPS recognition process by TLR4/MD-2 via LBP and CD14

Figure 1.5 shows the schematic diagram of LPS recognition process. Due to its amphipathic nature, LPS tends to form aggregates or micelles in the aqueous environment [44]. In the serum, a single LPS-binding protein (LBP) molecule binds to LPS micelles and catalyzes multi-rounds of LPS transfer to CD14. The LPS is then presented by CD14 to TLR4/MD-2, which leads to dimerization of the receptor complex and activates the innate immune pathway [45][46].

In 2007, the crystal structure of human MD-2 and tetra-acylated lipid IVa, the biosynthetic precursor of lipid A, was resolved [47]. In this structure, four acyl chains of the lipid IVa bind directly to the hydrophobic pocket of MD-2. Additionally, Lee et al. showed that binding of LPS causes the dimerization of TLR4/MD-2 complex [48]. In 2009, the structure of TLR4/MD-2/LPS complex was determined via X-ray crystallography. The dimerization interface of TLR4 is induced by the binding of LPS, with the LPS molecule directly connecting the two components. Additionally, five of six lipid A **1** acyl chains are buried inside the pocket, while the remaining chain is exposed to the surface of MD-2 and forms hydrophobic interaction with the phenylalanine residue of another TLR4/MD-2 complex, promoting dimer formation. The phosphate groups of LPS also contribute to the process of dimerization by forming ionic interaction with positively charged residues of TLR4 and MD-2 [49].

Dimerization of TLR4/MD-2 complex is followed by the activation of the intracellular immune signaling pathway (Figure 1.6), where downstream adaptor molecules such as MyD88/TIRAP (MyD88-dependent pathway) and TRIF/TRAM (TRIF-independent pathway) are recruited. The MyD88-dependent pathway activates the transcription factor NF-κB, which translocate to the

nucleus and induces the production of pro-inflammatory cytokines such as IL-6 and TNF-α. The TRIF-dependent pathway activates transcription factor IFN regulatory factor 3 (IRF3), which also translocate to the nucleus and induces the expression of antiviral type I interferon genes [50].

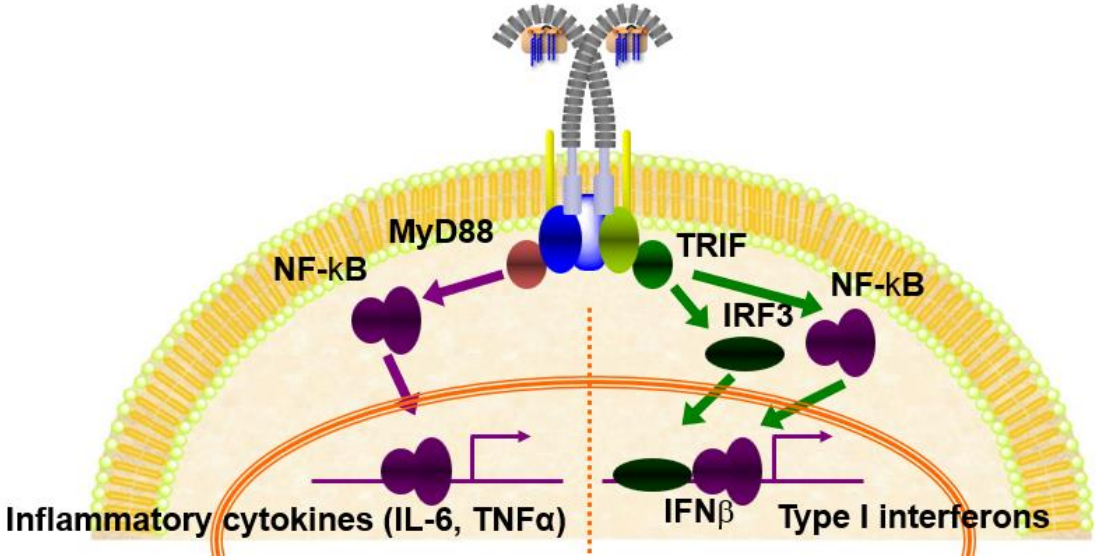

Figure 1.6: TLR4 signaling pathway

Section 2: Various TLR4 ligands

Item 1: Damage-associated molecular patterns (DAMPs)

Binding of PAMPs initiates an immune response, and excessive immune response can lead to severe inflammation, which results in cell necrosis and the subsequent release of damage-associated molecular patterns (DAMPs). DAMPs are intracellular components that function as endogenous danger signals and recognized by innate immune receptors, capable of activating the innate immune system by interacting with PRRs [51]. DAMPs play a major role in the pathogenesis of human diseases by inducing inflammation [52]. Examples of DAMPs include HMGB1 proteins (activate NF-κB signaling pathway by binding to TLR2, TLR4 and receptor for advanced glycation end products [53]), and heat-shock proteins (activation of TLR2, TLR4 and CD91 pathway [54]).

Previous research from our laboratory in collaboration with a German group had showed that a DAMP such as cardiolipin (CL) can regulate the immune response of a PAMP like *E. coli* lipid A **1** [55]. CL is a tetra-acylated diphosphatidylglycerol lipid that located in the inner mitochondrial membrane of bacteria, yeast, plants and animals. During cell stress or mitochondrial damage, CL translocate to the outer mitochondrial membrane or into the extracellular space [56]. CL can function as an antagonistic ligand and prevents LPS activation of TLR4 immune pathway.

In Mueller and Kusumoto et al. work [55], the *E. coli* lipid A **1** and CL (C18:2) **2** (figure 1.7) were mixed in chloroform at different molar ratios. After evaporation, the dry mixtures were resuspended in water to produce aggregate suspensions. Suspensions that contain only CL or contain only lipid A were prepared similarly.

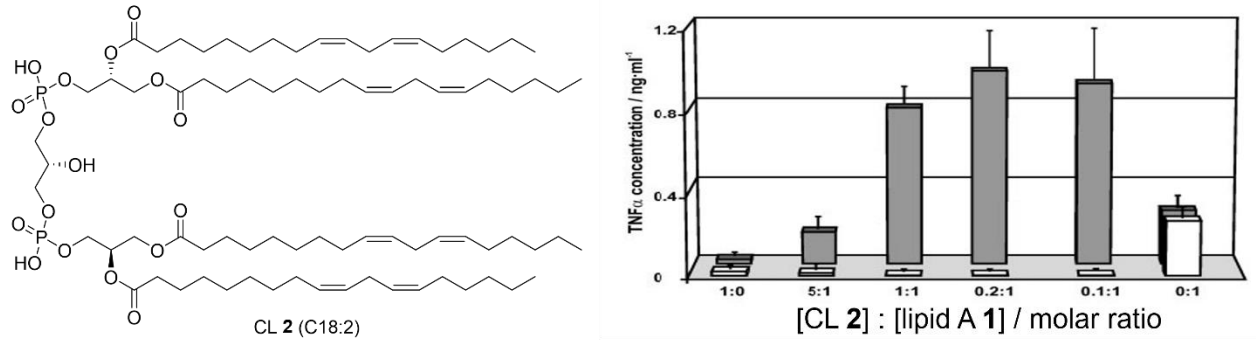

Figure 1.7: Left: Structure of CL (C18:2) **2**; Right: Immune function of aggregates containing lipid A **1** and CL (18:2) **2**

Figure 1.7 shows the result of TNF-α production after stimulation of human mononuclear cells (MNCs) by the aggregates. The white bar shows a simple mixture of lipid A **1**-only suspension and CL **2**-only suspension, where the introduction of CL **2** completely inhibited lipid A **1** activity, and an antagonistic effect was observed. On the other hand, the black bar shows the result of cells stimulation with mixed aggregates (CL **2** + lipid A **1** suspension). A boosting or antagonistic effect was observed depending on the molecular ratio between CL **2** and lipid A **1**.

In this same work, Mueller and Kusumoto et al. also prepared aggregates containing *E. coli* lipid A **1** and lipid IVa at different molecular ratios [55]. Lipid IVa, a precursor of lipid A **1**, acts as an agonistic ligand in mice but exhibits antagonistic effects in human [57]. When a mixture of lipid IVa-only suspension and lipid A **1**-only suspension was used to stimulate MNC, the production of TNF-α by lipid A **1** was suppressed because of lipid IVa antagonistic nature (white bar, figure 1.8). However, depending on the molecular ratio, mixed aggregates (lipid IVa + lipid A **1** suspension) induced either a higher or lower level of biological activity in comparison to stimulation with lipid A **1** alone (black bar, figure 1.8). These observations show that the immune function of lipid A **1** can be modified depending on the composition of its aggregate.

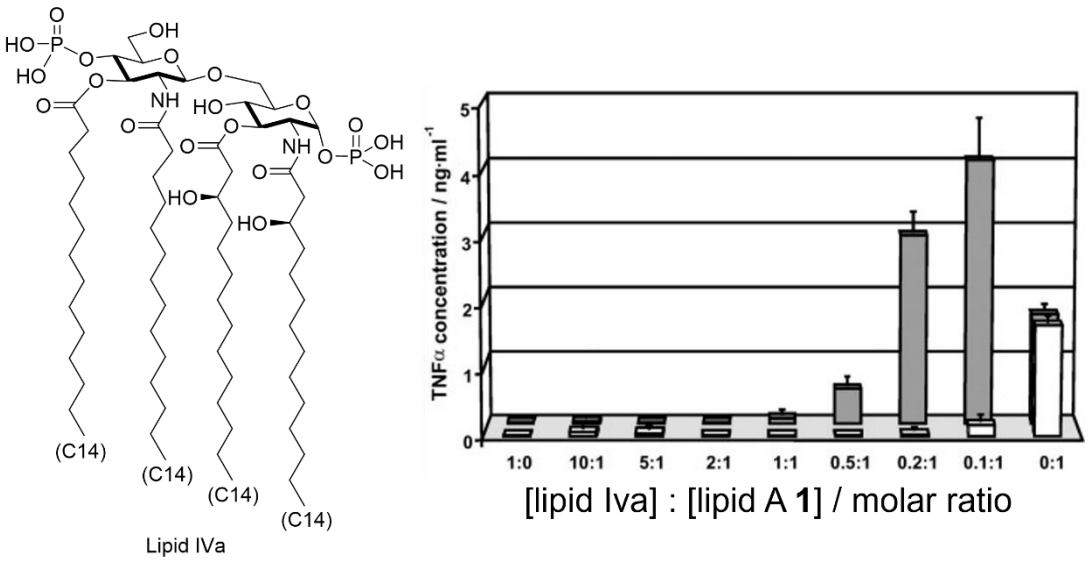

Figure 1.8: Left: Structure of lipid IVa; Right: Immune function of aggregates containing lipid A **1** and lipid IVa

Item 2: Ganglioside GM3

In another work performed in collaboration with our laboratory, Kanoh and Inokuchi et al. reported the effects of ganglioside GM3 on the immune function of LPS and lipid A **1** [58]. GM3 is a membrane-bound glycosphingolipid composed of three monosaccharide groups attached to a ceremide backbone (figure 1.9). GM3 is synthesized in the Golgi, then secreted into extracellular compartment or localized into plasma membrane as a component of membrane microdomains called lipid rafts [59]. Serum GM3 is composed of different fatty acids, including long-chain-fatty acid (LCFA: C16:0, C18:0, C20:0), very-long-chain-fatty-acid (VLCFA: C22:0, C23:0, C24:0), unsaturated VLCFA (C22:1, C24:1) and α-hydroxy VLCFA.

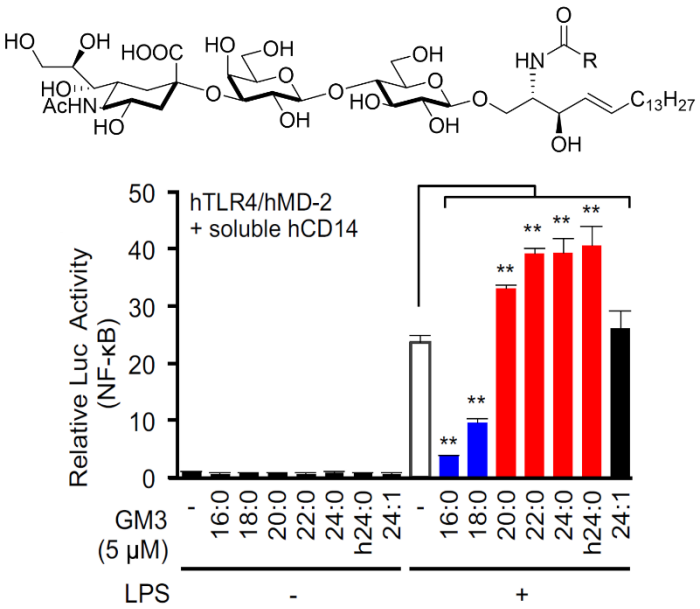

Figure 1.9: Top: Structure of GM3; Bottom: Co-stimulation of TLR4/MD-2 by GM3 species plus LPS (5 μg/mL)

Figure 1.9 presents the results of stimulating human peripheral blood monocytes (HPBM) by *E. coli* LPS and GM3. Cells were pre-treated with GM3 for 30 minutes before LPS was introduced to the cell culture medium. While GM3 alone did not exhibit any immunostimulatory effects on TLR4 signalling pathway, the immune function of LPS was synergistically enhanced by VLCFA-GM3 (red bar, figure 1.9) and antagonistically suppressed by LCFA-GM3 (blue bar, figure 1.9).

Item 3: Fatty acids potential role as ligands or regulators of innate immune function

Amphipathic compounds such as fatty acids, alongside DAMPs like CL, may act as ligands for TLR4, or they may play a role in the regulation of PAMPs immune function. Fatty acids are the major components of triglyceride, and the main contributors to dietary fat in humans. Fatty acids are available through digestion and absorption or synthesized by humans from nonlipid precursors (e.g. glucose) or from other fatty acids [60]. Different fatty acids can have specific metabolic, signaling or regulatory roles.

Saturated fatty acids, including stearic acid (C18:0), palmitic acid (C16:0), myristic acid (C14:0) and lauric acid (C12:0), are the most common fatty acids in diets, but they are also synthesized *de novo* in humans from carbohydrate or amino acid metabolism [61]. Saturated fatty acids are necessary for cell signaling as components of phospholipids, sphingolipids, gangliosides, and lipid raft structures, and some (e.g. palmitic acid, myristic acid) also function in acylation of membrane proteins for the anchoring of these proteins to the plasma membrane [62]. Oleic acid (C18:1) is the most prevalent *cis*-monounsaturated fatty acid (MUFA) in diet but also synthesized *de novo* by desaturation of stearic acid. Oleic acid was reported to lower cardiovascular risk by reducing blood lipid, mainly cholesterol, low-density-lipoprotein (LDL) cholesterol, and triglycerides [63].

Poly-unsaturated fatty acids (PUFAs) such as linoleic acid (C18:2) and linolenic acid (C18:3) are essential fatty acids that must be obtained from diet. PUFAs are necessary for normal brain development and function [64], necessary for synthesis of ceramides in the skin [65], and lower blood cholesterol concentrations. Docosahexaenoic acid (DHA, C22:6) can be obtained from diet or synthesized from linolenic acid, is a major component of brain and eye membranes [66] and is essential for visual and neural development of infants. *Trans*-unsaturated fatty acids such as elaidic acid (C18:1) are derived from *cis*-unsaturated fatty acids via industrial or cooking processes. *Trans*-unsaturated fatty acids are associated with higher blood LDL cholesterol concentration and higher risk of cardiovascular diseases [67].

Currently, there are multiple contrasting reports on the effects of different fatty acids on TLR4 signaling pathway and its downstream cytokines. Wong and Hwang et al. reported that lauric acid induces the dimerization and recruitment of TLR4/MD-2 receptor complex into lipid rafts and activates downstream pathway, while DHA inhibits LPS- or lauric acid- induced dimerization [68].

However, Erridge and Samani reported that saturated fatty acids alone cannot stimulate an immune response, and any observed activation of TLR4 pathway is caused by sample contamination with LPS [69]. Novak and Espat et al. reports that linolenic acid and DHA inhibit NF-κB activation, reducing the activation of TLR4 by LPS [70]. Based on these reports and others, there is not yet a clear consensus on the role of fatty acids in mediating TLR4-dependent signaling pathway.

Section 3: Lipid A as vaccine adjuvants

Item 1: Vaccine adjuvants

Vaccine is a preparation designed to safely induce an immune response and provides protection for the host against future infection by the same pathogen [71]. A vaccine can be derived from biological sources or synthesized using non-biological components. Vaccine typically contains antigen, a molecule that can bind to specific antibody or T-cell receptor. An antigen can exist on normal cells, cancer cells or microbes, and can be either proteins, peptides, polysaccharides, lipids or nucleic acids [72].

Vaccines are classified as either live (contain attenuated strains of the pathogen) or non-live (contain only components of a pathogen or killed whole organisms). Immunization with live viral or bacterial vaccines is a potential hazard in patients with immunodeficiencies of T cells, B cells and phagocytic cells [73]. On the other hand, non-live vaccines are safer, but also less immunogenic and potentially less effective. Therefore, vaccine adjuvants are often administered together with vaccine antigen to enhance the immunogenicity of vaccines [74]. A vaccine adjuvant can act as an immunostimulant (directly increasing the immune response to antigen) or as a delivery vehicle (controlled delivery of antigen to targeted site), and a combination of both is described as adjuvant system [75].

From 1920s to 1990s, insoluble aluminum salt (alum) was the only adjuvant included in commercial vaccines, such as vaccines against hepatitis B, diphtheria, tetanus and human papilloma virus [76]. Alum mechanism of action was not completely understood, but its adjuvant effects include inducing strong antibody response (Th2-biased) and activation of the NLRP3 inflammasome [77][78]. However, alum is less effective for stimulating Th1-response (cell-mediated immunity), which are essential for protection against intracellular pathogen like tuberculosis or HIV [79]. Alum also does not directly activate TLR and is ineffective when administering with poorly immunogenic antigens [80].

After alum, the next adjuvant approved for clinical use was the oil-in-water emulsion adjuvant MF59 that contains squalene, Tween 80 and Span 85 [81]. MF59 enhances both humoral and cell-mediated immune responses, although its mechanism of action remains unclear [82]. Since MF59, a few other adjuvants have been practically used, including the adjuvant system (AS)0 series developed by GlaxoSmithKline (GSK) [83].

The AS0 series combines the usage of adjuvant delivery modes (alum, emulsions, liposomes) with immunostimulants (TLR ligands). Currently, 5 adjuvant families were investigated in clinical trials, and 3 were officially included in licensed vaccines. AS01 is a liposomal formulation that contains 3D-MPL **3** (an agonist of TLR4, figure 1.11) and QS-21 (a potent immunostimulant saponin isolated from *Quillaja saponaria* tree bark) [84]. 3D-MPL **3** and QS-21 induce a synergistic activation of innate immunity and activate novel pathways not triggered by either component alone, increasing polyfunctional $CD4^+$ T cells expressing IL-2, IFN-γ and TNF-α [85]. AS01 is used in the shingles vaccine Shingrix and malaria vaccine Masquirix [86][87].

AS03 is a squalene in oil-in-water emulsion adjuvant that contains squalene, surfactant polysorbate 80 and α-tocopherol (vitamin E). α-tocopherol is an immunostimulant that enhances immune response by stimulating NF-κB and modulating the expression of cytokines such as CCL2 and IL-6 [88][89]. AS03 was approved for usage in influenza A (H5N1) vaccine and SARS-COV-2 recombinant protein vaccine [90] [91]. AS04 is a vaccine that contains 3D-MPL **3** adsorbed onto alum. AS04 stimulates immune response via a combination of TLR4-mediated innate immune signaling by 3D-MPL **3** and alum immunomodulatory properties [92]. AS04 is currently used in the hepatitis B virus (HBV) vaccine Fendrix and human papillomavirus (HPV) vaccine Cervavix [93][94].

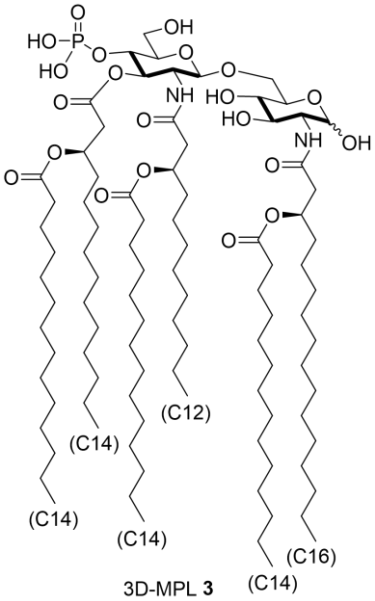

Figure 1.11: Structure of GSK's 3D-MPL **3**

Item 2: Lipid A structure-activity relationship

The ability to activate host immunity via TLR4-mediated innate immune pathway makes LPS and lipid A potential adjuvant candidates. As previously explained, TLR4 signaling pathways are either MyD88-dependent (triggers production of cytokines such as IL-6) or TRIF-dependent (triggers production of antiviral type I IFN) [50]. However, canonical *E. coli* LPS and its lipid A **1** are unsuitable as adjuvants because they simultaneously activate both pathways and induce severe inflammation that leads to lethal toxicity [95].

To ensure the safe use of lipid A as an adjuvant moiety, the inflammatory activity of lipid A must be attenuated. Previous structure-activity studies had demonstrated that the immune function of lipid A, including its inflammatory activity, can be regulated by modifying its structure, such as the number and length of acyl chains, as well as the charge of phosphate group [96]. GSK 3D-MPL **3** as shown in figure 1.11 is an attenuated monophosphoryl lipid A derived from Gram-negative bacterium *Salmonella enterica serovar Minnesota Re595* [97]. 3D-MPL **3** selectively activates the TRIF-dependent pathway while showing weaker stimulation of MyD88-dependent

pro-inflammatory cytokine IL-6 [98]. The ability to induce antiviral effects without causing severe inflammation makes 3D-MPL **3** a safe adjuvant molecule.

Item 3: Intestinal symbiotic bacteria *Alcaligenes faecalis*

In searching for safe lipid A molecules to be used as adjuvants, our laboratory has focused on symbiotic bacterial lipid A that could survive the host's immune response by promoting homeostasis. Obata et al. reported that several opportunistic bacteria, including *Alcaligenes faecalis* (*A. faecalis*), colonize the host's gut-associated lymphoid tissue (GALT), Peyer's patch (PP) (figure 1.12) [99]. Since the first discovery of *A. faecalis* inside PP, it has been reported that LPS extracted from *A. faecalis* shows weaker TLR4 activation than canonical *E. coli* LPS. In comparison to the high toxicity effect induced by *E. coli* LPS in vivo (hypothermia, lung inflammation, etc.), no excessive inflammation was observed in mice treated with *A. faecalis* LPS. *A. faecalis* LPS stimulates dendritic cells to induce antigen-specific mucosal IgA antibodies in the gastrointestinal tract (GI) tract through an IL-6 dependent mechanism [100]. Additionally, *A. faecalis* LPS induces low amount of nitric oxide (NO) and a low rate of apoptosis when co-cultured with DCs, suggesting a symbiotic relationship between DCs of the intestinal lymphoid tissues and *A. faecalis* [101].

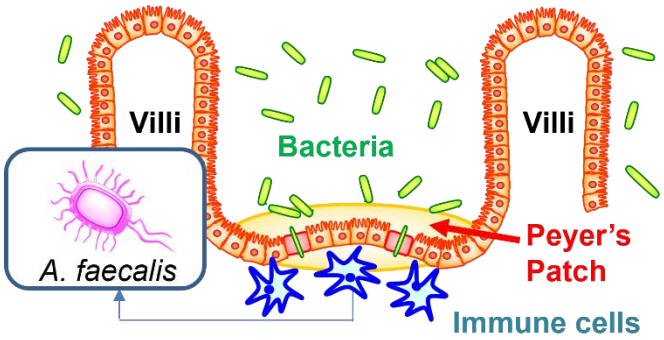

Figure 1.12: *A. faecalis* colonizes the gut-associated lymphoid tissue Peyer's patch

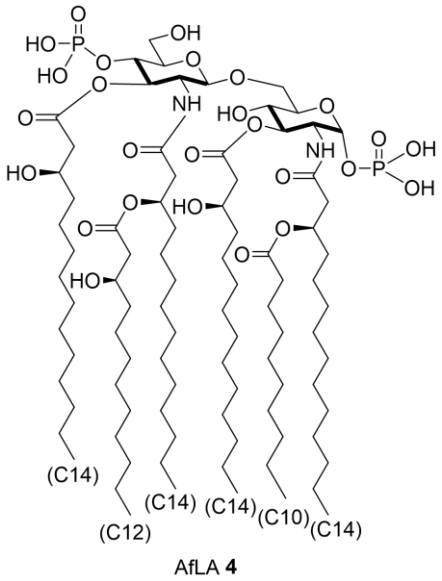

Figure 1.13: Structure of hexa-acylated *A. faecalis* lipid A **4** (AfLA)

Recently, our laboratory showed that *A faecalis* LPS contains a mixture of tetra-acylated, penta-acylated and hexa-acylated lipid A. Our laboratory successfully synthesized all three moieties and identified the active principle of *A. faecalis* LPS as hexa-acylated lipid A **4** (AfLA **4**), its structure shown in figure 1.13 [102]. In immunization study with ovalbumin (OVA) as an antigen via subcutaneous immunization, AfLA **4** demonstrated the ability to boost antigen-specific IgA and IgG production, and stimulated the preferred induction of Th17 cells, which are essential for mucosal immune defense [103]. Furthermore, immunization of mice with up to 1 µg of AfLA **4** caused no major side effects, such as lymphopenia and thrombocytopenia.

Most significantly, both *A. faecalis* LPS and AfLA **4** showed promising results as mucosal vaccine adjuvant. In nasal immunization study with pneumococcal surface protein A (PsPA) antigen of *Streptococcus pneumoniae*, AfLA **4** induced stronger mucosal IgA production compared to cholera toxin, which is a known potent immunogen for mucosal IgA production [104][105]. AfLA **4** also outperformed MPLA (an adjuvant derived from *Salmonella* bacterium like GSK's 3D-MPL **3**) and demonstrated stronger mucosal adjuvant activity when immunized nasally together with OVA [106][107].

These results suggested that AfLA **4** is a very promising candidate for the development of mucosal vaccine adjuvant. Currently, only a limited number of adjuvants are approved for practical use due to safety concerns. For example, while cholera toxin is approved as a mucosal vaccine adjuvant, its use is associated with problems such as Bell's palsy (facial weakness or paralysis), inflammation and diarrhea [108][109]. Furthermore, to date, there are only 9 mucosal vaccines approved for human use, none of which is synthetic (only live vaccines or whole-cell vaccines) [110]. Against diseases that target mucosal membrane such as influenza or cholera, mucosal vaccine can provide better protection compared to injection vaccines that only induce systemic response. In fact, majority of pathogens initiate their infection process at mucosal surfaces such as gastrointestinal or respiratory tract. Therefore, mucosal vaccines are crucial for eliciting localized mucosal immunity at the site of pathogen entry, preventing the establishment of the initial infection and blocking further disease transmission.

Item 4: Lipid nanoparticles as carriers for the delivery of vaccine materials

Lipid nanoparticles (LNPs) are nanosized carriers composed of lipids that assemble into well-defined structures, such as micelles, lipid bilayers, or solid lipid cores. They are designed to encapsulate and protect therapeutic or immunogenic agents (e.g., nucleic acids, proteins, peptides), enabling the efficient delivery of these agents to target cells or tissues while minimizing in vivo degradation [111]. By tailoring their properties to specific applications, LNPs, whether naturally assembled or engineered through methods such as microfluidics, can overcome limitations of traditional delivery systems, such as low efficacy, enzymatic degradation, or off-target side effects.

LNPs represent an advanced class of delivery systems that have evolved from earlier generation liposomes. Compared to liposomes, LNPs offer improved functionality, stability and delivery efficiency. GSK's AS01, which uses liposomes, has been successfully applied in vaccines for shingles and malaria, illustrating the early success of liposome-based adjuvants [112]. Similarly, liposome-based adjuvants addressed the problem of water solubility in earlier generation of cancer treatment [113]. Building on these foundational systems, modern LNPs platforms have revolutionized the delivery of nucleic acids and small molecules, with their role in mRNA vaccines for COVID-19 exemplifying their potential [114].

Structurally, LNPs are spherical nanoparticles formed by phospholipids (e.g., phosphatidylcholine, phosphatidylglycerol, etc.) dispersed in aqueous solution, often with additional stabilizers such as cholesterol. The organization and physicochemical properties of LNPs depend on the types and quantities of the constituent lipids, as well as the solution properties (such as ionic strength, pH) [115]. Their size typically ranges from 20 nm to 200 nm, but smaller LNPs with size ≤ 100 nm tend to exhibit enhanced cellular uptake and prolonged circulation time, which facilitate antigen presentation and immune cell activation [116][111]. LNPs are versatile delivery vehicles, capable of transporting both hydrophilic and hydrophobic drugs [117]. The surface charge of LNPs, including liposomes, is determined by the charge of the lipid head groups within their structure. This charge contributes to zeta potential, a key parameter representing the electrical potential at the interface between a particle's surface and the surrounding fluid. Particles with low zeta potential values (close to 0 mV) are prone to aggregate due to insufficient electrostatic repulsion. In contrast, particles with high zeta potential (≤-30 mV or ≥30 mV) exhibit strong repulsion forces that prevent aggregation [118].

The zeta potential of LNPs can be tuned based on their composition. For example, cationic lipids, such as dioleoyl-3-trimethylammonium propane (DOTAP), yield positively charged LNPs which enhance interaction with negatively charged cell membranes and promote cellular uptake via endocytosis [117]. However, it was also reported that cationic LNPs were unstable during storage and exhibited high cytotoxicity levels, both in vitro and in vivo [119][120]. In contrast, anionic lipids, such as 1,2-dioleoyl-sn-glycero-3-phosphoglycerol (DOPG), have also been explored. The inclusion of negatively charged lipids produces LNPs that generally demonstrate greater stability in solutions and lower cytotoxicity [121].

Despite their advantages, LNPs still have certain limitations including short circulation time and low in vivo stability. To address these challenges, various modifications have been developed to improve the functionality of LNPs. One notable approach is the incorporation of bio-compatible polymers, such as polyethylene glycol (PEG), onto the surface of LNPs. This process is known as PEGylation, which creates a stealth effect by introducing steric hindrance that prevents phagocytic cells from accessing the surface of LNPs and prolongs LNPs circulation time in bloodstream [122]. Moreover, PEGylation improves drug solubility by forming a water cloud around the polymer [123].

Section 4: Summary

Building on the information outlined in the introduction, this research was structured into two main parts. The first part focused on examining how the immune function of lipid A **1** can be modulated by altering its aggregate structure using simple amphipathic molecules such as fatty acids. This involved investigating the impact of aggregate composition and the state of mixed aggregate on the innate immune activity of lipid A **1**.

The second part of this research centered on the development of LNPs containing AfLA **4** as a mucosal vaccine adjuvant. Drawing on the insights gained from the first part, the lipid composition of LNPs was tailored and optimized to regulate their immune function. The adjuvanticity of LNPs containing AfLA **4** was then evaluated in vivo using ovalbumin (OVA) as a model antigen.

Chapter 2: Regulation of *Escherichia coli* lipid A immune function by amphipathic fatty acids

Section 1: Background

In the previous work by Mueller and Kusumoto et al. [55], it was observed that the composition of aggregates between *E. coli* lipid A **1** and cardiolipin (CL, C18:2) **2** could affect the immune function of lipid A **1**. Therefore, I wanted to investigate the modification of lipid A **1** aggregate structure by using simple amphipathic compounds like fatty acids.

Although previous studies had explored the role of fatty acids in immune signaling, there remains no clear consensus on whether fatty acids directly activate the TLR4-mediated signaling pathway or regulate the immune function of LPS or lipid A **1** [68][69][70]. Considering those prior results, in this chapter, the aggregate structure of *E. coli* lipid A **1** was modified using different fatty acids to investigate how the state of mixed aggregate and aggregate composition can affect lipid A **1** activity. Specifically, the effects of fatty acids chain length and degree of unsaturation on lipid A **1** immune function were examined. These findings were subsequently applied to the next phase of this research, which involved developing lipid nanoparticles containing lipid A and other amphipathic compounds as vaccine adjuvant materials.

Section 2: Aggregate sample preparation method

To evaluate the effect of fatty acids chain length on lipid A **1** immune function, stearic acid (C18:0) **5**, palmitic acid (C16:0) **6**, myristic acid (C14:0) **7**, and lauric acid (C12:0) **8** were used. To evaluate the effect of fatty acids degree of unsaturation on the immune function of lipid A **1**, oleic acid (C18:1) **9**, linoleic acid (C18:2) **10**, linolenic acid (C18:3) **11** and docosahexaenoic acid (DHA, C22:6) **12** were used. Figure 2.1 below shows the structure of all fatty acids that were examined in this research.

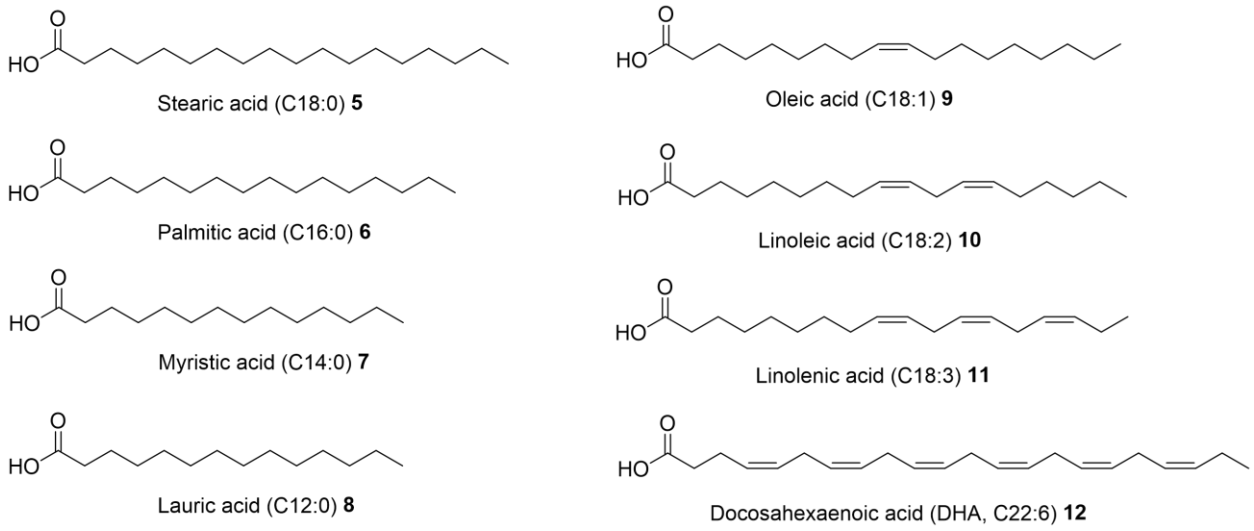

Figure 2.1: Structures of all fatty acids investigated

To investigate the effects of aggregates on the immune function of lipid A **1**, two sample preparation methods were constructed as shown in figure 2.2 below: simple mixing method (SMM) and homogenous mixing method (HMM). These methods were first developed by Mr. Ichinoo in our group, who prepared HMM and SMM samples containing cardiolipin and *E. coli* lipid A **1**, successfully reproducing the findings of Mueller and Kusumoto et al. [124]. The choice of method was expected to influence the proportion of mixed aggregates composed of multiple compounds versus aggregates consisting of a single compound.

For SMM, lipid A **1** and one fatty acid (chosen from fatty acids **5-12**) were separately dissolved in DMSO at appropriate concentrations. The samples were then diluted with physiological saline before being added continuously to cell culture medium. SMM samples were expected to form a mixture of two distinct aggregates composed of single components: lipid A **1**-only aggregates and fatty acids-only aggregates.

For HMM, lipid A **1** and one fatty acids (selected individually from fatty acid **5-12**) were mixed in tert-butyl alcohol (^{t}BuOH) and then lyophilized overnight. The mixture was then dispersed and homogenized in chloroform, which should result in a uniform solution. After evaporation to remove chloroform, HMM samples were dissolved in ^{t}BuOH, lyophilized overnight and dissolved in DMSO before being added to cell culture medium. HMM samples were expected to predominantly form mixed aggregates composed of both lipid A and fatty acid.

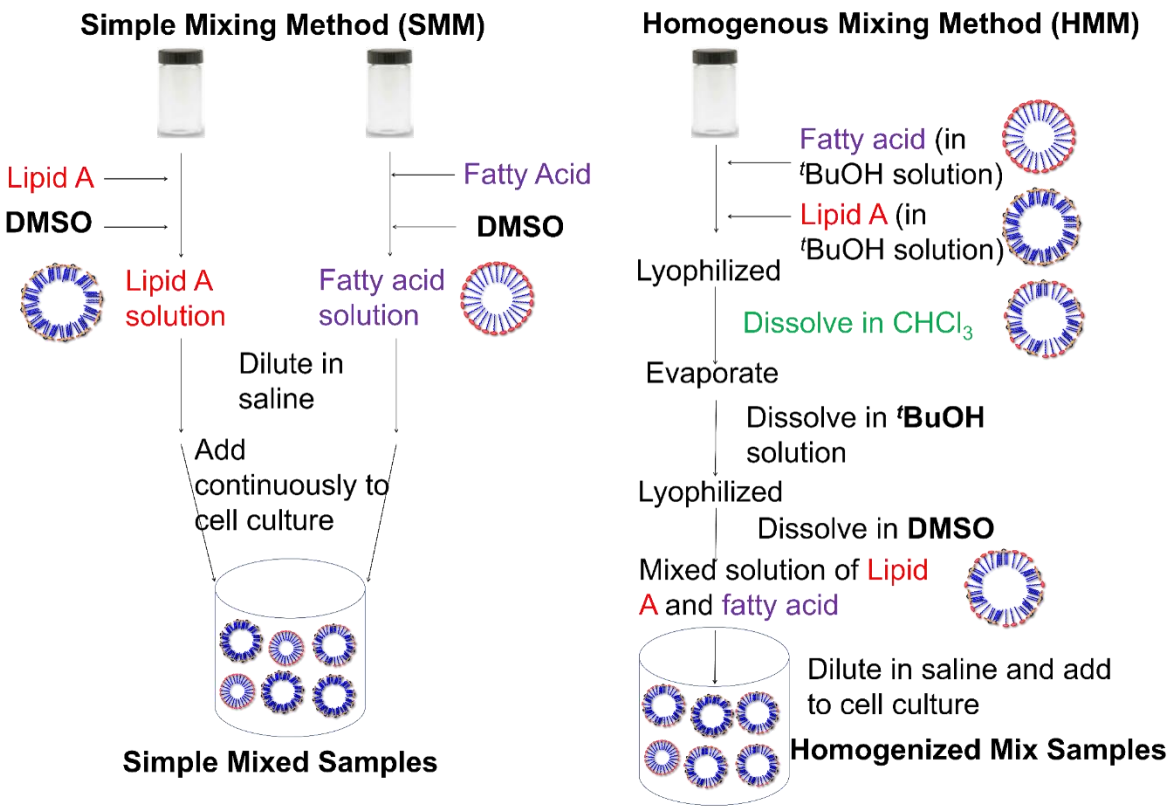

Figure 2.2: Aggregate sample preparation method

Section 3: Evaluation of SMM and HMM samples innate immune function

In this chapter, the innate immune function of all samples was evaluated using the HEK-Blue™ hTLR4 cell line. Previous studies have utilized cell lines expressing multiple receptors such as RAW264.7 or Ba/F3 cell lines [68][69][70]. Since this research aimed to examine the effect of fatty acids **5-12** on lipid A **1** TLR4-mediated immune pathway, a cell line that stably expresses TLR4/MD-2 receptor complex was chosen. This approach ensured that any observed immune activity could be attributed specifically to the TLR4/MD-2 signaling cascade. Specifically, innate immune function was measured via the activation of NF-κB, a transcription factor protein complex that is essential in regulating immune response of the TLR4/MD-2 signaling pathway [125]. The level of NF-κB activation was evaluated by the release of secreted alkaline phosphatase (SEAP), a reporter of gene expression.

First, the effects of fatty acid chain length on lipid A immune function were examined using lipid A **1** and saturated fatty acids **5-8**.

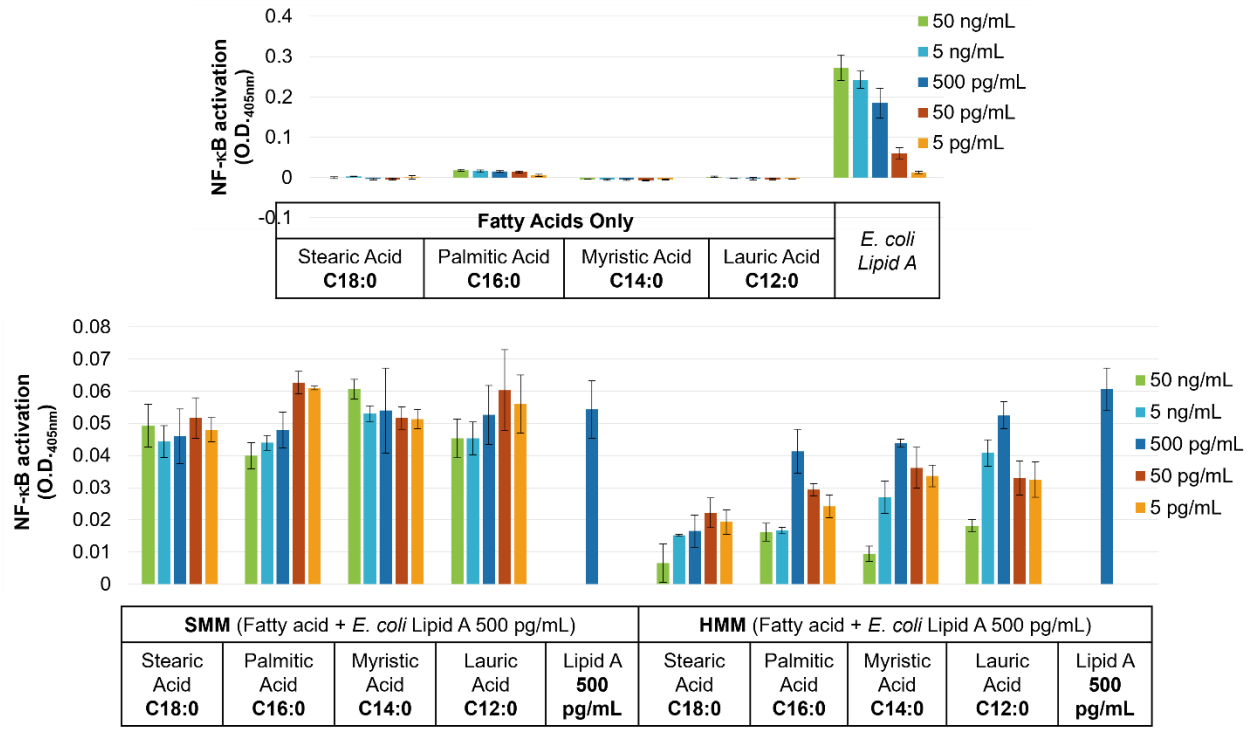

Figure 2.3: Top: Evaluation of NF-κB activation by saturated fatty acids **5-8** alone/ *E. coli* lipid A **1** alone. Bottom: Evaluation of NF-κB activation by SMM samples of saturated fatty acids **5-8** and *E. coli* lipid A **1** (500 pg/mL)/ HMM samples of saturated fatty acids **5-8** and *E. coli* lipid A **1** (500 pg/mL)

From figure 2.3, when HEK-Blue^{TM} hTLR4 cells were treated with only saturated fatty acids **5-8**, no immunostimulatory effect was observed. For SMM and HMM samples, each sample contain lipid A **1** at 500 pg/mL and one saturated fatty acid at concentration range from 50 ng/mL to 5 pg/mL. In the case of SMM, it was observed that changing the fatty acid concentration had no effect on the immune function of the SMM sample compared to the positive control, which contained only lipid A (500 pg/mL).

On the other hand, the HMM samples of all saturated fatty acids **5-8** exhibited an attenuation effect on the immune activity of lipid A **1**, and the attenuation effect occurred in a concentration-dependent manner. Additionally, it was observed that the as the acyl chain length decreased from stearic acid C18:0 **5** to lauric acid C12:0 **8**, the attenuation effect also decreased. Based on these results, changing the fatty acid chain length could affect the level of NF-κB activation by lipid A **1**, but only in HMM samples.

Next, the effects of the degree of unsaturation on lipid A **1** immune function were evaluated using unsaturated fatty acids **9-12**.

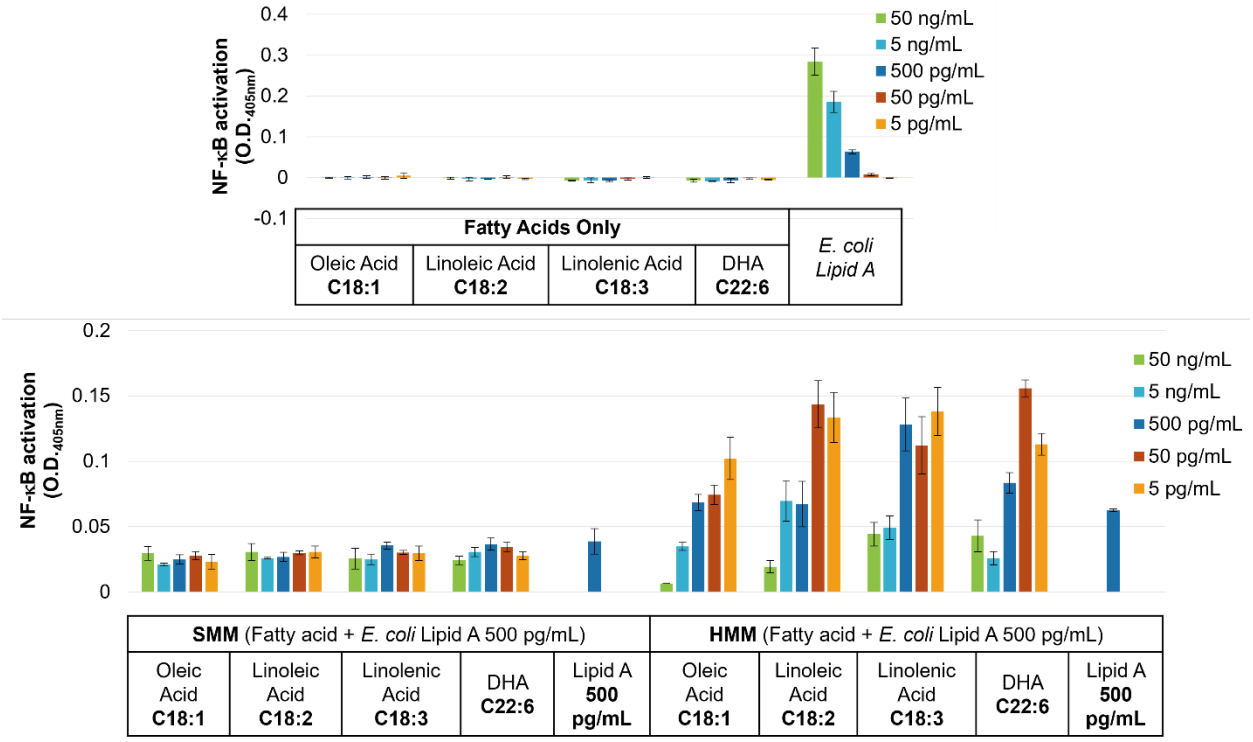

Figure 2.4: Top: Evaluation of NF-κB activation by unsaturated fatty acids **9-12** alone/ *E. coli* lipid A **1** alone. Bottom: Evaluation of NF-κB activation by SMM samples of unsaturated fatty acids **9-12** and *E. coli* lipid A **1** (500 pg/mL)/ HMM samples of unsaturated fatty acids **9-12** and *E. coli* lipid A **1** (500 pg/mL)

As shown in figure 2.4, treatment of HEK-Blue™ hTLR4 cells with only unsaturated fatty acids **9-12** did not induce any immunostimulatory activity. Similarly, when cells were treated with SMM samples that contained lipid A **1** (500 pg/mL) and one unsaturated fatty acid (concentration ranging from 50 ng/mL to 5 pg/mL), no change was observed in the level of NF-κB activation compared to cells treated with lipid A **1** alone.

Meanwhile, HMM samples showed a concentration-dependent attenuation effect at higher concentration of fatty acid, but as the fatty acid concentration decreased, a boosting effect was observed for all unsaturated fatty acids **9-12**. Furthermore, the attenuation effect weakened as the number of unsaturated bonds increased from one in oleic acid **9** to three in linolenic acid **11**. Thus, the degree of unsaturation of fatty acids appeared to influence the immune function of lipid A **1** in HMM samples, but not in SMM samples.

Based on the previous results (figure 2.3 and 2.4), SMM samples containing any fatty acids **5-12** had no effect on the activity of lipid A **1**, suggesting that these fatty acids **5-12** did not competitively inhibit MD-2 binding pocket. In contrast, HMM samples showed attenuation of lipid

A **1** activity, indicating an alternative mechanism by which fatty acids **5-12** could modulate the immune function of lipid A **1**. One possible explanation was that lipid A **1** activity was influenced by the structural properties of its aggregate. Therefore, a structural evaluation of aggregates containing lipid A **1** and fatty acids **5-12** was conducted.

Furthermore, the innate immune activity of lipid A **1** (500 pg/mL) was found to change depending on three factors: 1) sample preparation method (SMM or HMM); 2) the choice of fatty acid (saturated or unsaturated); 3) the concentration ratio of fatty acid to lipid A. It was considered that modifying any of these factors could alter the structural properties of the aggregates. Structural evaluation was thus performed to investigate the influence of these factors.

Section 4: Structural evaluation of aggregates by dynamic light scattering and transmission electron microscopy

To examine the differences between aggregates, structural evaluation was performed using dynamic light scattering (DLS) and transmission electron microscopy (TEM). DLS measures the sizes of aggregates as well as the polydispersity index (PI), which is a measure of aggregates homogeneity. A large PI value means that sample is more heterogenous and contains aggregates with different sizes, while a small PI value (approach 0) means that the sample contains more homogenous aggregates. On the other hand, TEM provides information about the size distribution and shape of aggregates in each sample.

As previously mentioned, from the in vitro results there were three factors that showed an effect on lipid A **1** immune function: 1) sample preparation method (HMM and SMM); 2) which fatty acid was used; 3) the concentration ratios between fatty acid and lipid A **1**. To evaluate the effect of different types of fatty acids, sample containing stearic acid (C18:0) **5** was chosen to represent saturated fatty acid**,** and sample containing linoleic acid (C18:2) **10** was chosen to represent unsaturated fatty acids. To evaluate the effect of concentration ratio, two concentration ratios of fatty acid to lipid A were chosen: 10:1 and 0.1:1 (Table 2.1).

Table 2.1: Difference in concentrations of samples for biological experiments and for DLS/TEM

Concentration Ratio (Fatty acid : lipid A)	Concentrations for biological experiments (Fatty acid : lipid A)	Concentrations for DLS/ TEM (Fatty acid : lipid A)
10:1	5 ng/mL : 500 pg/mL	10 µg/mL : 1 µg/mL
0.1:1	50 pg/mL : 500 pg/mL	0.1 µg/mL : 1 µg/mL

From table 2.1, although the concentrations of samples used for biological experiments ranged from 5 ng/mL to 50 pg/mL, these conditions could not be replicated in DLS measurements due to the detection limit of DLS. Instead, the same concentration ratios were maintained, with DLS experiments conducted at concentrations ranging from 10 µg/mL to 0.1 µg/mL. For TEM, while aggregates could be observed at lower concentrations, the range of 10 µg/mL to 0.1 µg/mL was applied due to technical constraints.

First, the effects of sample preparation method (SMM or HMM) on the aggregates formed and the immune function of lipid A **1** were shown in table 2.2 below.

Table 2.2: Effects of sample preparation method

Concentration Ratio (Fatty acid : lipid A)	10:1	10:1	10:1	10:1
Fatty acid	Stearic acid (C18:0)		Linoleic acid (C18:2)	
Sample preparation method	SMM	HMM	SMM	HMM
Effect on lipid A immune function in vitro	No effect	Attenuation effect	No effect	Attenuation effect
DLS	**Peak**: 525.5 ± 143.9 **PI**: 1.092 + 0.0903	**Peak**: 546.8 ± 35.8 **PI**: 0.296 ± 0.00658	**Peak**: 636.7 ± 99.2 **PI**: 0.761 ± 0.0481	**Peak**: 286.3 ± 7.6 **PI**: 0.303 ± 0.0584
TEM	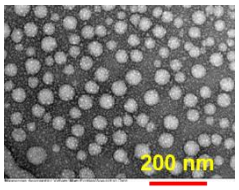 Aggregates size <100 nm 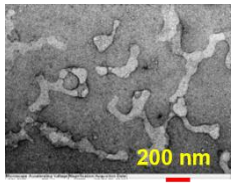 Amorphous aggregates size 300~1000 nm	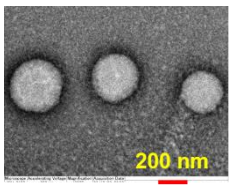 Aggregates size 100~500 nm	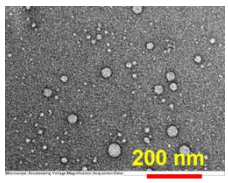 Aggregates size <50 nm 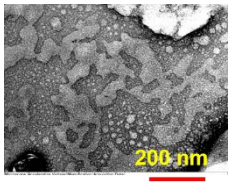 Amorphous aggregates size 300~1000 nm	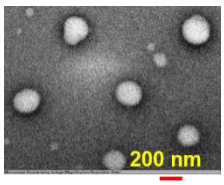 Aggregates size 100~300 nm

Table 2.2 above shows the summary of DLS, TEM and in vitro results of the SMM and HMM sample preparation methods. In the case of samples that contained saturated stearic acid (C18:0) **5** and lipid A **1** at concentration ratio 10:1, SMM sample showed no effect on the immune function of lipid A **1**, while HMM sample showed an attenuation effect. From the DLS results, the main difference was that HMM sample showed a lower PI value, which suggested that the HMM samples were relatively more homogenous. TEM results also showed a difference in the aggregates formed by SMM and HMM. The SMM sample contained a large amount of small size aggregates, but also many large amorphous aggregates with irregular structures. This was in contrast with HMM sample, where stearic acid (C18:0) **5** and lipid A **1** rearranged to form relatively homogenized large aggregates.

When comparing the results of SMM and HMM samples of unsaturated linoleic acid (C18:2) **10** and lipid A **1**, in vitro experiments showed no effect on lipid A **1** immune function for SMM, but an attenuation effect was observed for HMM (figure 2.4). The results of DLS and TEM showed that HMM sample had a lower PI value and formed large and relatively homogenized structure compared to the small and amorphous aggregates observed in SMM sample.

From these results, there seemed to be a correlation between the structures of the aggregates formed and the effects of these aggregates on the immune activity of lipid A **1**. DLS and TEM results showed that for both fatty acids, HMM samples formed large, relatively homogenous structures, which corresponded to an attenuation effect on lipid A **1** immune function. On the other hand, SMM samples consisted of many small aggregates or large but amorphous aggregates, which seemed to have no effect on the in vitro results.

Next, the effects of concentration ratio and the type of fatty acids on the structural characteristics of aggregates were evaluated.

Table 2.3: Effects of concentration ratios and types of fatty acids

Concentration Ratio (Fatty acid : lipid A)	10:1	0.1:1	10:1	0.1:1
Fatty acid	Stearic acid (C18:0)		Linoleic acid (C18:2)	
Sample preparation method	HMM	HMM	HMM	HMM
Effect on lipid A immune function *in vitro*	Attenuation effect	Attenuation effect	Attenuation effect	Boosting effect
DLS	**Peak**: 546.8 ± 35.8 **PI**: 0.296 ± 0.00658	**Peak**: 314.4 ± 22.7 **PI**: 0.447 ± 0.0301	**Peak**: 286.3 ± 7.6 **PI**: 0.303 ± 0.0584	**Peak**: 49.8 ± 0.891 **PI**: 0.418 ± 0.891
TEM	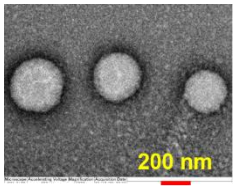 Aggregates size 100~300 nm	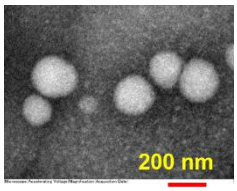 Aggregates size 100~300 nm	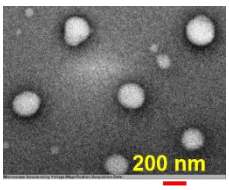 Aggregates size 100~300 nm	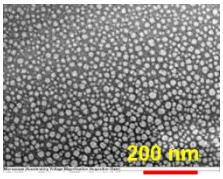 Aggregates size <50 nm 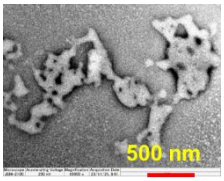 Amorphous aggregates 300~1000 nm

Table 2.3 above shows the summary of DLS, TEM and in vitro results of HMM samples at different concentration ratios of fatty acid and lipid A **1**. In the case of samples containing stearic acid (C18:0) **5**, an attenuation effect on lipid A **1** immune function was observed for both concentration ratios 10:1 and 0.1:1 (figure 2.3). The results of DLS and TEM were also similar for both concentration ratios. A relatively low PI value was observed in DLS, and large, relatively homogenous aggregates were observed in TEM.

On the other hand, for samples containing linoleic acid (C18:2), an attenuation effect was observed at concentration ratio 10:1, but a boosting effect on lipid A **1** innate immune activity

occurred at concentration ratio 0.1:1 (figure 2.4). At the concentration ratio 10:1, DLS and TEM results were similar to the results of stearic acid (C18:0) **5**, where a low PI value and large, relatively homogenous aggregates were observed. However, at the concentration ratio 0.1:1, TEM showed a large amount of small size aggregates and large amorphous aggregates. Additionally, evaluation by DLS showed a higher PI value compared to the PI value at concentration ratio 10:1.

Based on these results, a correlation between the aggregates structures and the effect of mixed aggregates on lipid A **1** immune function was observed. For HMM samples containing stearic acid (C18:0) **5**, many relatively homogenous aggregates were observed at both concentration ratios 10:1 and 0.1:1, which corresponded to an attenuation effect on lipid A **1** immune activity at both ratios. Meanwhile, HMM samples containing linoleic acid (C18:2) **10** showed an attenuation effect at concentration ratio 10:1, but a boosting effect at ratio 0.1:1. This was reflected in the results of DLS and TEM, where relatively homogenous aggregates were observed at ratio 10:1 but missing at ratio 0.1:1. Instead, many small size aggregates and large amorphous aggregates were observed. The DLS and TEM data for HMM samples of palmitic acid **6** exhibited a similar trend with stearic acid **5**, while data for HMM samples of linolenic acid **11** showed similar tendency to linoleic acid **10**. These DLS and TEM results are provided in the supporting information (Table S1).

Section 5: Discussion and conclusion

In the previous work by Mueller and Kusumoto et al. [55], it was reported that the innate immune activity of lipid A was affected by the composition of suspensions containing *E. coli* lipid A **1** and cardiolipin (CL, C18:2) **2**. When lipid A **1**-only suspension and CL **2**-only suspension were mixed together, an antagonistic effect was observed. On the other hand, mixed suspensions that contained both lipid A **1** and CL **2** showed a boosting or antagonistic effect depending on the ratios of these two compounds.

Taking the results of previous work into consideration, the effects of mixed aggregate and aggregate compositions on the immune function of lipid A were investigated. To achieve this, the aggregate of lipid A **1** was modified using amphipathic fatty acids **5-12**, and the level of innate immune response was measured via the level of NF-κB activation.

When HEK-Blue^{TM} hTLR4 cells were treated with only fatty acids, all saturated and unsaturated fatty acids **5-12** showed no innate immune activity (figure 2.3 and 2.4). From this result, fatty acids were not agonist of TLR4/MD-2 receptor complex. In previous work using Ba/F3 and RAW264.7 cell lines, it was reported that saturated fatty acids could elicit immunostimulatory effect by inducing dimerization and recruitment of TLR4/MD-2 receptor complex into the lipid raft regions of cell membrane [68]. However, when using a cell line that stably expressed TLR4/MD-2 receptor complex, no immune activation was observed for all fatty acids. As the cell lines in previous works expressed multiple receptors, it was possible that the fatty acids could activate immune function

using other signaling pathways such as TLR2-mediated pathway, or by triggering caspase-4/5/11 which led to the activation of Nod-like receptor 3 (NLRP3) inflammasome [126][127].

Samples that contained lipid A **1** and one fatty acids (chosen from fatty acids **5-12**) were then prepared using either simple mixing method (SMM) or homogenous mixing method (HMM). When HEK-Blue^{TM} hTLR4 cells were treated with SMM samples, there were no changes in the immune function of lipid A **1** compared to control that contained only lipid A (figure 2.3 and 2.4). This was observed for all fatty acids regardless of chain length or degree of unsaturation. This suggested that when lipid A **1** and fatty acids **5-12** were simply mixed together, fatty acids did not competitively inhibit MD-2 binding pocket to inhibit lipid A **1** immune function. This was different from previous results where unsaturated fatty acid like linoleic acid (C18:2) **10** and docosahexaenoic acid (22:6) **12** inactivated the NF-κB signaling pathway and reduced LPS and lipid A-induced innate immune activity [70]. However, previous works also used RAW264.7 cells which expressed multiple immune receptors, compared to HEK-Blue^{TM} hTLR4 which stably expressed TLR4/MD-2 receptor complex. If fatty acids could modulate immune activity through pathways outside TLR4, this experiment system may not be able to detect such phenomenon.

On the other hand, when treatment of HEK-Blue^{TM} hTLR4 cells were performed using HMM samples, effects on the immune function of lipid A **1** were observed. In the case of samples containing saturated fatty acids, a concentration-dependent attenuation effect was observed for all saturated fatty acids **5-8** (figure 2.3). Furthermore, this attenuation effect was strongest for stearic acid (C18:0) **5** and decreased as the acyl chain length decreased to 12 carbons of lauric acid (C12:0) **8**.

There were several factors that may explain the decrease in the attenuation effect as the number of carbon atoms decreased. The longer fatty acid chains of stearic acid (C18:0) **5** and palmitic acid (C16:0) **6** enhanced Van der Waals force, leading to tighter packing of the mixed aggregates of lipid A **1** and fatty acids. Tighter packing resulted in more rigid and thermodynamically stable aggregates, which could prevent the presentation of lipid A to LBP or TLR4/MD2. Additionally, the larger hydrophobic region of stearic acid (C18:0) **5** and palmitic acid (C16:0) **6** may also integrate into cellular membrane, affecting membrane fluidity and disrupting the function of membrane receptor proteins [128].

On the other hand, the shorter chains of myristic acid (C14:0) **7** and lauric acid (C12:0) **8** reduced the Van der Waals force, resulting in less stable aggregates. This reduced the prevention of lipid A transfer to LBP and TLR4, leading to a decrease in the attenuation effect. The shorter hydrophobic regions of myristic acid (C14:0, 7) and lauric acid (C12:0, 8) were also less disruptive to the cell membrane, and therefore had a smaller impact on the function of membrane receptor proteins [128].

In the case of HMM samples containing lipid A **1** and one unsaturated fatty acid **9-12**, an attenuation effect was observed at higher fatty acid to lipid A concentration ratio, and a boosting

effect was observed at lower concentration ratio (figure 2.4). Additionally, the attenuation effect decreased as the degree of unsaturation increased from one double bond of oleic acid (C18:1) **9** to three double bonds of linolenic acid (C18:3) **11**.

There were several factors that could explain the stronger attenuation effect and weaker boosting effect of mono-unsaturated oleic acid (C18:1) **9** compared to poly-unsaturated linoleic acid (C18:2) **10** and linolenic acid (C18:3) **11**. As oleic acid **9** contained only a single double bond, it formed a tighter and more organized packing compared to the poly-unsaturated fatty acids, reducing the presentation of lipid A **1** to LBP. In contrast, the additional double bonds of linoleic acid **10** and linolenic acid **11** introduced more kinks to the fatty acid chain, which significantly disrupted aggregate packing. This disruption increased the accessibility of lipid A **1** to LBP and TLR4. Furthermore, poly-unsaturated fatty acids inserted into membrane may increase the membrane fluidity, thereby promoting the recruitment of TLR4 [129].

As fatty acids **5-12** did not suppress lipid A **1** activity by competitively inhibited MD-2 binding pocket (based on SMM results), an alternative mechanism by which fatty acids **5-12** could modulate the immune function of lipid A **1** should be considered. One possible hypothesis was that lipid A **1** activity could be influenced by the structures of its aggregate. Additionally, it was observed that the immune function of lipid A **1** changed depending on three factors: 1) sample preparation method (SMM or HMM); 2) type of fatty acids (saturated or unsaturated); 3) concentration ratios of fatty acids to lipid A. Therefore, it was hypothesized that modifying any of these three factors could alter the structural properties of the aggregates formed, which required structural evaluation by DLS and TEM to verify. First, when compared the DLS results of SMM and HMM samples, it was observed that HMM sample had a higher degree of homogeneity based on a lower polydispersity index (PI) (table 2.2). The TEM results showed that SMM samples formed many small size aggregates and large amorphous aggregates, while HMM samples rearranged into large and relatively homogenous aggregate structures. SMM samples also showed no effect on the immune function of lipid A **1**, which suggested that the fatty acids and lipid A **1** in SMM were phase-separated and not reorganized into a unified structure. The small size aggregates could be incomplete structures that contained only lipid A **1** or only fatty acids, while the large amorphous aggregates were irregular and structurally unstable, which could indicate poor compatibility between lipid A **1** and fatty acids. These amorphous aggregates may be easy to collapse, which allowed lipid A **1** to be available to LBP. In this way, lipid A **1** may retain its biological conformation and could continue to activate TLR4 effectively.

Meanwhile, the large, relatively homogenous aggregates in HMM samples suggested that fatty acids and lipid A **1** were structurally integrated. The tighter packing of lipid A **1** and fatty acids in these relatively homogenous mixed aggregate structures could lead to a more rigid and stable structure, which prevented the presentation of lipid A **1** to LBP and TLR4/MD-2 complex.

Next, the effects of the types of fatty acid (saturated and unsaturated) as well as the effects of concentration ratios between fatty acid and lipid A **1** on the innate immune activity of lipid A **1** were evaluated (table 2.3). At concentration ratios 10:1 and 0.1:1 (fatty acid:lipid A), HMM samples of saturated stearic acid (C18:0) **5** showed attenuation effect. The DLS and TEM results at these two concentration ratios were similar, where large, relatively homogenous aggregates were observed. As explained previously, this kind of homogenous morphology may lead to tighter packing, which resulted in reduced interaction between lipid A **1** and LBP.

In the case of HMM samples of unsaturated linoleic acid (C18:2) **10**, an attenuation effect was observed at concentration ratio 10:1 and a boosting effect was observed at concentration ratio 0.1 (fatty acid:lipid A). At concentration ratio 10:1, large, relatively homogenous aggregates were formed that were structurally similar to aggregates containing stearic acid **5**. However, at concentration ratio 0.1:1, many small aggregates and large amorphous aggregates were observed. It was possible that these morphologies had lower stability and were easier to collapse, which led to easier transfer of lipid A to TLR4/MD-2 receptor complex via LBP. Thus, a boosting effect was observed.

In conclusion, by preparing aggregates that contained lipid A **1** and simple amphipathic fatty acids **5-12** using SMM or HMM, it was shown that aggregate composition and state of mixed aggregates could regulate the immune function of lipid A **1**. Additionally, the morphologies of the aggregates that were formed may be directly correlated with the observed immune activity.

For future experiments, one possibility is the usage of fluorescent or biotin-labeled lipid A to tract its surface accessibility to LBP. Another possibility is binding assay to measure the direct binding of lipid A aggregates to TLR4/MD-2 receptor complex using surface plasmon resonance (SPR), which measures molecular interactions in real time. Additionally, molecular dynamics simulations can be performed to simulate the interactions between lipid A and different fatty acids to predict aggregate stability and lipid packing, and how the aggregate structure might interact with TLR4/MD-2 receptor complex.

The results from this chapter demonstrated that aggregates containing amphipathic fatty acids could influence the immune function of lipid A. This understanding was utilized in the subsequent chapter, focusing on the development of lipid nanoparticles incorporating lipid A as vaccine adjuvant materials. By incorporating more complex amphipathic compounds into lipid nanoparticles, the aim was to develop vaccine adjuvants that could enhance the innate immune activity of lipid A.

Chapter 3: Development of lipid nanoparticles containing *Alcaligenes faecalis* lipid A as vaccine adjuvant materials

Section 1: Background

Item 1: Self-adjuvating vaccines

Traditional vaccines typically consist of a physical mixture of antigens and adjuvants. In contrast, self-adjuvating vaccines integrate antigen and adjuvant into a single complex, either through covalent or non-covalent conjugations [130]. Since innate immune ligands are commonly used as adjuvants in self-adjuvating vaccine, this strategy enhances vaccine delivery and immunogenicity by facilitating efficient phagocytosis of the adjuvant-antigen complex by antigen-presenting dendritic cells that recognize these ligands (figure 3.1) [131]. In addition to promoting antigen uptake, the adjuvant also activates innate immunity, triggering a signaling cascade that promotes antibody production (adaptive immunity).

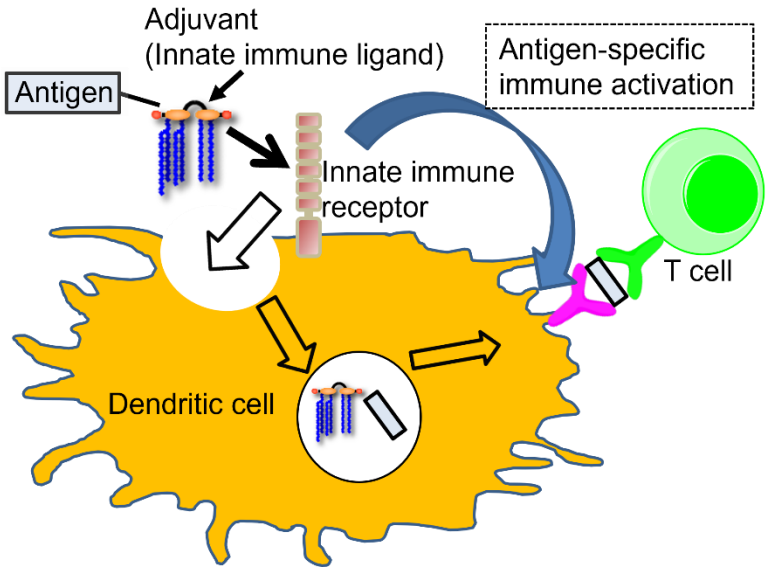

Figure 3.1: Self-adjuvating vaccine strategy

By ensuring that both antigen and adjuvant are simultaneously uptake by the same immune cell, self-adjuvating vaccines enable a coordinated antigen-specific immune response [132]. Furthermore, self-adjuvating vaccines eliminate the need for additional adjuvants such as Freund's adjuvant. This not only reduces the inflammation caused by adjuvants but also has the added benefit of simplifying vaccine formulation and enhancing consistency. Additionally, self-adjuvating strategy allows for the formation of adjuvant-antigen complex with high degree of homogeneity, which is essential for quality control [130].

There have been multiple reports of synthetic covalent self-adjuvating vaccines, including those that utilized agonistic ligands of TLR2 (lipopeptides such as diacylated Pam_2CSK_4, and triacylated Pam_3CSK_4) and TLR4 (MPLA) [130][131]. Here, the focus is on self-adjuvating vaccines that are formulated via non-covalent conjugations. Our laboratory had previously synthesized co-assembling vaccines composed of lipidated HER2-derived antigenic CH401 peptide and a lipophilic adjuvant (Pam_3CSK_4, α-GalCer, or lipid A **1**) [133]. However, this work instead focused on self-adjuvating vaccines that are lipid nanoparticles (LNP), inspired by the mRNA LNP vaccines that became popular during the COVID-19 pandemic.

Item 2: Lipid nanoparticles as a vaccine platform

Nucleic acid-based vaccines utilizing mRNA were first conceptualized more than three decades ago and demonstrated several advantages over traditional vaccine platforms [134]. Unlike conventional methods, mRNA vaccines can be manufactured through a cell-free process, allowing for both rapid and cost-effective large-scale production [135]. Additionally, a single mRNA vaccine can encode multiple antigens, which can enhance the immune response against resilient pathogen or targeting multiple pathogens or variants with a single vaccine formulation [136][137]. Despite these advantages, early mRNA vaccines faced many challenges, including low stability, poor efficacy or excessive immune stimulation.

The COVID-19 pandemic marked a pivotal moment for mRNA vaccine technology [138]. mRNA vaccines developed by Pfizer-BioNTech and Moderna showed high efficacy against SARS-CoV-2. Most importantly, these vaccines addressed the limitations of mRNA-based platforms by employing lipid nanoparticles (LNPs) as delivery vehicles. LNPs provided a protection barrier for mRNA against enzymatic degradation by nucleases in the host body. This ensured the successful delivery of the genetic code for SARS-CoV-2 spike protein to the target cells. Additionally, the use of ionizable cationic lipids in LNPs facilitated the cellular uptake of negatively charged mRNA, enabling it to cross the anionic lipid bilayer of the cell membrane.

Beyond their in vivo benefits, LNPs vaccines also offer the practical advantage of scalability, enabling the rapid production of large quantities of vaccine. The success of mRNA vaccines during the COVID-19 pandemic demonstrated the potential of LNPs as a reliable and versatile platform for vaccine development. Inspired by these advancements, this research focused on designing LNPs incorporating lipid A as a vaccine adjuvant to further explore their potential in enhancing immune responses.

Item 3: Lipid A as vaccine adjuvant

As previously explained, LPS and lipid A have the potential to act as vaccine adjuvants because they exhibit immunostimulatory effect via TLR4-mediated signaling pathway, which are either MyD88-dependent or TRIF-dependent [50]. Unfortunately, canonical *E. coli* LPS and its lipid A **1** excessively stimulate both pathways, leading to lethal toxicity [52].

However, the immune function of lipid A can be attenuated by modifying its structure, such as GlaxoSmithKline (GSK) 3D-MPL **3** (figure 1.11), a monophosphoryl lipid A derived from Gram-negative bacterium *Salmonella enterica serovar Minnesota Re595* [97]. Most importantly, 3D-MPL **3** selectively activates TRIF-dependent pathway without severe inflammation and can be used as a safe adjuvant [98]. 3D-MPL **3** was applied to GSK AS0 series, which combined the usage of adjuvant delivery modes (alum, emulsions, liposomes) with immunostimulants. One of these is AS01, a liposomal formulation containing 3D-MPL **3** and QS-21 (an immunostimulatory saponin) that has already been used in vaccines for shingles and malaria [86][87].

On the other hand, our laboratory has focused on symbiotic bacterial lipid A that could survive the host's innate immune response by promoting homeostasis. Specifically, we studied Alcaligenes *faecalis* (*A. faecalis*), an opportunistic bacterium that was reported to colonize the gut-associated lymphoid tissues (GALT), Peyer's patch (PP) [99]. *A. faecalis* was found to establish and maintain a homeostatic environment in the PPs by activating the immune system without causing harmful responses. The extracted LPS fraction from *A. faecalis* showed weaker TLR4 agonistic activity compared to canonical E. coli LPS, and it could promote IL-6 induction from DCs, which in turn enhanced IgA production without inducing toxicity [100].

Our laboratory successfully synthesized the hexa-acylated form of *A. faecalis* lipid A **4** (AfLA **4**, figure 1.13) and showed that it is the active principle of *A. faecalis* LPS [102]. In intranasal immunization study using mice, *A. faecalis* LPS and AfLA **4** showed promising results as mucosal vaccine adjuvant. AfLA **4** outperformed MPLA (an adjuvant derived from *Salmonella* bacterium similar to GSK's 3D-MPL **3**) and cholera toxin (a well-known immunogen for mucosal IgA production) [104][105][106][107]. These results suggest that AfLA **4** is a highly promising candidate for mucosal vaccine adjuvant.

Building on prior results of AfLA **4** as an adjuvant, this chapter focused on the development and assessment of LNPs containing AfLA **4**, both in vitro and in vivo. Based on the findings of previous chapter, where the introduction of amphipathic compounds at varying concentrations was shown to modulate the innate immune activity of lipid A, this research investigated whether modifying the lipid composition of LNPs with different amphipathic compounds at different concentrations can influence the immune function of AfLA **4** in LNPs. Additionally, this study evaluated how these modifications could impact the efficacy of LNP vaccines in murine experiments.

Section 2: Development of lipid nanoparticles using thin-film hydration method

In the initial investigation, the composition of LNPs was modified according to GSK AS01B composition, which originally contained 3D-MPL **3**, QS-21, DOPC and cholesterol [139]. DOPC promoted the formation of nanoparticles, while cholesterol was included to stabilize the liposome and prevent leakage.

As this research focused on the activity of AfLA **4**, QS-21 was not used in the preparation of LNPs. The LNPS were prepared using the thin-film hydration method, where lipids solution of DOPC, cholesterol and AfLA **4** were mixed together in chloroform [140]. After evaporation to remove the chloroform, a thin lipid film was produced. Hydration of the lipid film was then performed using phosphate buffered saline (PBS), and the LNPs were formed via agitation.

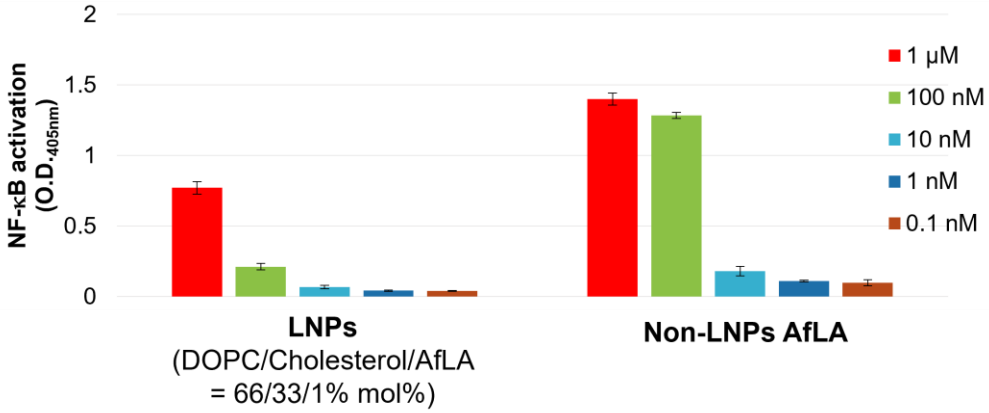

Figure 3.2: Evaluation of NF-κB activation by LNPs containing AfLA **4** and non-LNPs AfLA **4**

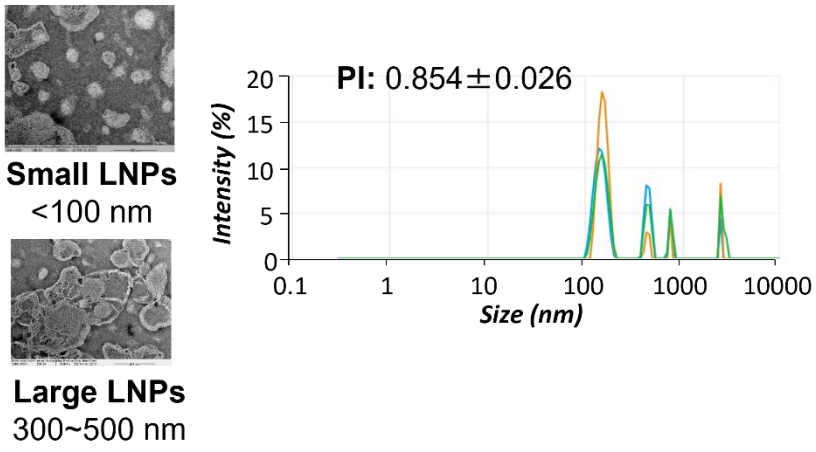

Figure 3.3: Structural evaluation of LNPs containing AfLA **4** using DLS and TEM

The innate immune function of the LNPs formed were then evaluated using HEK-Blue^{TM} hTLR4 cell line by measuring the level of NF-κB activation (figure 3.2). Structural evaluation of LNPs was also performed using DLS and TEM.

From figure 3.2, it was observed that AfLA **4** could maintain innate immune activity even when incorporated into LNPs. However, the result of DLS showed a high polydispersity index (PI), which meant that the LNPs formed were not homogenous (figure 3.3). This was reflected in the TEM result, which showed multiple large LNPs of different sizes.

Although the immune function of AfLA **4** in LNPs was confirmed, the LNPs formed by thin-film hydration method were not homogenous enough to function as vaccine adjuvant. Therefore, the LNPs preparation method and the LNPs composition were modified to improve LNPs quality.

Section 3: Development of lipid nanoparticles containing DOTAP and *Alcaligenes faecalis* lipid A using microfluidic

Item 1: Optimization of lipid nanoparticles preparation and quantification of lipid A in lipid nanoparticles

To improve the quality of the LNPs formed, a microfluidic device called iLiNP was used. iLiNP was developed by Professor Manabu Tokeshi group at Hokkaido University [141]. The iLiNP device is a baffle mixer device with a zigzag-shaped microchannel, which allows for rapid mixing and dilution of the lipid solution in the aqueous buffer solution (figure 3.4). By changing the flow rate and flow rate ratio between lipid and buffer solution, it was possible to synthesize homogenous LNPs population with the desired size ≤100 nm, which could improve circulation time and prevent uptake by phagocytes [116][111].

In addition to using the iLiNP, the composition of LNPs was modified to mimic the design philosophy of mRNA Covid-vaccine [114]. In addition to the neutral phospholipid (DSPC **13** and DOPC **14**) and cholesterol **15**, a polyethylene glycol lipid DMG-PEG 2000 **16** and an ionizable cationic lipid DOTAP **17** were introduced (figure 3.5). As AfLA **4** are negatively charged, the inclusion of the positively charged DOTAP **17** should help anchor the lipid A more strongly into LNPs lipid compartments. Additionally, the adsorption of cationic LNPs with negatively charged cell membrane are electrostatically favored, which

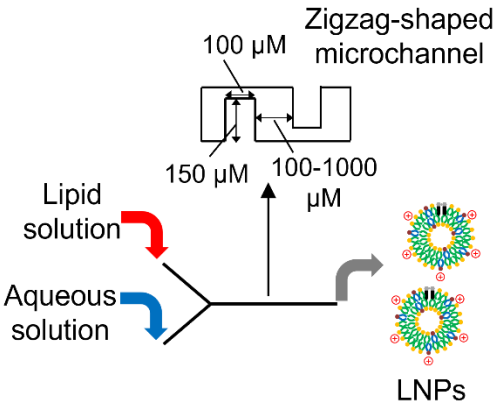

Figure 3.4: Overview of iLiNP

should lead to an increase in endocytosis of the LNPs. This can ensure that both AfLA **4** and antigen reached the same antigen-presenting cells, leading to efficient T cell activation [117]. On the other hand, DMG-PEG 2000 **16** are biocompatible polymers that prevent phagocytes from accessing LNPs surfaces due to steric hindrance and help increase LNPs circulation time [122]. Thanks to the water cloud surrounding the polymer, PEGylation also improves drug solubility [123].

To ensure the solubility of all compounds, the lipid solution was ethanol:DMSO at 6:4 ratio. For the aqueous solution, 25 mM acetate buffer at pH 4.0 was used to maintain the positive charge of DOTAP **17**. The flow rate of the lipid solution was 125 µL/min and the flow rate of the aqueous solution was 375 µL/min. Slower flow rates were also examined, but there was no significant change in the physical properties of the LNPs formed (similar sizes and zeta potential) and no change in the innate immune activity of the LNPs. Therefore, speed was prioritized to decrease sample preparation time. After LNPs were synthesized, dialysis was performed to remove any lipids that were not incorporated into the LNPs.

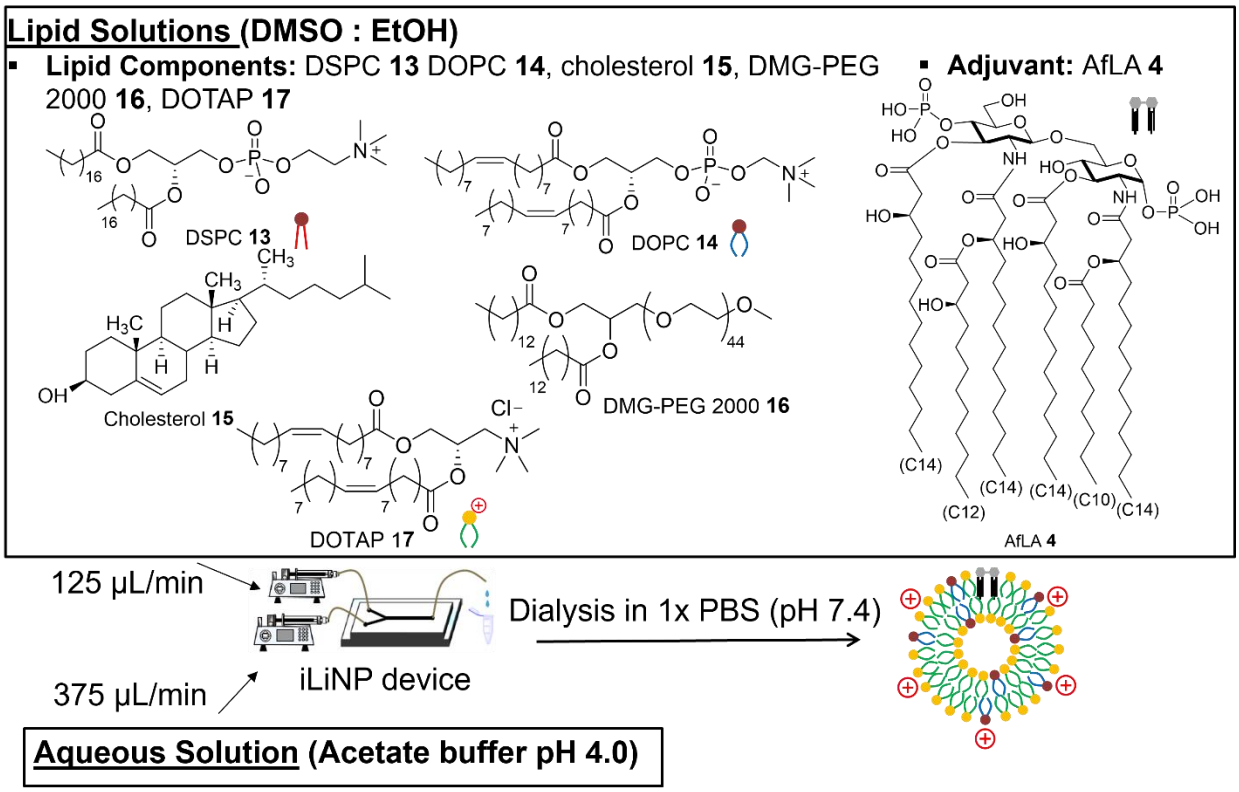

Figure 3.5: Preparation of LNPs vaccine using iLiNP

As part of the research purpose was to investigate whether changing lipid compositions of LNPs can synergistically enhance the activity of AfLA **4** in LNPs, different compositions were evaluated. Based on the lipid composition of Moderna mRNA vaccine [114], the concentrations of cholesterol **15** (38 mol%), DMG-PEG 2000 **16** (1.5 mol%) and AfLA **4** (1 mol%) were kept constants for all samples. However, the effects of DOTAP **17** and the neutral phospholipid on the immune activity of AfLA **4** were considered. The findings from the previous chapter showed that different concentrations of amphipathic compounds could affect the immune function of lipid A. Therefore, to investigate the LNPs composition that could elicit the strongest AfLA **4** immune activity, either saturated DSPC **13** or unsaturated DOPC **14** was used, and the ratio of DSPC **13**/DOTAP **17** or DOPC **14**/ DOTAP **17** was modified. Table 3.1 and 3.2 below show the physical properties of the LNPs synthesized by iLiNP.

Table 3.1: Physical properties of DSPC **13**/DOTAP **17** LNPs by DLS and TEM

AfLA = 1 mol% Cholesterol = 38 mol% DMG-PEG = 1.5 mol% DSPC:DOTAP = x:y mol%	**10:49.5 mol%**	**29.7:29.7 mol%**	**49.5:10 mol%**	**59.5:0 mol%**
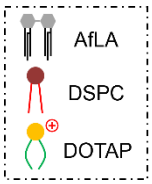	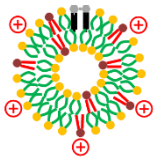		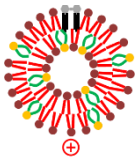	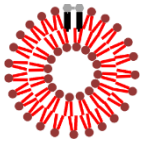
DLS	**Peak:** 48.3 ± 4.57 nm **PI**: 0.343 ± 0.0386 **Zeta**: +27.8 ± 2.98 mV	**Peak:** 84.1 ± 2.58 nm **PI:** 0.339 ± 0.0132 **Zeta:** +20.2 ± 1.88 mV	**Peak:** 64.1 ± 4.85 nm **PI:** 0.205 ± 0.0273 **Zeta:** +7.3 ± 3.15 mV	**Peak:** 50.7 ± 2.85 nm **PI:** 0.321 ± 0.0265 **Zeta:** -10.2 ± 1.37 mV
TEM	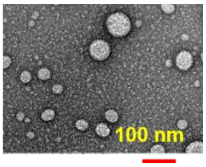 LNPs size <100 nm	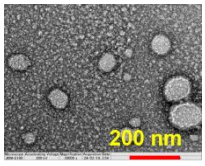 LNPs size <100 nm	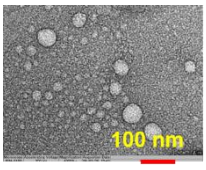 LNPs size <100 nm	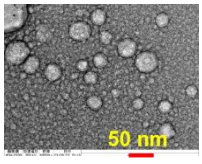 LNPs size <100 nm

Table 3.1 above shows the physical properties of the LNPs at different concentration ratios of DSPC **13** and DOTAP **17**. All LNPs had sizes <100nm, but there was no correlation between the concentrations of DOTAP and the sizes of the LNPs. All LNPs also had much lower PI compared to LNPs prepared by thin-film hydration method. Additionally, as the concentration of DOTAP decreased, the zeta potential of the LNPs also decreased. When there was no DOTAP, the negative charge of AfLA **4** contributed to the negative zeta potential. The results of TEM also support DLS findings, where all compositions formed LNPs structure with size <100 nm.

Table 3.2: Physical properties of DOPC **14**/DOTAP **17** LNPs by DLS and TEM

AfLA = 1 mol% **Cholesterol = 38 mol%** **DMG-PEG = 1.5 mol%** **DOPC:DOTAP = a:b mol%**	**10:49.5 mol%**	**29.7:29.7 mol%**	**49.5:10 mol%**	**59.5:0 mol%**
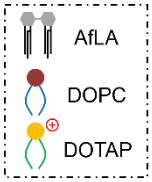	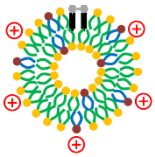	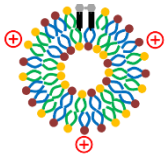	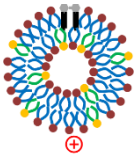	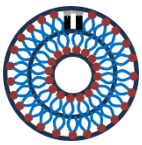
DLS	**Peak:** 45.3 ± 4.32 nm **PI:** 0.415 ± 0.0425 **Zeta:** +28.3 ± 1.35 mV	**Peak:** 36.2 ± 2.91 nm **PI:** 0.331 ± 0.0685 **Zeta:** +19.9 ± 1.82 mV	**Peak:** 34.3 ± 1.82 nm **PI:** 0.365 ± 0.0308 **Zeta:** +11.7 ± 2.72 mV	**Peak:** 26.1 ± 2.33 nm **PI:** 0.257 ± 0.0816 **Zeta:** -5.8 ± 2.05 mV
TEM	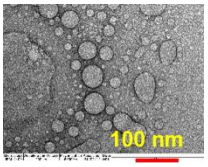 LNPs size <100 nm	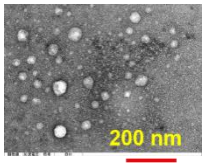 LNPs size <50 nm	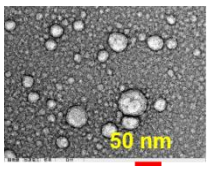 LNPs size <50 nm	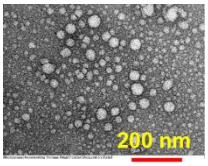 LNPs size <50 nm

Table 3.2 above shows the physical properties of LNPs with different concentration ratios of DOPC **14** and DOTAP **17**. All LNPs had sizes <100 nm, but the sizes were lower than the LNPs containing DSPC **13**. The PI values were lower than the LNPs prepared by thin-film hydration method, and the zeta potential value decreased as concentration of DOTAP **17** decreased. LNPs structure with size <50 nm were also observed in TEM, corresponding to DLS results.

After synthesis of LNPs, the quantification of AfLA **4** in each LNP sample was performed using liquid chromatography – mass spectrometry (LC/MS) (column: UHPLC PEEK Column InertSustain C18 3µm, 2.1×100mm). Solvent A was 10 mM ammonia in methanol/water (8/2) and solvent B was 10 mM ammonia in isopropanol. The eluent was collected at a flow rate of 0.2 mL/min and a linear gradient of 0% to 95% solvent B over 33 minutes. The results of quantitative analysis were summarized in table 3.3 below.

Table 3.3: Quantification of AfLA in LNPs samples by LC/MS

AfLA = 1 mol% **Cholesterol = 38 mol%** **DMG-PEG = 1.5 mol%** **DSPC:DOTAP = x:y mol%**	**10:49.5 mol%**	**29.7:29.7 mol%**	**49.5:10 mol%**	**59.5:0 mol%**
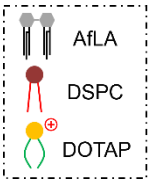	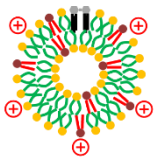	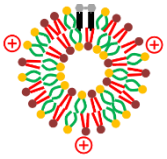	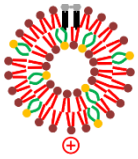	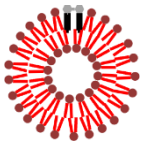
Lipid A retention %	**91.2%**	**82.0%**	**67.8%**	**67.5%**
AfLA = 1 mol% **Cholesterol = 38 mol%** **DMG-PEG = 1.5 mol%** **DOPC:DOTAP = a:b mol%**	**10:49.5 mol%**	**29.7:29.7 mol%**	**49.5:10 mol%**	**59.5:0 mol%**
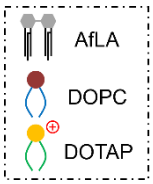	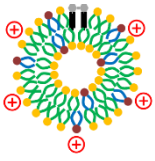	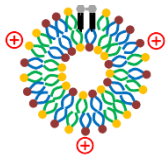	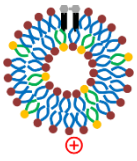	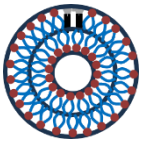
Lipid A retention %	**74.3%**	**78.6%**	**58.5%**	**60.3%**

From table 3.3 above, it could be observed that all samples had retained between 60% to 90% of AfLA **4**. For both LNPs contain either DSPC **13** or DOPC **14**, as the concentration of DOTAP **17** increased, the lipid A retention% also increased. This could be explained by the electrostatic interaction between positve charge of DOTAP **17** and negative charge of AfLA **4**, which promoted the incorporation of lipid A into the LNPs lipid compartments.

Item 2: in vitro evaluation of lipid nanoparticles samples containing DOTAP **17** and AfLA **4** using human cell lines

The innate immune function of all LNPs samples containing DOTAP **17** and AfLA **4** was evaluated using HEK-Blue™ hTLR4 and THP-1 cell lines. First, the level of NF-κB activation was evaluated by the SEAP reporter assay using HEK-Blue™ hTLR4 cells.

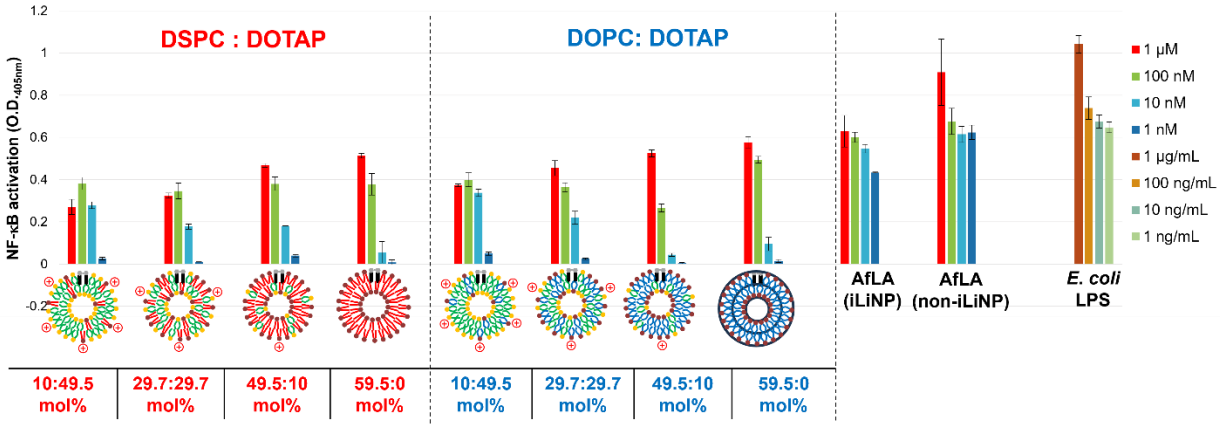

Figure 3.6: Evaluation of NF-κB (HEK-Blue™ hTLR4) activation by LNPs containing DOTAP **17** and AfLA **4**

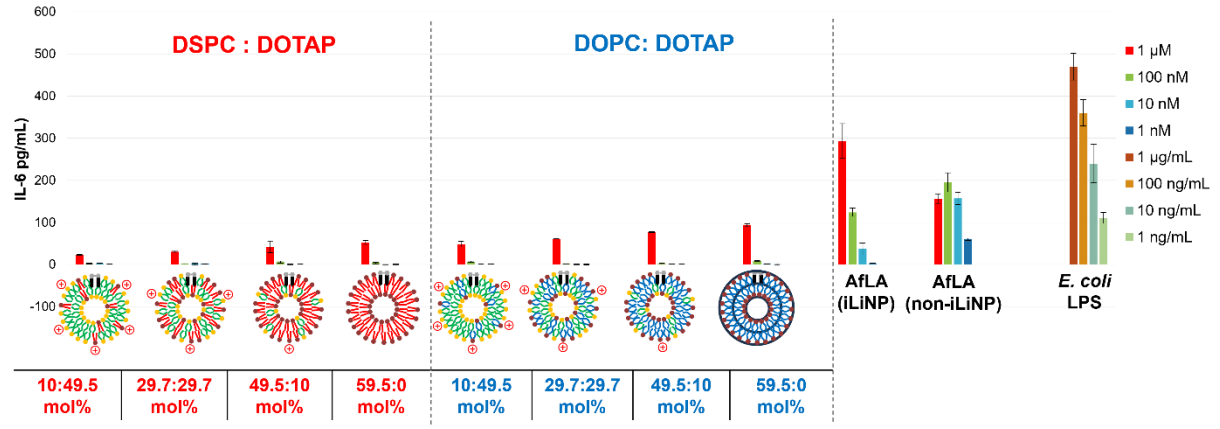

Figure 3.7: Evaluation of IL-6 (THP-1) inducing ability by LNPs containing DOTAP **17** and AfLA **4**

From figure 3.6 above, when HEK-Blue™ hTLR4 cells were treated with LNPs samples containing AfLA **4**, innate immunity activation was observed for all samples, but the level of immune activity was weaker than non-iLiNP AfLA **4**. LNPs containing AfLA **4** without other lipids components were also prepared, and showed weaker activity compared to non-iLiNP AfLA **4**. Furthermore, the activity of LNPs containing AfLA **4** was attenuated as DOTAP concentration increased. Additionally, LNPs containing DOPC **14** showed a slightly stronger level of NF-κB activation compared to LNPs containing DSPC **13**.

Next, the ability of LNPs samples to induce IL-6 cytokine was evaluated in phorbol 12-myristate 13-acetate (PMA)-differentiated THP-1 cells using enzyme-linked immunosorbent assay (ELISA). From figure 3.7, all LNPs samples were able to induce IL-6, although the levels of induced IL-6 cytokine were weaker than non-iLiNP AfLA **4** and *E. coli* LPS. Similar to the result of NF-κB activation, LNPs containing DOPC **14** showed stronger level of IL-6 induction compared to LNPs containing DSPC **13**.

As previously explained, the adjuvant 3D-MPL **3** developed by GSK selectively activates TRIF-dependent pathway and shows weaker stimulation of MyD88-dependent pro-inflammatory cytokine IL-6 [98]. Here, the possibility of selective activation of TLR4 signaling by the developed LNPs material was evaluated by comparing LNPs ability to induce MyD88-dependent IL-6 and TRIF-dependent MCP-1.

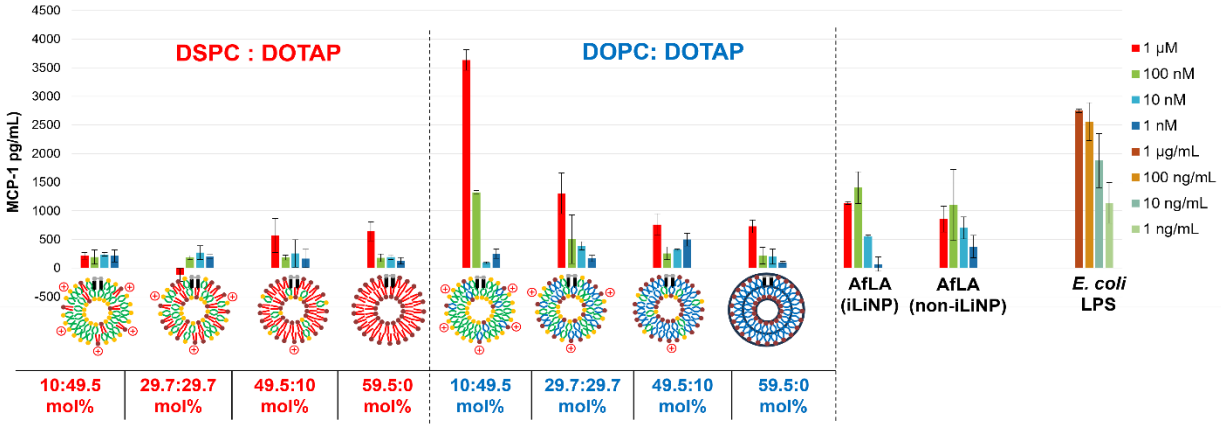

Figure 3.8: Evaluation of MCP-1 (THP-1) inducing ability by LNPs containing DOTAP **17** and AfLA **4**

Figure 3.8 shows that LNPs containing DOPC **14** and DOTAP **17** at 10:49.5 mol% and 29.7:29.7 mol% induced stronger MCP-1 activation compared to the other LNPs samples. Notably, there was a distinct difference in the immune profile of various LNPs regarding MyD88-dependent IL-6 activation (figure 3.7) and TRIF-dependent MCP-1 activation (figure 3.8). Specifically, while LNPs containing DOPC **14**/DOTAP **17** showed reduced IL-6 activation compared to non-iLiNP AfLA **4**, they demonstrated a TRIF-biased selectivity in TLR4 signaling.

Item 3: Investigation on enhancing AfLA **4** immune activity in lipid nanoparticles using amphipathic compounds

From the result of in vitro experiments, all LNPs samples showed weaker immune activity compared to non-iLiNP AfLA **4**. To enhance the activity of AfLA **4** in LNPs, amphipathic compounds were introduced to LNPs. From the previous report, it was known that cardiolipin (CL) could boost the immune activity of lipid A [55]. Similarly, the findings from the previous chapter

showed that unsaturated fatty acids could also enhance lipid A immune function. Therefore, CL (C18:1) **18**, CL (C18:2) **2**, linoleic acid (C18:2) **10** and linolenic acid (C18:3) **11** were added to LNPs containing DOPC **14** and DOTAP **17** (figure 3.9). Innate immune activity was then evaluated by SEAP reporter assay using HEK-Blue™ hTLR4 cells.

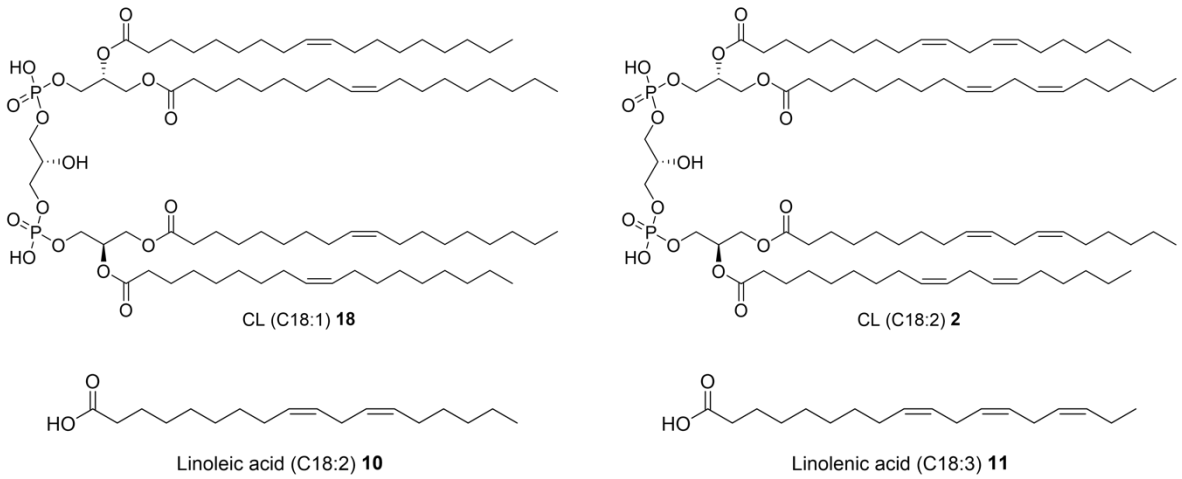

Figure 3.9: Structure of amphipathic compounds introduced to LNPs

From figure 3.10, the introduction of unsaturated linoleic acid (C18:2) **10** and linolenic acid (C18:3) **11** did not enhance the level of NF-κB activation by LNPs containing AfLA **4**. On the other hand, the addition of either CL (C18:1) **18** or CL (C18:2) **2** led to an increase in LNPs AfLA **4** innate immune activity, but the level of activity was still weaker than non-iLiNP AfLA **4**. Based on these results, the enhancement effect of cardiolipin was further investigated.

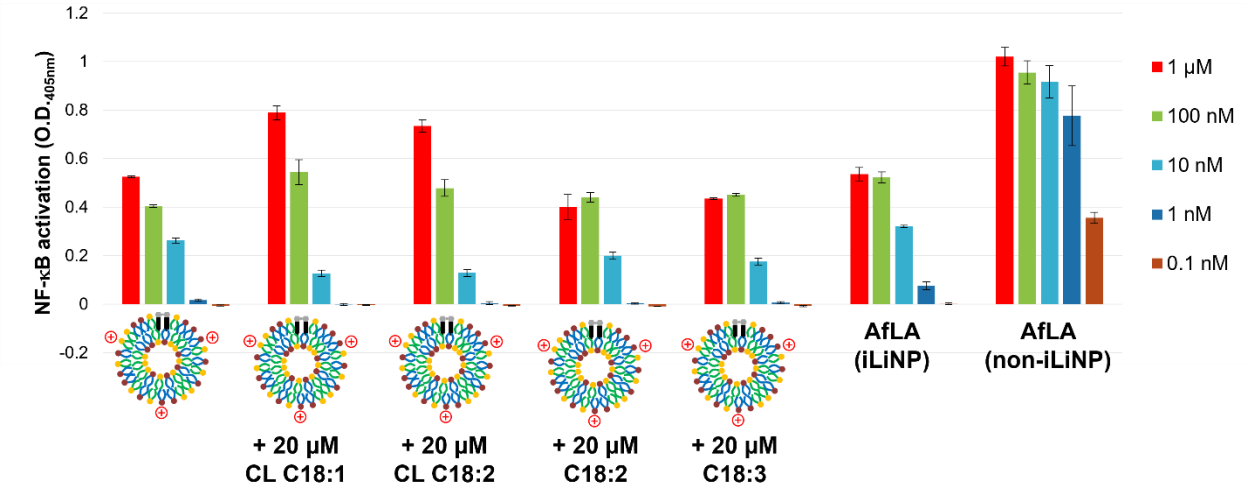

Figure 3.10: Evaluation of NF-κB (HEK-Blue™ hTLR4) activation by LNPs after addition of amphipathic compounds

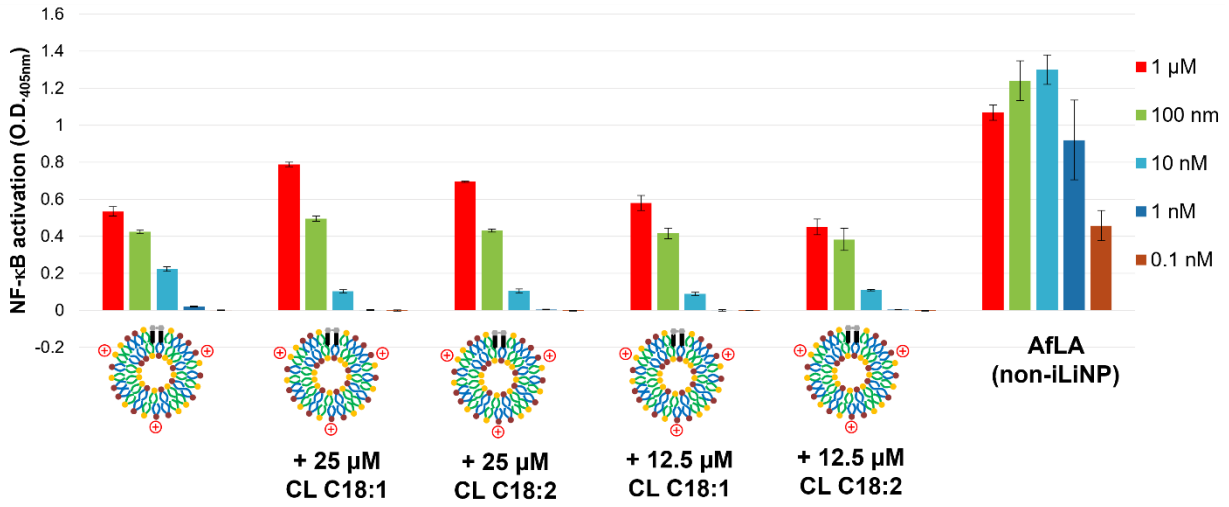

Figure 3.11: Evaluation of NF-κB (HEK-Blue™ hTLR4) activation by LNPs after addition of cardiolipin

From figure 3.11, it could be observed that when the concentration of either CL (C18:1) **18** or CL (C18:2) **2** was increased from 12.5 µM to 25 µM, the level of NF-κB activation of LNPs containing AfLA **4** was increased. However, due to cardiolipin solubility in this solvent system, it was difficult to incorporate a higher concentration of cardiolipin. Therefore, the enhancement effect of cardiolipin was not examined further.

Item 4: in vitro evaluation of lipid nanoparticles samples containing DOTAP **17** and AfLA **4** using mice cell lines

Before performing in vivo experiments, the innate immunity activity of LNPs samples was also evaluated using mice cell lines HEK-Blue™ mTLR4 and RAW264.7. HEK-Blue™ mTLR4 stably expressed TLR4/MD-2 receptor complex and was used to evaluate the level of NF-κB activation.

Figure 3.12 below shows that the level of NF-κB activation by non-iLiNP **4** was saturated when using HEK-Blue™ mTLR4. On the other hand, although innate immune activity was confirmed for all LNPs samples, there were no observable differences compared to the human system. Next, the ability of LNPs sample to induce IL-6 cytokine was evaluated using mice macrophage RAW 264.7 by enzyme-linked immunosorbent assay (ELISA), as shown in figure 3.13.

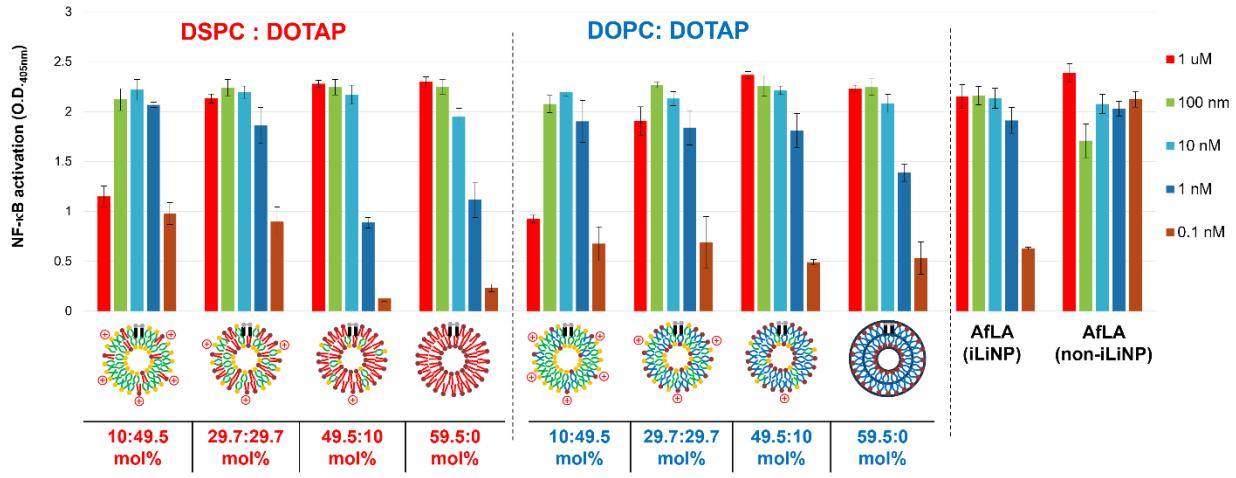

Figure 3.12: Evaluation NF-κB (HEK-Blue^{TM} mTLR4) activation by LNPs containing DOTAP **17** and AfLA **4**

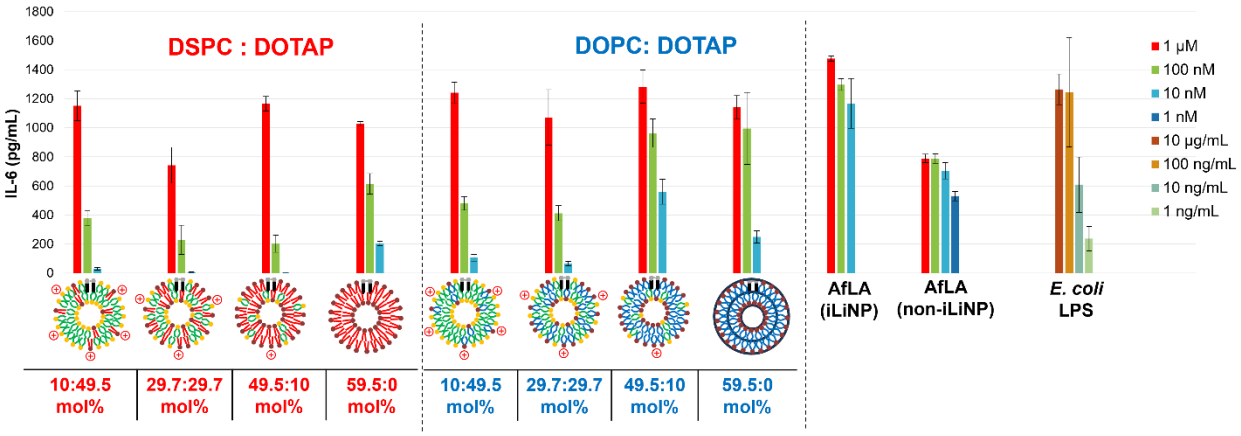

Figure 3.13: Evaluation of IL-6 (RAW264.7) inducing ability by LNPs containing DOTAP **17** and AfLA **4**

From figure 3.13, the ability to induce IL-6 was confirmed for all samples. LNPs containing DOPC **14** also showed slightly stronger immune activity compared to LNPs containing DSPC **13**, which was consistent with the tendency observed in experiments using human cell lines.

Item 5: in vivo evaluation of lipid nanoparticles samples containing DOTAP **17** and AfLA **4** using mice

As the purpose of this research was to evaluate the adjuvanticity of AfLA **4** in LNPs, in vivo murine experiments were performed. The adjuvant functions of all LNP samples were evaluated using BALB/c mice. Ovalbumin (OVA), a protein in chicken egg whites, was used as a model antigen. For immunization purposes, OVA was simply mixed with LNPs after LNPs synthesis.

First, to evaluate the systemic protection ability of LNPs containing AfLA **4**, mice were subcutaneously immunized with 1 μg of OVA alone, or 1 μg of OVA plus 1 μg of AfLA **4** in LNPs, or 1 μg of OVA plus 1 μg of non-iLiNP AfLA **4**. Mice were immunized twice on day 0 and day 7, and mice serum were collected on day 14. ELISA was then performed to measure the level of OVA-specific IgG antibody production.

To evaluate the effect of DOTAP **17** on the adjuvanticity of AfLA **4**, LNPs containing different ratios of DOPC **14** and DOTAP **17** were selected for immunization: 10:49.5 mol%, 29.7:29.7 mol% and 59.5:0 mol%.

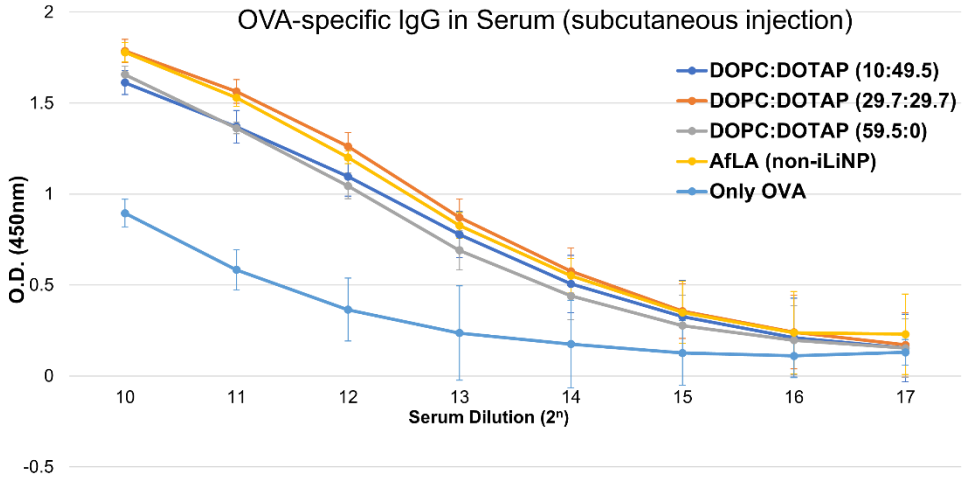

Figure 3.14: Enhancement of OVA-specific IgG antibodies by LNPs samples in vivo: mice (all samples n=6) were subcutaneously immunized on day 0 and day 7 with 1 μg of OVA alone, or 1 μg of OVA plus 1 μg of AfLA **4** in LNPs, or 1 μg of OVA plus 1 μg of non-iLiNP AfLA **4**. On day 14, mice serum was collected for evaluation of IgG antibodies by ELISA

From figure 3.14, mice immunized with either LNPs containing AfLA **4** or non-iLiNP AfLA **4** showed a higher level of OVA-specific serum IgG production compared to mice immunized with only OVA. Furthermore, all LNPs samples containing AfLA **4** showed similar level of IgG production to non-iLiNP AfLA **4**. The immune activity of AfLA **4** in LNPs was attenuated in vitro (figure 3.6 and 3.7) but was successfully recovered in vivo.

Additionally, from the results of in vitro experiments, samples with low DOTAP **17** concentration showed higher level of NF-κB ability and higher IL-6 inducing ability compared to samples containing higher DOTAP **17** concentrations (figure 3.6 and 3.7). However, in vivo results showed that in the case of subcutaneous immunization using BALB/c mice, changing the DOTAP **17** concentration had no significant effect on the ability of AfLA **4** in LNPs to induce OVA-specific IgG.

Next, to evaluate the ability of LNPs containing AfLA **4** for the development of mucosal vaccine adjuvant, BALB/c mice were intranasally immunized twice on day 0 and day 7. On day 21, mice serum, nasal wash and bronchoalveolar lavage fluid (BALF) were collected and ELISA was then performed to measure the level of OVA-specific IgA and IgG antibody production. For intranasal immunization, mice were immunized with 5 µg of OVA alone, or 5 µg of OVA plus 1 µg of AfLA **4** in LNPs, or 5 µg of OVA plus 1 µg of non-iLiNP AfLA **4**.

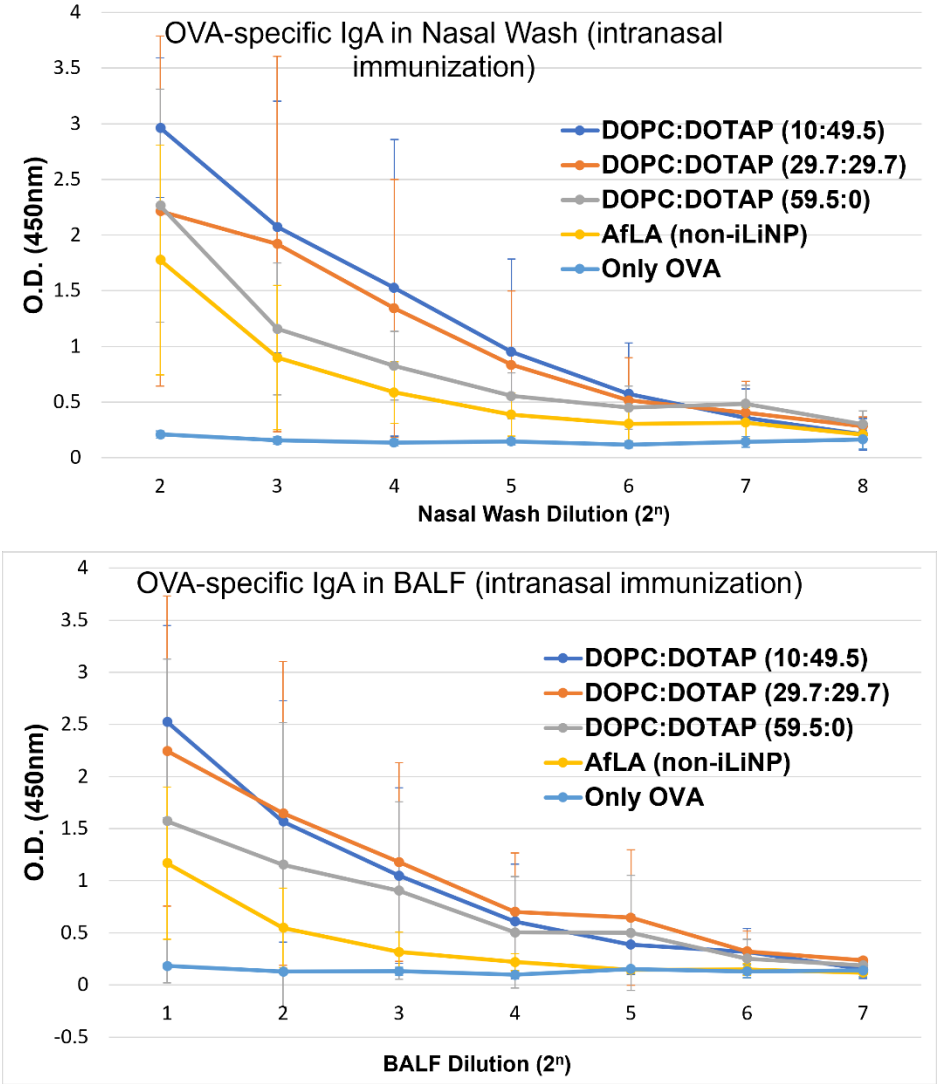

Figure 3.15: Enhancement of OVA-specific IgA antibodies by LNPs samples in nasal wash (Top) and BALF (bottom): mice (all samples n=4) were intranasally immunized on day 0 and day 7 with 5 µg of OVA alone, or 5 µg of OVA plus 1 µg of AfLA **4** in LNPs, or 5 µg of OVA plus 1 µg of non-iLiNP AfLA **4**. On day 21, nasal wash and BALF were collected for evaluation of IgA antibodies by ELISA.

As shown in figure 3.15, mice immunized with either LNPs containing AfLA **4** or non-iLiNP AfLA **4** produced more OVA-specific IgA in both upper respiratory tract (nasal wash), and lower

respiratory tract (BALF) compared to mice immunized with OVA alone. More interestingly, all LNPs samples showed stronger adjuvanticity compared to non-iLiNP AfLA **4**. Even though the innate immune activity of AfLA **4** in LNPs was attenuated in vitro (figure 3.6 and 3.7), in vivo results showed a successful robust enhancement effect of IgA production compared to non-iLiNP AfLA **4**. Additionally, LNPs containing DOPC **14** and DOTAP **17** at 10:49.5 mol% showed the strongest mucosal adjuvant function. Next, the ability of LNPs containing AfLA **4** to induce systemic antibody production via intranasal immunization were also evaluated.

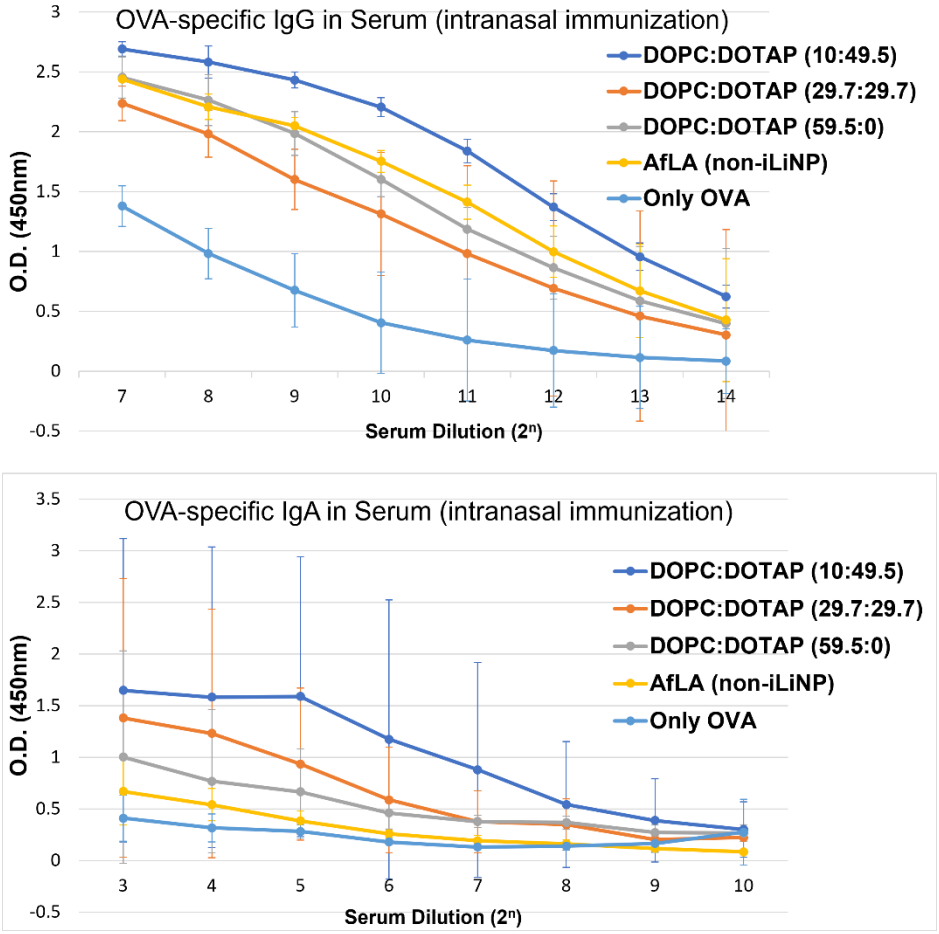

Figure 3.16: Enhancement of OVA-specific antibodies by LNPs samples in serum: IgG (Top) and IgA (bottom): mice (all samples n=4) were intranasally immunized on day 0 and day 7 with 5 μg of OVA alone, or 5 μg of OVA plus 1 μg of AfLA **4** in LNPs, or 5 μg of OVA plus 1 μg of non-iLiNP AfLA **4**. On day 21, mice serum was collected for evaluation of IgA and IgG antibodies by ELISA.

From figure 3.16, the results of serum antibodies production were similar to antibodies production in nasal wash and BALF. LNPs containing DOPC **14** and DOTAP **17** at ratio 10:49.5 mol% showed the strongest production of both IgA and IgG antibodies, even stronger than non-

iLINP AfLA **4**. These results demonstrated that LNPs containing AfLA **4** could be promising candidates for mucosal vaccine adjuvants, capable of inducing both systemic and mucosal immune protection.

Section 4: Development of lipid nanoparticles containing *Alcaligenes faecalis* lipid A by modification of surface charge

Item 1: Preparation of lipid nanoparticles containing different surface charges

In the previous section, the cationic lipid DOTAP **17** was used for the synthesis of LNPs. The advantages of DOTAP **17** are its ability to anchor AfLA **4** into LNPs lipids compartments by electrostatic interaction with the negative charge of AfLA **4**, and to promote adsorption of LNPs to the negatively charged cell membrane. This could ensure that both AfLA **4** and antigen reached the same antigen-presenting cells, leading to efficient T cell activation [117]. On the other hand, it was reported that cationic LNPs were unstable in storage and showed high level of cytotoxicity in vitro and in vivo [119][120].

In this section, LNPs containing either anionic DOPG **19** or ss-OP **20** were also prepared (figure 3.17). Anionic LNPs were reported to demonstrate greater stability in blood and lower cytotoxicity compared to cationic LNPs [121]. On the other hand, ss-OP **20** is a pH-responsive and reducing condition-responsive lipid [142]. As ss-OP possesses a tertiary amine head group instead of a quaternary amine, it has no charge under neutral conditions in the blood. When ss-OP **20** was taken up into the cells by endocytosis and transported to the endosomes, it became cationic due to the weakly acidic conditions within the endosome. Additionally, ss-OP **20** should also respond to the reducing conditions in the cells by cleaving the disulfide bond of its head group to generate a thiol. This thiol could attack the ester of the linker connecting the acyl chain with the head group, promoting the decomposition of the LNPs and releasing the vaccine material.

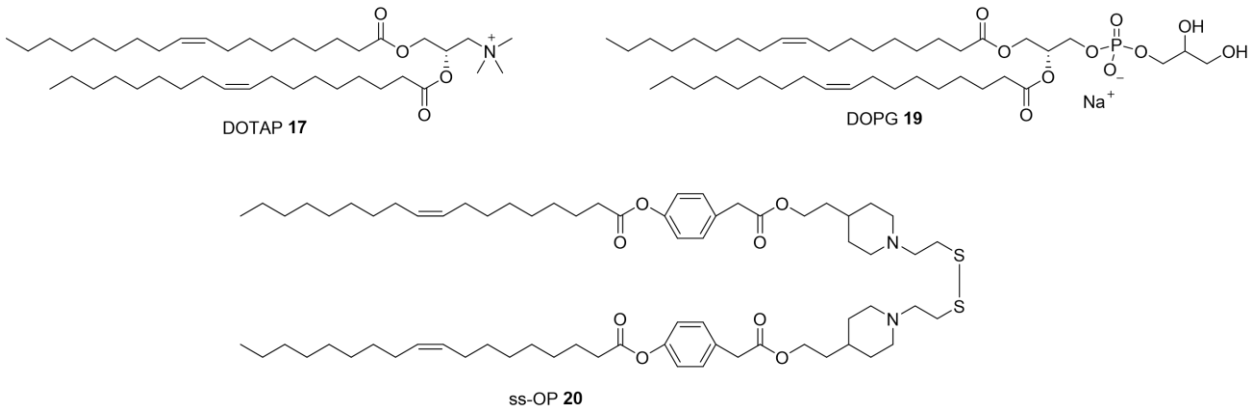

Figure 3.17: Structure of DOTAP **17**, DOPG **19** and ss-OP **20**

Similar to the LNPs prepared in the previous section, the concentrations of cholesterol **15** (38 mol%), DMG-PEG 2000 **16** (1.5 mol%) and AfLA **4** (1 mol%) were kept constants for all samples. To evaluate the effects of surface charge, DOPC **14** were used for all samples and kept constant at 10 mol%. DOTAP **17** or DOPG **19** or ss-OP **20** were used at 49.5 mol%. Table 3.3 below shows the physical properties of the LNPs synthesized by iLiNP.

Table 3.3: Properties of LNPs with different surface charges

AfLA = 1 mol% Cholesterol = 38 mol% DMG-PEG = 1.5 mol%	**DSPC:DOTAP 10:49.5 mol%**	**DOPC:DOTAP 29.7:29.7 mol%**	**DOPC:DOPG 49.5:10 mol%**	**DOPC:ss-OP 59.5:0 mol%**
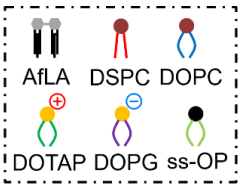	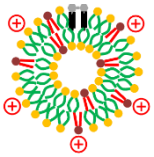	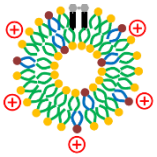	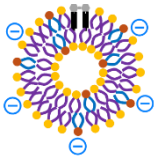	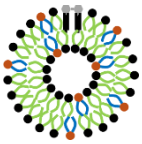
DLS	**Peak:** 42.5 ± 3.35 nm **PI**: 0.346 ± 0.0521 **Zeta**: +29.1 ± 3.57 mV	**Peak:** 44.8 ± 3.46 nm **PI:** 0.378 ± 0.0415 **Zeta:** +27.5 ± 2.55 mV	**Peak:** 25.9 ± 1.77 nm **PI:** 0.314 ± 0.0241 **Zeta:** -30.5 ± 1.04 mV	**Peak:** 43.9 ± 3.59 nm **PI:** 0.282 ± 0.0291 **Zeta:** -17.4 ± 3.24 mV

From table 3.3 above, all LNPs had size <100 nm, which should be optimal for the purpose of drug delivery as it prolongs circulation time and prevents clearance [116][111]. The PI values were also relatively low, and the zeta potential reflected the surface charges of the lipid compositions. The in vitro and in vivo experiments were then performed using these samples.

Item 2: in vitro evaluation of lipid nanoparticles samples with different surface charges

The innate immune function of all LNPs samples containing AfLA **4** were evaluated using HEK-Blue™ hTLR4 and THP-1 cell lines. First, the level of NF-κB activation was evaluated by the SEAP reporter assay using HEK-Blue™ hTLR4 cells. As shown in figure 3.18 below, LNPs that contained anionic DOPG **19** and pH-responsive ss-OP **20** showed stronger innate immune activity compared to LNPs containing DOTAP **17**. However, all LNPs containing AfLA **4** still showed a weaker immune function compared to non-iLiNP AfLA **4**.

The ability of LNPs samples to induce IL-6 (MyD88-dependent) and MCP-1 (TRIF-dependent) were also evaluated using PMA-differentiated THP-1 cells by ELISA. Figure 3.19 below shows that LNPs containing DOPG **19** and ss-OP **20** showed higher level of IL-6 induction compared to DOTAP **17** LNPs. This result was in accordance with the result of NF-κB activation. However, *E. coli* LPS still induced the highest level of IL-6 induction.

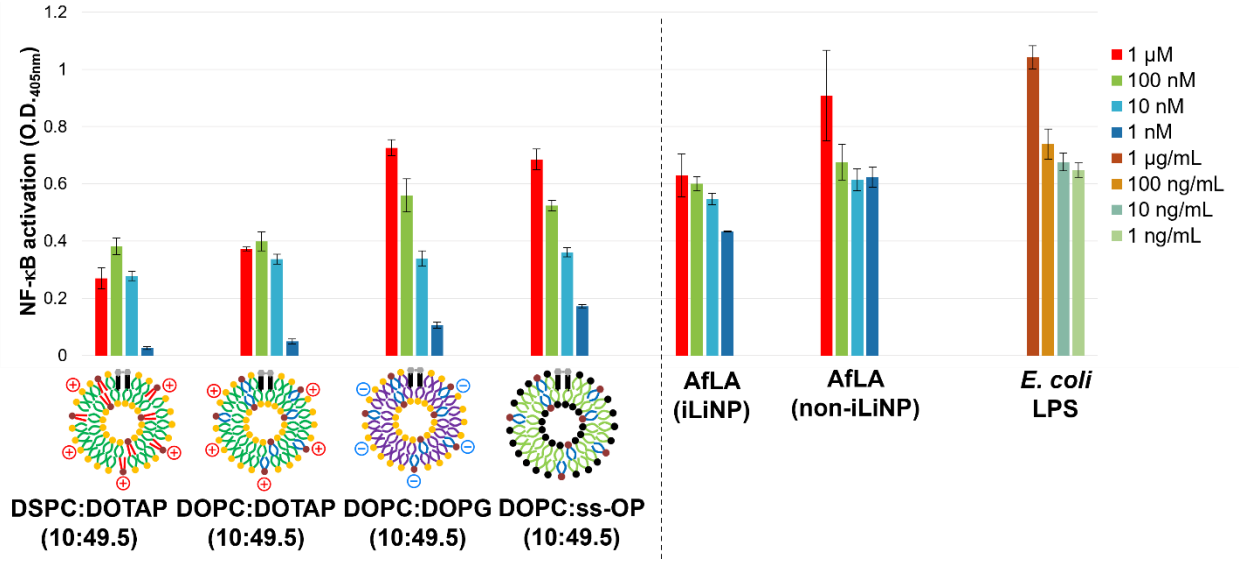

Figure 3.18: Evaluation of NF-κB (HEK-Blue™ hTLR4) activation by LNPs with different surface charges

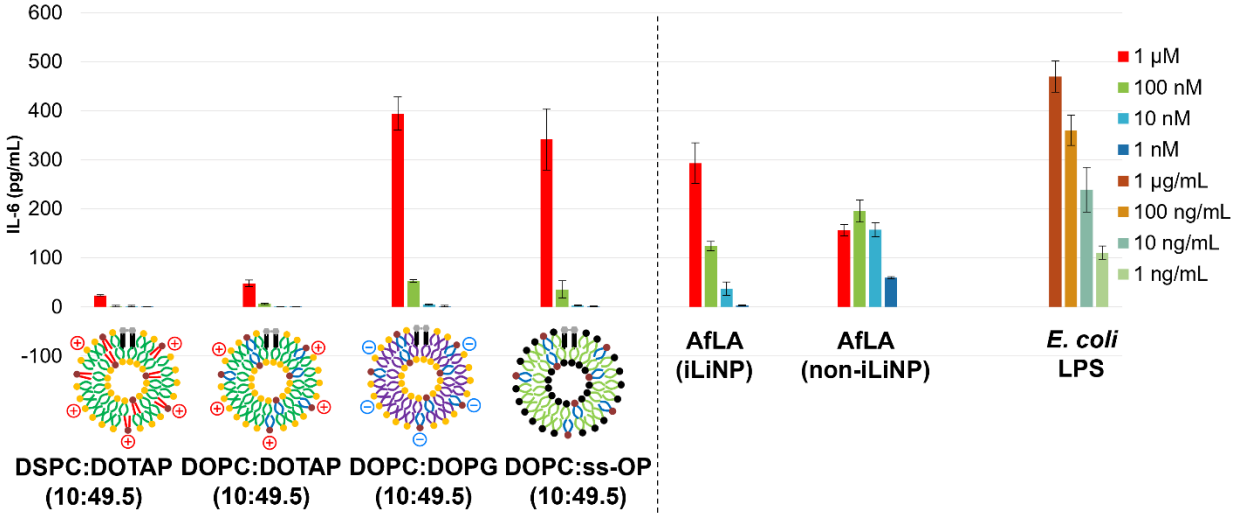

Figure 3.19: Evaluation of IL-6 (THP-1) inducing ability by LNPs with different surface charges

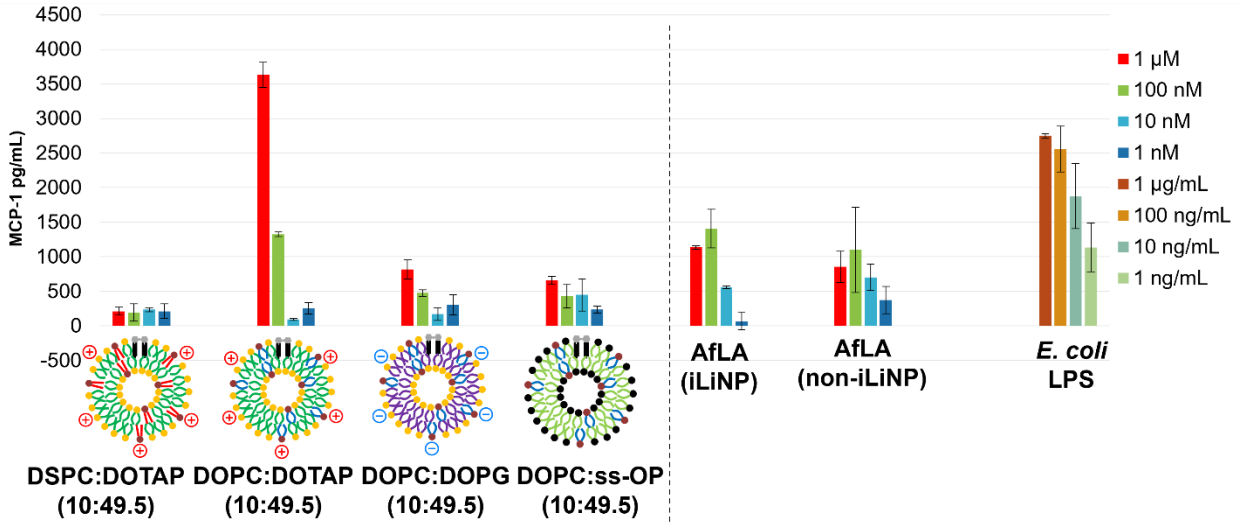

Figure 3.20: Evaluation of MCP-1 (THP-1) inducing ability by LNPs with different surface charges

Interestingly, figure 3.20 above shows that LNPs containing DOPC **14** and DOTAP **17** at 10:49.5 mol% had the strongest MCP-1 induction ability compared to the other LNPs samples and compared to non-iLiNP AfLA **4**. This was completey different from the result of IL-6 induction and NF-κB activation (figure 3.18 and 3.19), where DOPC **14**/ DOTAP **17** LNPs showed weaker immune activity compared to LNPs containing DOPG **19** or ss-OP **20.**

From the IL-6 and MCP-1 result, LNPs containing DOPC **14**/DOTAP **17** exhibited a TRIF-biased selectivity in TLR4 signaling. It is known that MyD88-dependent signaling is associated with TLR4 activation at the cell surface, whereas TRIF-dependent signaling occurs after TLR4 is internalized into endosomes. The results of IL-6 and MCP-1 suggested the possibility that TLR4 signaling could be influenced by the surface charges of LNPs.

Item 3: in vivo evaluation of lipid nanoparticles samples with different surface charges using mice

To evaluate the adjuvanticity of LNPS containing AfLA **4**, in vivo experiments were performed using BALB/c mice and OVA was used as the antigen. For immunization purposes, OVA was mixed with LNPs after the preparation of LNPs.

To evaluate the systemic immune response of LNPs with different surface charges, mice were subcutaneously immunized with 1μg of OVA alone, or 1 μg of OVA plus 1 μg of AfLA **4** in LNPs, or 1 μg of OVA plus 1 μg of non-iLiNP AfLA **4**. Mice were immunized twice on day 0 and day 7,

and mice serum was collected on day 14. ELISA was then performed to measure the level of OVA-specific IgG antibody production.

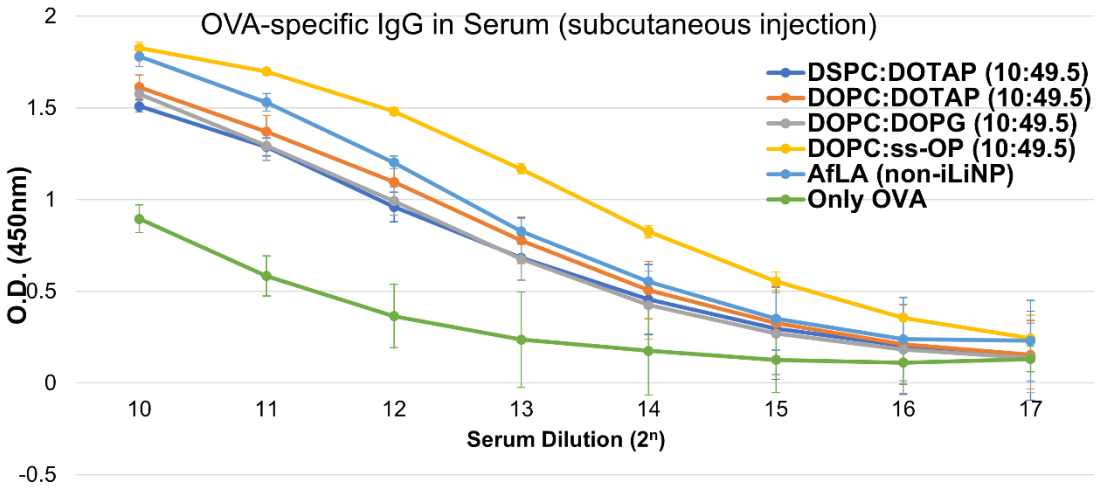

Figure 3.21: Enhancement of OVA-specific IgG antibodies by LNPs samples in vivo: mice (all samples n=6) were subcutaneously immunized on day 0 and day 7 with 1 μg of OVA alone, or 1 μg of OVA plus 1 μg of AfLA **4** in LNPs, or 1 μg of OVA plus 1 μg of non-iLiNP AfLA **4**. On day 14, mice serum was collected for evaluation of IgG antibodies by ELISA.

As shown in figure 3.21, mice immunized with either LNPs containing AfLA **4** or non-iLiNP AfLA **4** showed a higher level of OVA-specific serum IgG production compared to mice immunized with only OVA. Interestingly, LNPs sample containing DOPC **14** and ss-OP **20** at 10:49.5mol% showed slightly stronger IgG production compared to non- AfLA **4**. Even though the innate immune activity of AfLA **4** in LNPs was attenuated in vitro (figure 3.18), its immune function was recovered in vivo and LNPs successfully induced OVA-specific serum IgG production at a comparable level to non-iLiNP AfLA **4**. Additionally, no significant differences were observed between cationic and anionic LNPs in their ability to induce serum IgG production.

The effects of lipid compositions on IgG subclass induction were also evaluated. Cationic LNPs were reported to increase the stimulation of Th1-type response and enhance the production of IgG2a and IgG3 subclass [143]. On the other hand, anionic LNPs were reported to remain in circulation longer, leading to sustained antigen presentation and enhance antibody-mediated response. Thus, anionic LNPs could stimulate a Th2-biased response and enhance IgG1 subclass production.

To evaluate IgG subclass induction, the productions of OVA-specific IgG1, IgG2a, IgG2b and IgG3 were measured using LNPs containing DOTAP **17**, DOPG **19** or ss-OP **20**.

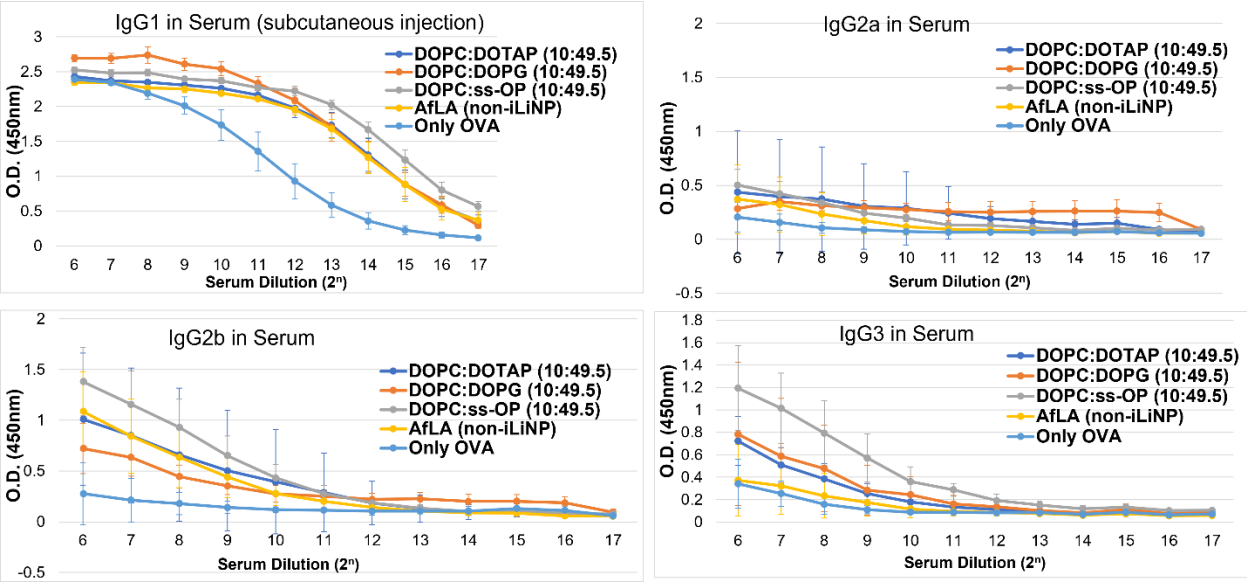

Figure 3.22: Enhancement of OVA-specific IgG antibodies subclass by LNPs samples in vivo: mice (all samples n=6) were subcutaneously immunized on day 0 and day 7 with 1 μg of OVA alone, or 1 μg of OVA plus 1 μg of AfLA **4** in LNPs, or 1 μg of OVA plus 1 μg of non-iLiNP AfLA **4**. On day 14, mice serum was collected for evaluation of IgG antibodies subclass by ELISA. Top: IgG1 (Left), IgG2a (Right); Bottom: IgG2b (Left), IgG3 (Right).

From figure 3.22, it could be observed that LNPs containing ss-OP **20** induced the highest level of IgG2b and IgG3 titer (Th1-type) than non-iLiNP AfLA **4** and other LNPs samples. However, the major subclass induced by ss-OP **20** LNPs were still IgG1, which is Th2-biased. Additionally, all LNPs samples showed stronger IgG3 production compared to non-iLiNP AfLA **4**.

The dominant production of IgG1 (Th2-biased) suggested that LNPs containing ss-OP **20** were stable in circulation, enabling sustained antigen presentation and enhancing antibody-mediated response. On the other hand, one possible hypothesis for the high IgG2b and IgG3 titer (Th1-type) was that the inclusion of ss-OP **20** may promote endocytosis by APCs, facilitating better cross-presentation of antigen via MHC-I pathway.

The mucosal adjuvant functions of LNPs were also evaluated. BALB/c mice were intranasally immunized twice on day 0 and day 7. On day 21, mice serum, nasal wash and bronchoalveolar lavage fluid (BALF) were collected and ELISA was then performed to measure the level of OVA-specific IgA and IgG antibody production. For intranasal immunization, mice were immunized with 5 μg of OVA alone, or 5 μg of OVA plus 1 μg of AfLA **4** in LNPs, or 5 μg of OVA plus 1 μg of non-iLiNP AfLA **4**.

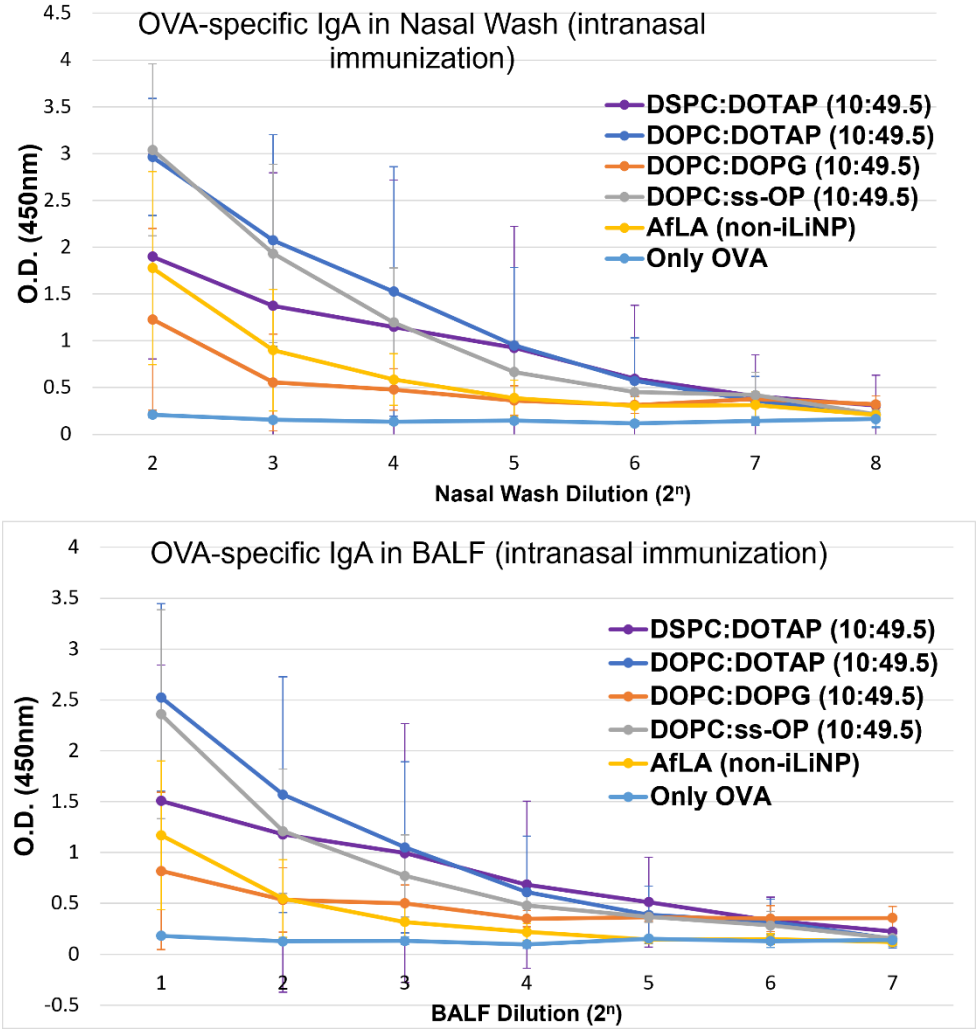

Figure 3.23: Enhancement of OVA-specific IgA antibodies by LNPs samples in nasal wash (Top) and BALF (bottom): mice (all samples n=4) were intranasally immunized on day 0 and day 7 with 5 μg of OVA alone; or 5 μg of OVA plus 1 μg of AfLA **4** in LNPs; or 5 μg of OVA plus 1 μg of non-iLiNP AfLA. On day 21, nasal wash and BALF were collected for evaluation of IgA antibodies by ELISA.

From figure 3.23, mice immunized with either LNPs or non-iLiNP AfLA **4** produced more OVA-specific IgA in both upper and lower respiratory tract. Interestingly, LNPs containing DOPC **14** and DOTAP **17** (10:49.5 mol%) and LNPs containing DOPC **14** and ss-OP **20** both showed stronger adjuvanticity compared to non-iLiNP AfLA **4**. This was also different from the result of serum IgG production from subcutaneous immunization, where only LNPs containing ss-OP **20** had a higher IgG titer compared to non-iLiNP AfLA **4** (figure 3.21). Next, the ability of LNPs

containing AfLA **4** to induce systemic antibody production via intranasal immunization was also evaluated.

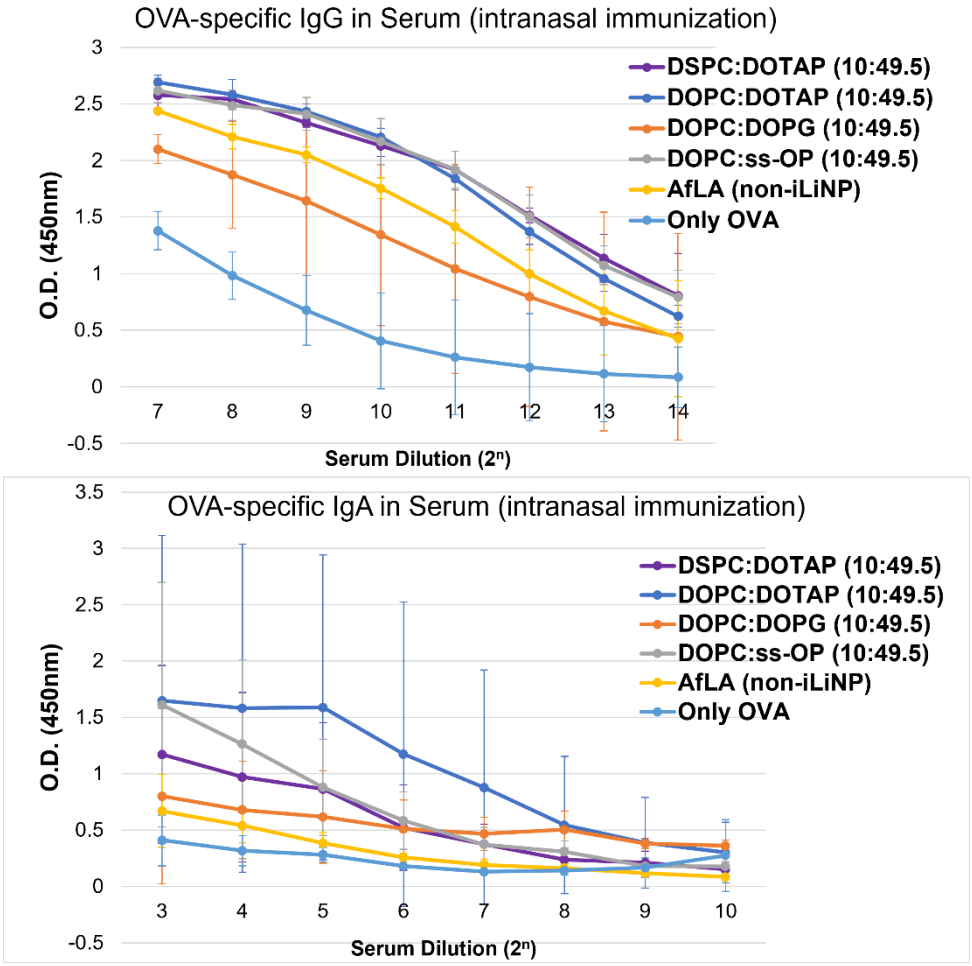

Figure 3.24: Enhancement of OVA-specific antibodies by LNPs samples in serum: IgG (Top) and IgA (bottom): mice (all samples n=4) were intranasally immunized on day 0 and day 7 with 5 μg of OVA alone; or 5 μg of OVA plus 1 μg of AfLA **4** in LNPs; or 5 μg of OVA plus 1 μg of non-iLiNP AfLA **4**. On day 21, nasal wash and BALF were collected for evaluation of IgA antibodies by ELISA.

From figure 3.24, LNPs containing DOTAP **17** or ss-OP **20** showed the strongest production of serum IgG antibodies and IgA antibodies, even stronger than non-iLiNP AfLA **4**. These results were consistent with the results of IgA antibodies production in the respiratory tract (nasal wash and BALF, figure 3.23). Taken everything into account, LNPs containing DOPC **14**/DOTAP **17** and DOPC **14**/ss-OP **20** at 10:49.5 mol% were two compositions that showed slightly stronger adjuvanticity than other formulations. They can be selected for further evaluation on their ability to act as effective mucosal vaccine adjuvants to induce both systemic and mucosal immune response.

Section 5: Evaluation of lipid nanoparticles stability in storage and after lyophilization

In addition to in vitro and in vivo evaluations of LNPs, the stability of LNPs over long-term storage and after lyophilization were also investigated for future research. First, quantitative analysis using LC/MS were performed at 1 day after synthesis and 1 month after synthesis where LNPs samples were stored at 4°C.

Table 3.4: Quantification of AfLA **4** in LNPs samples by LC/MS after 1 month in storage

AfLA = 1 mol% **Cholesterol = 38 mol%** **DMG-PEG = 1.5 mol%** **DSPC:DOTAP = x:y mol%**	**10:49.5 mol%**	**29.7:29.7 mol%**	**49.5:10 mol%**	**59.5:0 mol%**
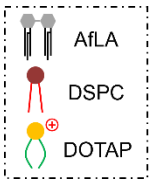	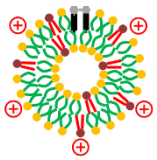	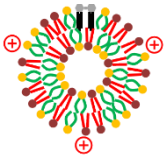	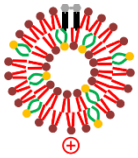	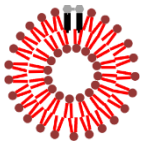
Lipid A retention % (1 day after synthesis)	**91.2%**	**82.0%**	**67.8%**	**67.5%**
Lipid A retention % (1 month after synthesis)	**87.5%**	**83.5%**	**65.8%**	**70.5%**
AfLA = 1 mol% **Cholesterol = 38 mol%** **DMG-PEG = 1.5 mol%** **DOPC:DOTAP = a:b mol%**	**10:49.5 mol%**	**29.7:29.7 mol%**	**49.5:10 mol%**	**59.5:0 mol%**
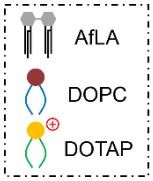	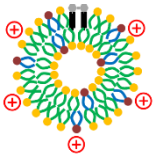	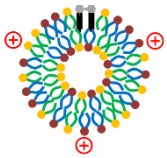	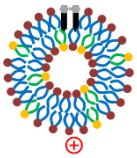	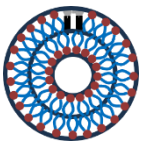
Lipid A retention % (1 day after synthesis)	**74.3%**	**78.6%**	**58.5%**	**60.3%**
Lipid A retention % (1 month after synthesis)	**72.4%**	**75.6%**	**62.5%**	**60.1%**

From table 3.4 above, it could be observed that after 1 month storage at 4°C, there were almost no changes in lipid A retention%. In the future, the retention of OVA in LNPs after 1 month storage will also be evaluated. Next, the changes in physical properties of LNPs after 1 month storage at 4°C were evaluated.

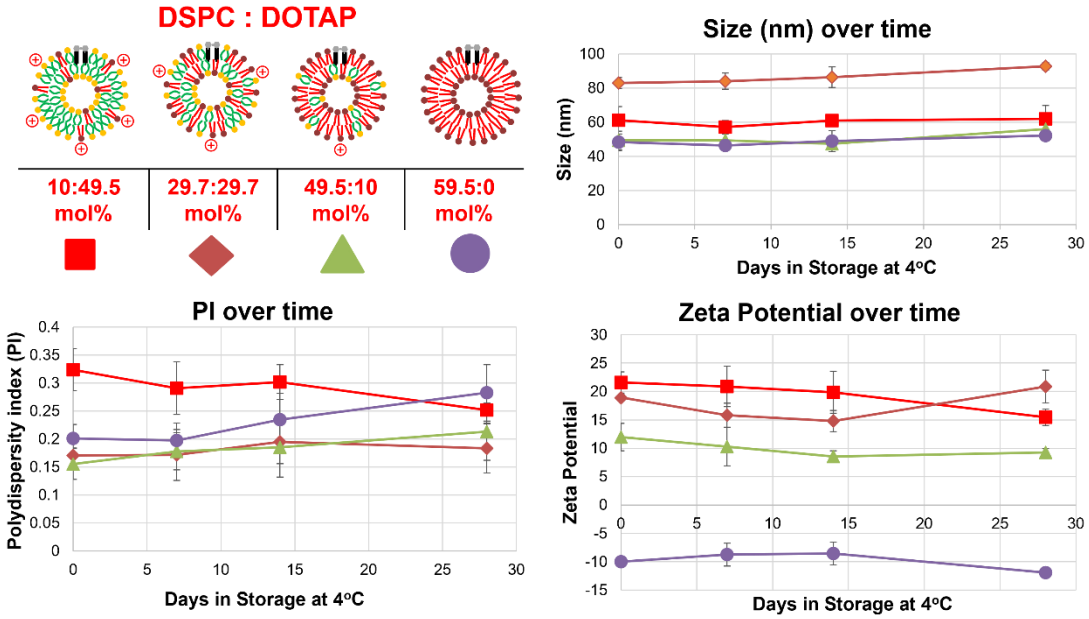

Figure 3.25: Physical properties of DSPC **13**/DOTAP **17** LNPs after 1 month in storage

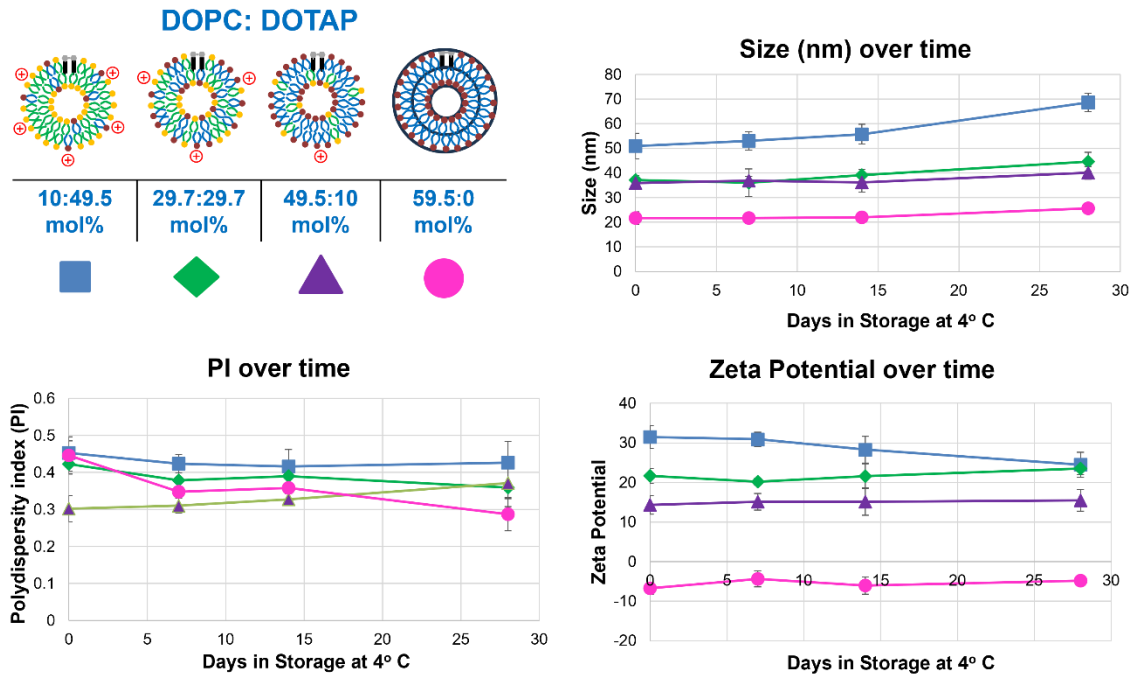

Figure 3.26: Physical properties of DOPC **14**/DOTAP **17** LNPs after 1 month in storage

Figure 3.25 showed the changes in physical properties of LNPs containing DSPC **13** and DOTAP **17** after 1 month in storage at 4°C. Although all LNPs showed a small increase in size, there were almost no significant changes in PI or Zeta potential over time. Similarly, LNPs containing DOPC **14** and DOTAP **17** also showed a small increase in size after 1 month in storage, but no significant changes in PI or zeta potential (figure 3.26). The levels of NF-κB activation of LNPs samples after 1 month storage were also evaluated as shown in figure 3.27 below.

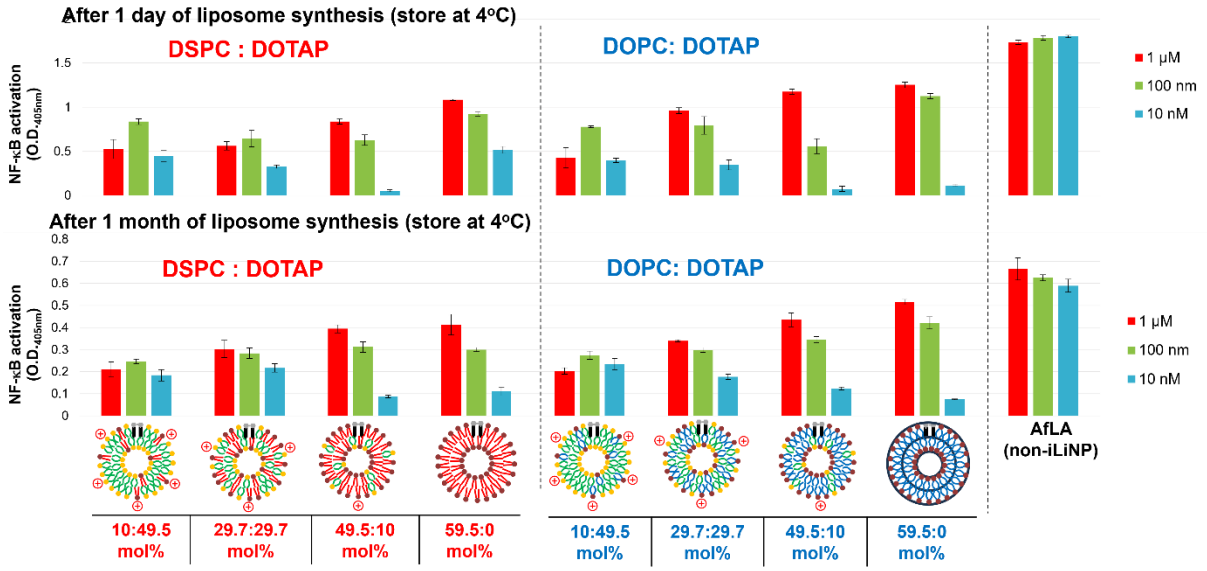

Figure 3.27: Evaluation of NF-κB (HEK-Blue™ hTLR4) activation by LNPs containing DOTAP **17**and AfLA **4** after 1 day (Top) and 1 month (Bottom) in storage at 4°C

From figure 3.27, it could be observed that there were no changes in innate immune activity of all LNPs samples after 1 month in storage at 4°C. This confirmed that the LNPs were stable up to 1 month in this condition.

In addition to evaluating the stability of LNPs in storage, the stability of LNPs after lyophilization was also investigated. Samples were desalted and washed with 5% sucrose before lyophilized. Samples were then reconstituted in PBS, and their physical properties were examined.

Table 3.5: Physical properties of DSPC **13**/DOTAP **17** LNPs before and after lyophilization (measured by DLS)

AfLA = 1 mol% Cholesterol = 38 mol% DMG-PEG = 1.5 mol% DOPC:DOTAP = a:b mol%		**10:49.5 mol%**	**29.7:29.7 mol%**	**49.5:10 mol%**	**59.5:0 mol%**
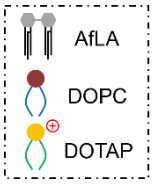		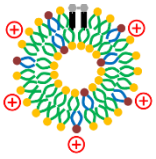	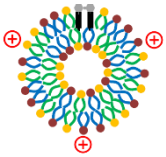	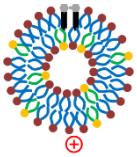	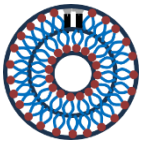
Size (nm)	**Before**	**45 nm**	**38 nm**	**39 nm**	**23 nm**
	After	**60 nm**	**56 nm**	**70 nm**	**38 nm**
Polydispersity index	**Before**	**0.41**	**0.37**	**0.42**	**0.29**
	After	**0.46**	**0.41**	**0.38**	**0.35**
Zeta potential (mV)	**Before**	**+18**	**+10**	**+3**	**-8**
	After	**+13**	**+6**	**+2**	**-11**

Table 3.6: Physical properties of DOPC **14**/DOTAP **17** LNP before and after lyophilization (measured by DLS)

AfLA = 1 mol% Cholesterol = 38 mol% DMG-PEG = 1.5 mol% DSPC:DOTAP = x:y mol%		**10:49.5 mol%**	**29.7:29.7 mol%**	**49.5:10 mol%**	**59.5:0 mol%**
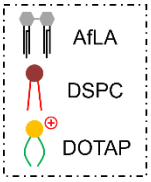		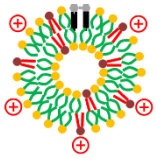		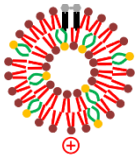	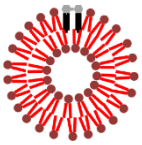
Size (nm)	**Before**	**55 nm**	**90 nm**	**85 nm**	**54 nm**
	After	**120 nm**	**110 nm**	**102 nm**	**60 nm**
Polydispersity index	**Before**	**0.45**	**0.28**	**0.31**	**0.29**
	After	**0.47**	**0.30**	**0.33**	**0.33**
Zeta potential (mV)	**Before**	**+20**	**+12**	**+3**	**-10**
	After	**+15**	**+9**	**+2**	**-13**

From table 3.5 and table 3.6, it was observed that after lyophilization, all LNPs samples showed an increase in size, possibly due to aggregation during the lyophilization process. However, there were almost no significant differences in PI and zeta potential. The innate immune activity of samples was also examined to see if the process of lyophilization could affect the immune function of AfLA **4** in LNPs (figure 3.28). Even though there was an increase in size for all samples after lyophilization, there were no significant effects on the innate immune activity of samples.

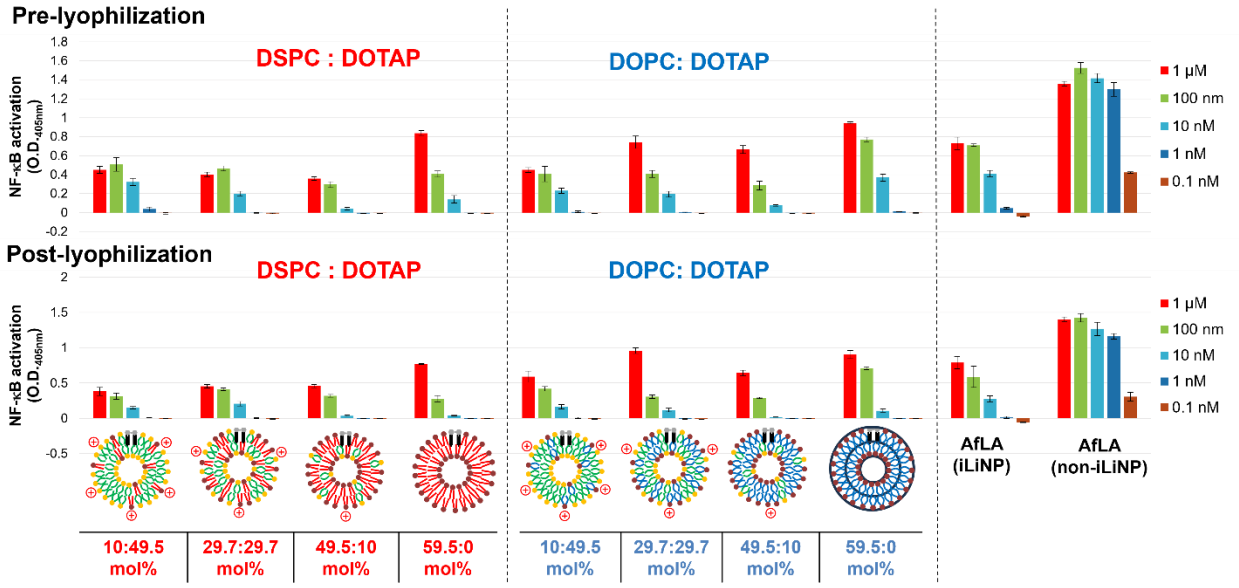

Figure 3.28: Evaluation of NF-κB (HEK-Blue^{TM} hTLR4) activation by LNPs containing DOTAP **17** and AfLA **4** before lyophilization (Top) and after lyophilization (Bottom)

Section 6: Discussion and conclusion

Alcaligenes faecalis (*A. faecalis*) lipid A (AfLA **4**) was previously synthesized by our laboratory and showed remarkable results as a mucosal vaccine adjuvant candidate. In intranasal immunization studies using mice, it showed a stronger enhancement effect on mucosal IgA production compared to both MPLA (an adjuvant derived from *Salmonella* bacterium) and cholera toxin (a well-known immunogen for mucosal IgA production) [104][105][106][107].

Inspired by the AS0 series developed by GSK which combined liposomes delivery system with the monophosphoryl lipid A 3D-MPL **3** and by mRNA LNPs vaccines that were popularized during the COVID-19 pandemic, this chapter focused on the development of LNPs containing AfLA **4** as vaccine adjuvant materials. Additionally, based on the results of previous chapter which showed that the introduction of amphipathic compounds can modulate the innate immune activity of lipid A, this chapter investigated how to synergistically enhance the immune function of AfLA **4** in

LNPs using different amphipathic compounds. Finally, this chapter evaluated the efficacy of LNP vaccines in mice.

First, the effects of changing the ratio between neutral lipid DSPC **13** or DOPC **14** and cationic lipid DOTAP **17** on the immune function of AfLA **4** in LNPs were evaluated. The results of in vitro experiments using human cell lines showed that all LNPs could elicit an immune response, but the levels of response were weaker than non-liposome AfLA **4** (figure 3.6 and 3.7). This could be explained by the physical encapsulation of AfLA **4** in the lipid compartments of LNPs as well as PEGylation using DMG-PEG **16**, which could hinder the accessibility of AfLA **4** by LBP and TLR4.

Based on figure 3.6, in vitro experiments showed that LNPs containing high DOTAP **17** concentrations showed a suppression in immune activity. This could be explained by the electrostatic interaction between positive charge of DOTAP **17** and negative charge of AfLA **4**, which could anchor AfLA **4** more tightly inside LNP lipid compartments and prevent interaction of AfLA **4** with LBP and TLR4. Additionally, LNPs containing DOPC **14** showed slightly stronger innate immune activity compared to LNPs containing DSPC **13** (figure 3.6). This result was similar to the findings of previous chapters, where the presence of unsaturated acyl chain decreased the stability of LNPs and allowed easier interaction of AfLA **4** with LBP and TLR4.

Figure 3.29 and 3.30 below shows the correlation between surface charge of LNPs (zeta potential) with LNPs innate immune activity. In both figures, as the concentration of DOTAP **17** increased, the value of zeta potential also increased. The positive charge of DOTAP **17** could electrostatically interact with AfLA **4** negative charge, and anchored AfLA **4** more tightly into the LNP, which led to a decrease in presentation of AfLA **4** to LBP and TLR4. Therefore, a decrease in LNP immune function was observed as DOTAP **17** concentration increased.

On the other hand, for LNPs containing DSPC **13** and DOTAP **17** (figure 3.29), there was no clear correlation between the size of LNP and the innate immune activity of AfLA **4** in LNPs. However, in the case of LNPs containing DOPC **14** and DOTAP **17** (figure 3.30), as the concentration of DOTAP **17** increased, the sizes of the LNPs formed also increased, and the activity of LNPs decreased.

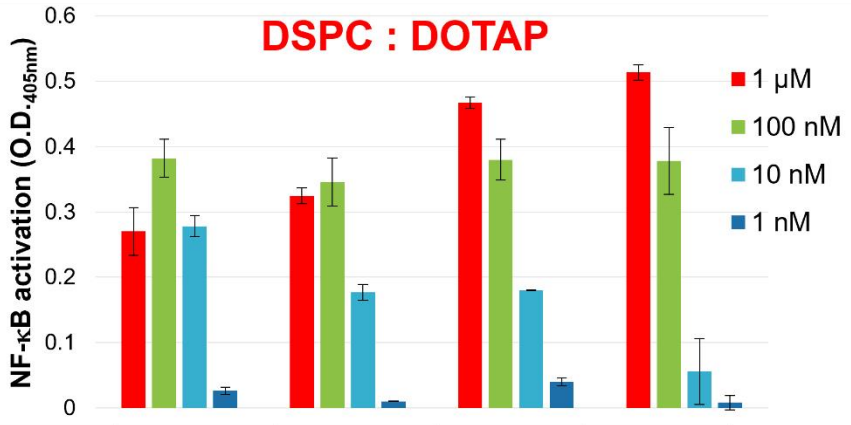

AfLA = 1 mol% Cholesterol = 38 mol% DMG-PEG = 1.5 mol% DSPC:DOTAP = x:y mol%	10:49.5 mol%	29.7:29.7 mol%	49.5:10 mol%	59.5:0 mol%
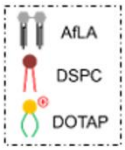				
Size (nm)	**48 nm**	**84 nm**	**64 nm**	**50 nm**
Polydispersity index	**0.34**	**0.34**	**0.20**	**0.32**
Zeta Potential (mV)	+27	+20	+7	-10

Figure 3.29: Correlation between LNPs size/ zeta potential and LNPs in vitro immune activity for LNPs containing DSPC **13**/ DOTAP **17**

One possible explanation why DSPC **13** and DOPC **14** LNPs behaved differently regarding size change with respect to change in DOTAP **17** concentration was due to the difference in their lipid phase behavior. At physiological temperature, DOPC **14** has a fluid, disordered structure that formed loosely packed bilayers while DSPC **13** has a gel-phase structure that formed tightly packed bilayers. When DOTAP **17** was introduced to the fluid DOPC **14** bilayer, electrostatic repulsion between DOTAP **17** molecules led to swelling of LNPs size. In contrast, the rigid structure of DSPC **13** bilayer may resist changes in swelling by electrostatic repulsion when DOTAP **17** was introduced [144].

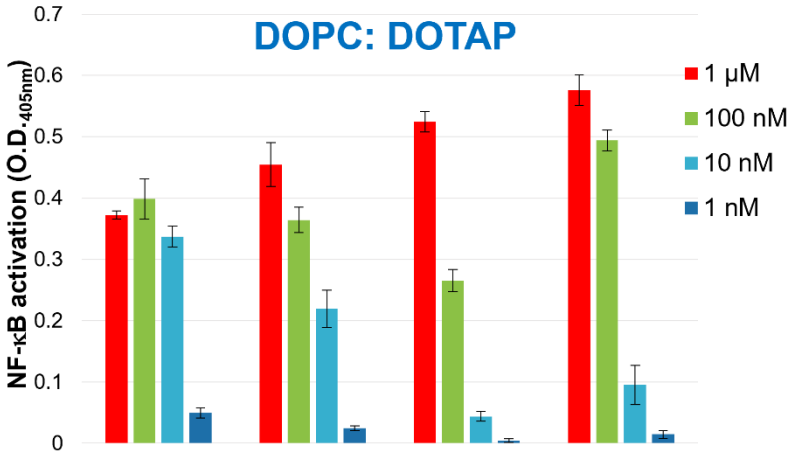

AfLA = 1 mol% Cholesterol = 38 mol% DMG-PEG = 1.5 mol% DOPC:DOTAP = a:b mol%	10:49.5 mol%	29.7:29.7 mol%	49.5:10 mol%	59.5:0 mol%
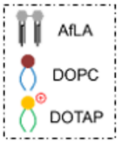				
Size (nm)	**45 nm**	**36 nm**	**34 nm**	**26 nm**
Polydispersity index	**0.41**	**0.33**	**0.36**	**0.25**
Zeta Potential (mV)	**+28**	**+19**	**+11**	**-5**

Figure 3.30: Correlation between LNPs size/ zeta potential and LNPs in vitro immune activity for LNPs containing DOPC **13**/ DOTAP **17**

Afterwards, the effects of changing the concentration of DOTAP **17** on the immune activity of LNPs containing AfLA **4** were evaluated in vivo using ovalbumin (OVA) as the model antigen. Specifically, LNPs containing three different ratios of DOPC **14** and DOTAP **17** were administered to mice subcutaneously or intranasally. After subcutaneous injection, all LNPs containing AfLA **4** showed similar level of serum OVA-specific IgG production compared to non-iLiNP AfLA **4** (figure 3.14). The immune activity of AfLA **4** in LNPs was attenuated in vitro but successfully recovered in vivo. There were a few factors that could explain the difference between in vitro and in vivo results. In the case of in vivo, LNPs could be taken up by antigen-presenting cells more efficiently due to mechanisms like opsonization and phagocytosis, which improved the delivery of LNPs AfLA **4** to immune cels [145]. Furthermore, by using LNPs as a delivery vehicle, AfLA **4** was protected from degradation by enzymes or clearance by the bloodstream. Additionally, the factor of controlled release should also be considered. The gradual release of AfLA **4** from LNPs

could lead to a sustained activation of immune cells over time, thus leading to a stronger immune response compared to in vitro activation [146].

After intranasal immunization, all LNPs containing DOPC **14** and DOTAP **17** showed an even stronger mucosal adjuvanticity compared to non-iLiNP AfLA **4**, eliciting higher IgA titers in both upper respiratory tract (nasal wash) and lower respiratory tract (BALF) (figure 3.15). To explain the differences in results between subcutaneous and intranasal immunizations, there could be a few reasons. Intranasal immunization directly targeted the mucosal-associated lymphoid tissue (MALT), where LNPs could adhere to the mucosal epithelium and readily taken up by dendritic cells and macrophages, facilitating antigen presentation [147]. Additionally, non-iLiNP AfLA **4** may be more susceptible to degradation by enzymes in the nasal cavity compared to the protection provided by the LNPs delivery vehicle. Finally, intranasal immunization allowed for efficient lymph node targeting. LNPs could deliver AfLA **4** to the draining cervical lymph nodes, which should enhance the level of mucosal and systemic immunity [148].

Next, the effects of surface charges on the immune function of AfLA **4** in LNPs were examined using cationic DOTAP **17**, anionic DOPG **19** and pH-responsive ss-OP **20**. The results of in vitro experiments showed that LNPs containing DOPG **19** or ss-OP **20** stimulated a higher level of NF-κB activation and higher IL-6 inducing ability compared to LNPs containing DOTAP **17** (figure 3.18 and 3.19). This may be explained by the electrostatic interaction between the positive charge of DOTAP **17** and negative charge of AfLA **4**, which could anchor AfLA **4** more tightly in the lipids compartments of LNPs. This could hinder the ability of AfLA **4** to interact with LBP and TLR4.

The possibility of selective activation of TLR4 signaling by LNPs with different compositions was evaluated by comparing MyD88-dependent IL-6 and TRIF-dependent MCP-1 (figure 3.19 and 3.20). LNPs containing DOPC **14** and DOTAP **17** at 10:49.5 mol% induced stronger MCP-1 activation compared to other LNP samples, but weaker IL-6 activation compared to LNP containing DOPG **19** or ss-OP **20**.

It is known that MyD88-dependent signaling is associated with TLR4 activation at the cell surface, whereas TRIF-dependent signaling occurs after TLR4 is internalized into endosomes. Cationic DOTAP **17** could promote enhanced endocytosis of LNPs, and once inside the cell, destabilization of LNPs could lead to better exposure of AfLA **4** to endosomal TLR4/MD-2 receptor complex. However, an enhancement of endocytosis might limit the time AfLA **4** spent interacting with surface TLR4, which reduced MyD88-dependent signaling. Based on these results, there is a possibility to control either MyD88-dependent or TRIF-dependent TLR4 pathway by modification of LNPs surface charges.

The effects of LNPs surface charges on the adjuvanticity of AfLA **4** in LNP were evaluated by both subcutaneous injection and intranasal immunization with OVA as the antigen. In the case of subcutaneous injection, LNPs containing ss-OP **20** showed the strongest level of serum OVA-

specific IgG production, even higher than non-liposome AfLA **4** (figure 3.21). The immune activity of AfLA **4** in LNPs, which was attenuated in vitro (figure 3.18), was recovered in vivo and led to an enhancement of antibodies production. One possible explanation was that non-iLiNP AfLA **4** was more prone to degradation by enzymes and clearance from the bloodstream.

The effects of lipids compositions on IgG subclass induction were also evaluated. LNPs containing ss-OP **20** induced the highest level of IgG2b and IgG3 titer (Th1-type) than non-iLiNP AfLA **4** (figure 3.22). It could be hypothesized that the structure of LNPs provide protection for AfLA **4** from degradation, which should ensure a prolonged exposure to immune cells and may lead to a robust class switching to IgG2b and IgG3 [149].

Finally, the results of intranasal immunization showed that LNPs containing DOPC **14**/DOTAP **17** and DOPC **14**/ss-OP **20** (10:49.5 mol%) both induced higher levels of OVA-specific IgA production compared to non-iLiNP AfLA **4** (figure 3.23). While future experiments are necessary to understand the mechanisms behind the efficacy of these vaccine formulations, one possible hypothesis was that intranasal immunization directly targeted the MALT so LNPs could adhere to the mucosal epithelium [147]. LNPs could then be readily taken up by DCs and macrophages, which should lead to an efficient antigen presentation to T cells.

In conclusion, while the results of in vitro experiments showed that all LNPs samples had lower innate immune activity compared to non-iLiNP AfLA **4**, in vitro results showed that many LNPs samples had higher adjuvanticity than non-iLiNP AfLA **4**. Specifically, LNPs containing DOPC **14**/DOTAP **17** and DOPC **14**/ss-OP **20** at 10:49.5 mol% were two compositions that showed slightly stronger adjuvanticity compared to other formulations. As the results of these experiments, these two are selected for further evaluation on their mucosal vaccine adjuvant functions.

Chapter 4: Summary and Future Outlook

Section 1: Summary

The host innate immune system can be activated by either pathogen-associated molecular patterns (PAMPs) derived from bacteria, viruses, fungi, etc. or by damage-associated molecular patterns (DAMPs) released from damage or dying cells [12][51]. Lipopolysaccharides (LPS) and their active center glycolipid lipid A (such as *E. coli* lipid A **1** or *A. faecalis* lipid A **4**) are representative PAMPs from Gram-negative bacteria and recognized by host's TLR4/MD-2 receptor [38][39].

In aqueous environment, lipid A tends to form aggregates due to its amphipathic nature. Our previous studies in collaboration with a German group had highlighted that the formation of aggregates containing lipid A **1** and cardiolipin (CL, C18:2) **2** could significantly affect lipid A **1** innate immune activity [55]. In this study, to evaluate the effects of aggregate compositions and state of mixed aggregates on lipid A **1**, simple amphipathic fatty acids **5-12** were used to modify lipid A **1** aggregate.

To prepare mixed aggregates of lipid A **1** and fatty acids **5-12**, two different sample preparation methods were employed: simple mixing method (SMM) or homogenous mixing method (HMM). SMM samples were expected to form a mixture of two distinct aggregates composed of single components: lipid A **1**-only aggregates and fatty acids-only aggregates, whereas HMM samples were expected to predominantly form mixed aggregates composed of both lipid A **1** and fatty acid.

Innate immunity activity was measured using HEK-Blue^{TM} hTLR4 cell line, which stably expressed TLR4/MD-2 receptor complex. This was different from previous studies about fatty acids which used cell lines that expressed multiple receptors.

When HEK-Blue^{TM} hTLR4 cells were treated with only fatty acids, all saturated and unsaturated fatty acids **5-12** showed no innate immune activity, which suggested that they were not agonistic ligands of TLR4/MD-2 receptor complex (figure 2.3, 2.4). SMM samples that contained lipid A **1** and one fatty acid (chosen from fatty acids **5-12**) also showed no changes in the immune function of lipid A **1**. However, HMM samples that contained saturated stearic acid (C18:0) **5** or palmitic acid (C16:0) **6** or myristic acid (C14:0) **7** or lauric acid (C12:0) **8** showed a concentration-dependent attenuation effect that decreased as acyl chain length decreased from 18 carbons of stearic acid **5** to 12 carbons of lauric acid **8** (figure 2.3). This was possibly because the longer chain length enhanced Van der Waals force, which led to tighter packing and formed more stable aggregates. Van der Waals force decreased as chain length decreased, so lipid A **1** became more exposed to lipid-binding protein (LBP) and TLR4.

On the other hand, HMM samples that contained unsaturated oleic acid (C18:1) **9** or linoleic acid (C18:2) **10** or linolenic acid (C18:3) **11** or docosahexaenoic acid (DHA, C22:6) **12** showed

an attenuation effect at higher fatty acid to lipid A concentration ratio, and a boosting effect at lower concentration ratio (figure 2.4). The attenuation effect decreased as the degree of unsaturation increased from one double bond of oleic acid **9** to three double bonds of linolenic acid **11**. One possible reason was that the additional double bonds introduced more kinks to the fatty acid chains, which disrupted the aggregate packing and increased lipid A **1** accessibility to LBP and TLR4. Poly-unsaturated fatty acids could also insert themselves into membrane, increasing membrane fluidity and promoting the recruitment of TLR4.

As fatty acids **5-12** did not suppress lipid A **1** activity by competitively inhibited MD-2 binding pocket (based on SMM results), an alternative mechanism by which fatty acids **5-12** could modulate the immune function of lipid A **1** should be considered. One possible explanation was that lipid A **1** activity could be influenced by the structures of its aggregate, so structural evaluations were then performed using dynamic light scattering (DLS) and transmission electron microscopy (TEM).

Moreover, it was observed that the immune function of lipid A **1** changed depending on three factors: 1) sample preparation method (SMM or HMM); 2) type of fatty acids (saturated or unsaturated); 3) concentration ratios of fatty acids to lipid A. Therefore, it was hypothesized that modifying any of these three factors could alter the structural properties of the aggregates formed, which required structural evaluation by DLS and TEM to verify (table 2.2, 2.3).

First, the structural properties of HMM and SMM samples were compared. HMM samples showed a higher degree of homogeneity where samples rearranged into large, relatively homogenous aggregates structures, while SMM samples formed many small size aggregates and large amorphous aggregates (table 2.2). These amorphous aggregates may be structurally unstable and easy to collapse, which allowed lipid A **1** to be available to LBP and TLR4. On the other hand, the relatively homogenous morphology of HMM samples suggested that fatty acids and lipid A **1** may be structurally integrated into mixed aggregates, and the tighter packing led to a more rigid structure and prevented the presentation of lipid A **1** to LBP and TLR4.

At fatty acid:lipid A 10:1 concentration ratio, the HMM samples of stearic acid **5** or linoleic acid **10** both showed large, relatively homogenous aggregates. However, at 0.1:1 fatty acid:lipid A concentration ratio, many small aggregates and large amorphous aggregates were observed for HMM samples of linoleic acid **10** (table 2.3). It was possible that this morphology had lower stability and was easier to collapse, which led to the easier transfer of lipid A **1** to TLR4/MD-2 receptor complex via LBP.

From these results, it was shown that aggregate compositions and state of mixed aggregates could regulate the immune function of lipid A **1**. These findings were then utilized in the development of LNPs containing lipid A as vaccine adjuvant materials, which incorporating more complex amphipathic compounds.

However, *E. coli* lipid A **1** is unsuitable as adjuvant as it overstimulates both the MyD88-dependent and TRIF-dependent pathway of TLR4-mediated signaling cascade, leading to lethal toxicity [50][95]. Instead, our laboratory focused on *Alcaligenes faecalis* (*A. faecalis*), a symbiotic bacterium that colonizes the gut-associated lymphoid tissues (GALT), Peyer's patch (PP) [99]. *A. faecalis* was found to establish and maintain a homeostatic environment in the PPs by activating the immune system without causing harmful responses. The extracted LPS fraction from *A. faecalis* showed weaker TLR4 agonistic activity than canonical E. coli LPS, and it could promote IL-6 induction from DCs, which, in turn, enhanced IgA production without toxicity [100].

Our laboratory successfully synthesized *A. faecalis* lipid A **4** (AfLA **4**), the active principle of *A. faecalis* LPS. In intranasal immunization studies using mice, AfLA **4** showed a stronger enhancement effect on mucosal IgA production compared to both MPLA (an adjuvant derived from *Salmonella* bacterium) and cholera toxin (a well-known immunogen for mucosal IgA production) [104][105][106][107].

Inspired by GSK AS0 series and mRNA-based LNP COVID-19 vaccines, LNPs containing AfLA **4** were synthesized using the microfluidic iLiNP device to function as mucosal vaccine adjuvants [141]. Additionally, the effects of different amphipathic compounds on the immune function of AfLA **4** in LNPs were evaluated both in vitro and in vivo.

Specifically, there were two LNPs compositions that showed slightly more promising results in vivo: DOPC **14** and cationic DOTAP **17** (10:49.5 mol%); DOPC **14** and pH-responsive and reducing condition-responsive ss-OP **20** (10:49.5 mol%). Although the levels of innate immune activity of AfLA **4** in these LNPs were attenuated in vitro (lower NF-κB activation and lower IL-6 inducing ability) compared to non-iLiNP AfLA **4** (figure 3.6, 3.7, 3.18, 3.19), their activity recovered in vitro. When LNPs containing AfLA **4** were intranasally immunized with the antigen ovalbumin (OVA), they induced higher OVA-specific IgA titers in both upper (nasal wash) and lower respiratory tract (BALF) (figure 3.23). These LNPs were also capable of inducing systemic immune response, evidenced by the higher serum IgG and IgA titers compared to non-iLiNP AfLA **4** (figure 3.28).

There were a few factors that might explain the differences between in vitro and in vivo results. In the case of in vivo results, LNPs could be taken up by antigen-presenting cells more efficiently by opsonization and phagocytosis [145]. Furthermore, AfLA **4** in LNPs was protected from degradation by enzymes, and the gradual release of AfLA **4** from LNPs could lead to a sustained activation of immune cells over time [146]. Additionally, intranasal immunization directly targeted the mucosal-associated lymphoid tissue (MALT), where LNPs could adhere to the mucosal epithelium and were readily taken up by dendritic cells and macrophages, facilitating antigen presentation [147]. Intranasal immunization might also allow for efficient lymph node targeting, delivering AfLA **4** to the draining cervical lymph nodes, which enhanced the level of mucosal and systemic immunity [148].

Furthermore, selective activation of TLR4 signaling by LNPs with different compositions was also evaluated by comparing MyD88-dependent IL-6 and TRIF-dependent MCP-1 (figure 3.19 and 3.20). LNPs containing DOPC **14** and DOTAP **17** at 10:49.5 mol% induced stronger MCP-1 activation compared to other LNP samples, but weaker IL-6 activation compared to LNP containing DOPG **19** or ss-OP **20**. As TRIF-dependent signaling occurs after endocytosis of TLR4 while MyD88-dependent signaling is associated with TLR4 activation at the cell surface, there is a possibility that LNPs surface charges could control the signaling pathway of lipid A, targeting either MyD88-dependent or TRIF-dependent pathway. Further studies are necessary to examine this possibility.

In conclusion, LNPs containing DOPC **14**/DOTAP **17** and DOPC **14**/ss-OP **20** at 10:49.5 mol% were two compositions that showed slightly stronger adjuvanticity than non-iLiNP AfLA **4**, and their potential to function as effective mucosal vaccine adjuvants that can induce both systemic and mucosal immune response should be further evaluated.

Section 2: Future outlook

For future experiments regarding the effects of aggregate compositions and state of mixed aggregates on lipid A **1** immune function, one possibility is the usage of fluorescent or biotin-labeled lipid A to tract its surface accessibility to LBP in different aggregate compositions. Another possibility is binding assay to measure the direct binding of lipid A aggregates to TLR4/MD-2 receptor complex using surface plasmon resonance (SPR), which measures molecular interactions in real time. Additionally, molecular dynamics simulations can be performed to simulate the interactions between lipid A and different fatty acids to predict aggregate stability and lipid packing, and how the aggregate structure might interact with TLR4/MD-2 receptor complex.

For the development of vaccine adjuvant materials containing AfLA **4**, the full cytokine profile is necessary to investigate the differences in adjuvanticity of different lipid compositions. This includes cytokines such as IL-12, IL-10 and TNF-α, which can allow for a more comprehensive understanding of the different T-cells polarization (Th1, Th2 and Th17). Additionally, fluorescently labeled LNPs should be synthesized to study cellular uptake, localization and endosomal escape in vitro by cell imaging and flow cytometry. This way, it might be possible to investigate whether different LNPs compositions can affect the activation of endosomal TLR4 versus surface TLR4 at different degrees. Finally, stability profile as well as physical properties of LNPs mixing with OVA need to be measured. In the future, antigens other than OVA (e.g. influenza hemagglutinins and neuraminidase surface proteins) should also be investigated to determine the suitability of LNPs containing AfLA **4** as mucosal vaccine adjuvants.

References

1) Marshall, J. S., Warrington, R., Watson, W., & Kim, H. L. (2018). An Introduction to Immunology and Immunopathology. *Allergy, Asthma & Clinical Immunology*, *14*(S2). https://doi.org/10.1186/s13223-018-0278-1

2) Costa, F. G., & Horswill, A. R. (2022). Overcoming pH defenses on the skin to establish infections. *PLOS Pathogens*, *18*(5), e1010512. https://doi.org/10.1371/journal.ppat.1010512

3) Zanin, M., Baviskar, P., Webster, R., & Webby, R. (2016). The interaction between respiratory pathogens and mucus. *Cell Host & Microbe*, *19*(2), 159–168. https://doi.org/10.1016/j.chom.2016.01.001

4) Turvey, S. E., & Broide, D. H. (2010). Innate Immunity. *Journal of Allergy and Clinical Immunology*, *125*(2), S24–S32. https://doi.org/10.1016/j.jaci.2009.07.016

5) Aristizábal, B., & González., Á. (2013). *Autoimmunity from bench to bedside*. Bogota El Rosario University Press.

6) Netea, M. G., Schlitzer, A., Placek, K., Joosten, L. A. B., & Schultze, J. L. (2019). Innate and Adaptive Immune Memory: an Evolutionary Continuum in the Host's Response to Pathogens. *Cell Host & Microbe*, *25*(1), 13–26. https://doi.org/10.1016/j.chom.2018.12.006

7) Sheu, K. M., Luecke, S., & Hoffmann, A. (2019). Stimulus-specificity in the responses of immune sentinel cells. *Current Opinion in Systems Biology*, *18*, 53–61. https://doi.org/10.1016/j.coisb.2019.10.011

8) Lim, J. J., Grinstein, S., & Roth, Z. (2017). Diversity and Versatility of Phagocytosis: Roles in Innate Immunity, Tissue Remodeling, and Homeostasis. *Frontiers in Cellular and Infection Microbiology*, *7*(191). https://doi.org/10.3389/fcimb.2017.00191

9) Uribe-Querol, E., & Rosales, C. (2017). Control of Phagocytosis by Microbial Pathogens. *Frontiers in Immunology*, *8*. https://doi.org/10.3389/fimmu.2017.01368

10) Vivier, E., Tomasello, E., Baratin, M., Walzer, T., & Ugolini, S. (2008). Functions of natural killer cells. *Nature Immunology*, *9*(5), 503–510. https://doi.org/10.1038/ni1582

11) Stone, K. D., Prussin, C., & Metcalfe, D. D. (2010). IgE, mast cells, basophils, and eosinophils. *Journal of Allergy and Clinical Immunology*, *125*(2), S73–S80. https://www.ncbi.nlm.nih.gov/pmc/articles/PMC2847274/

12) Mogensen, T. H. (2009). Pathogen Recognition and Inflammatory Signaling in Innate Immune Defenses. *Clinical Microbiology Reviews*, *22*(2), 240–273. https://doi.org/10.1128/cmr.00046-08

13) Kumar, H., Kawai, T., & Akira, S. (2011). Pathogen Recognition by the Innate Immune System. *International Reviews of Immunology*, *30*(1), 16–34. https://doi.org/10.3109/08830185.2010.529976

14) Takeuchi, O., & Akira, S. (2010). Pattern Recognition Receptors and Inflammation. *Cell*, *140*(6), 805–820. https://doi.org/10.1016/j.cell.2010.01.022

15) Loo, Y.-M., & Gale, M. (2011). Immune Signaling by RIG-I-like Receptors. *Immunity*, *34*(5), 680–692. https://doi.org/10.1016/j.immuni.2011.05.003

16) Chen, G., Shaw, M. H., Kim, Y.-G., & Nuñez, G. (2009). NOD-Like Receptors: Role in Innate Immunity and Inflammatory Disease. *Annual Review of Pathology: Mechanisms of Disease*, *4*(1), 365–398. https://doi.org/10.1146/annurev.pathol.4.110807.092239

17) Geijtenbeek, T. B. H., & Gringhuis, S. I. (2009). Signalling through C-type lectin receptors: shaping immune responses. *Nature Reviews Immunology*, *9*(7), 465–479. https://doi.org/10.1038/nri2569

18) Canton, J., Neculai, D., & Grinstein, S. (2013). Scavenger receptors in homeostasis and immunity. *Nature Reviews Immunology*, *13*(9), 621–634. https://doi.org/10.1038/nri3515

19) International Cytokine Society. (2006). *Cytokines, Chemokines, and Their Receptors*.

20) Murphy, K. M., Weaver, C., Mowat, A., Berg, L., Chaplin, D., Janeway, C. A., Travers, P., & Walport, M. (2017). *Janeway's immunobiology* (9th ed.). New York London Gs, Garland Science, Taylor & Francis Group.

21) Arango Duque, G., & Descoteaux, A. (2014). Macrophage Cytokines: Involvement in Immunity and Infectious Diseases. *Frontiers in Immunology*, *5*(491). https://doi.org/10.3389/fimmu.2014.00491

22) Paolini, R., Bernardini, G., Molfetta, R., & Santoni, A. (2015). NK cells and interferons. *Cytokine & Growth Factor Reviews*, *26*(2), 113–120. https://doi.org/10.1016/j.cytogfr.2014.11.003

23) Mukaida, N. (1998). Interleukin-8 (IL-8) and monocyte chemotactic and activating factor (MCAF/MCP-1), chemokines essentially involved in inflammatory and immune reactions. *Cytokine & Growth Factor Reviews*, *9*(1), 9–23. https://doi.org/10.1016/s1359-6101(97)00022-1

24) Ziblat, A., Nuñez, S. Y., Raffo Iraolagoitia, X. L., Spallanzani, R. G., Torres, N. I., Sierra, J. M., Secchiari, F., Domaica, C. I., Fuertes, M. B., & Zwirner, N. W. (2018). Interleukin (IL)-23 Stimulates IFN-γ Secretion by CD56bright Natural Killer Cells and Enhances IL-18-Driven Dendritic Cells Activation. *Frontiers in Immunology*, *8*. https://doi.org/10.3389/fimmu.2017.01959

25) Tominaga, K., Yoshimoto, T., Torigoe, K., Kurimoto, M., Matsui, K., Hada, T., Okamura, H., & Nakanishi, K. (2000). IL-12 synergizes with IL-18 or IL-1β for IFN-γ production from human T cells. *International Immunology*, *12*(2), 151–160. https://doi.org/10.1093/intimm/12.2.151

26) Zhang, J.-M., & An, J. (2007). Cytokines, Inflammation, and Pain. *International Anesthesiology Clinics*, *45*(2), 27–37. https://doi.org/10.1097/AIA.0b013e318034194e

27) Marshall, J. S., Warrington, R., Watson, W., & Kim, H. L. (2018b). An Introduction to Immunology and Immunopathology. *Allergy, Asthma & Clinical Immunology*, *14*(S2). https://doi.org/10.1186/s13223-018-0278-1

28) Wieczorek, M., Abualrous, E. T., Sticht, J., Álvaro-Benito, M., Stolzenberg, S., Noé, F., & Freund, C. (2017). Major Histocompatibility Complex (MHC) Class I and MHC Class II Proteins: Conformational Plasticity in Antigen Presentation. *Frontiers in Immunology*, *8*(1). https://doi.org/10.3389/fimmu.2017.00292

29) Groscurth, P., & Filgueira, L. (1998). Killing Mechanisms of Cytotoxic T Lymphocytes. *Physiology*, *13*(1), 17–21. https://doi.org/10.1152/physiologyonline.1998.13.1.17

30) Walker, J. A., & McKenzie, A. N. J. (2017). TH2 cell development and function. *Nature Reviews Immunology*, *18*(2), 121–133. https://doi.org/10.1038/nri.2017.118

31) Schroeder, H. W., & Cavacini, L. (2010). Structure and function of immunoglobulins. *Journal of Allergy and Clinical Immunology*, *125*(2), S41–S52. https://doi.org/10.1016/j.jaci.2009.09.046

32) Sandquist, I., & Kolls, J. (2018). Update on regulation and effector functions of Th17 cells. *F1000Research*, *7*, 205. https://doi.org/10.12688/f1000research.13020.1

33) Akira, S., Takeda, K., & Kaisho, T. (2001). Toll-like receptors: critical proteins linking innate and acquired immunity. *Nature Immunology*, *2*(8), 675–680. https://doi.org/10.1038/90609

34) Medzhitov, R., Preston-Hurlburt, P., & Janeway, C. A. (1997). A human homologue of the Drosophila Toll protein signals activation of adaptive immunity. *Nature*, *388*(6640), 394–397. https://doi.org/10.1038/41131

35) Molteni, M., Gemma, S., & Rossetti, C. (2016). The Role of Toll-Like Receptor 4 in Infectious and Noninfectious Inflammation. *Mediators of Inflammation*, *2016*, 1–9. https://doi.org/10.1155/2016/6978936

36) Poltorak, A. (1998). Defective LPS Signaling in C3H/HeJ and C57BL/10ScCr Mice: Mutations in Tlr4 Gene. *Science*, *282*(5396), 2085–2088. https://doi.org/10.1126/science.282.5396.2085

37) Shimazu, R., Akashi, S., Ogata, H., Nagai, Y., Fukudome, K., Miyake, K., & Kimoto, M. (1999). MD-2, a Molecule that Confers Lipopolysaccharide Responsiveness on Toll-like Receptor 4. *Journal of Experimental Medicine*, *189*(11), 1777–1782. https://doi.org/10.1084/jem.189.11.1777

38) Avila-Calderón, E. D., Ruiz-Palma, M. del S., Aguilera-Arreola, Ma. G., Velázquez-Guadarrama, N., Ruiz, E. A., Gomez-Lunar, Z., Witonsky, S., & Contreras-Rodríguez, A. (2021). Outer Membrane Vesicles of Gram-Negative Bacteria: An Outlook on Biogenesis. *Frontiers in Microbiology*, *12*. https://doi.org/10.3389/fmicb.2021.557902

39) Kusumoto, S., & Koichi Fukase. (2006). Synthesis of endotoxic principle of bacterial lipopolysaccharide and its recognition by the innate immune systems of hosts. *The Chemical Record*, *6*(6), 333–343. https://doi.org/10.1002/tcr.20098

40) Maldonado, R. F., Sá-Correia, I., & Valvano, M. A. (2016). Lipopolysaccharide modification in Gram-negative bacteria during chronic infection. *FEMS Microbiology Reviews*, *40*(4), 480–493. https://doi.org/10.1093/femsre/fuw007

41) Kusumoto, S., Koichi Fukase, & Shiba, T. (2010). Key structures of bacterial peptidoglycan and lipopolysaccharide triggering the innate immune system of higher animals: Chemical synthesis and functional studies. *Proceedings of the Japan Academy. Series B, Physical and Biological Sciences*, *86*(4), 322–337. https://doi.org/10.2183/pjab.86.322

42) Imoto, M., Yoshimura, H., Sakaguchi, N., Kusumoto, S., & Shiba, T. (1985). Total synthesis of Escherichia coli lipid A. *Tetrahedron Letters*, *26*(12), 1545–1548. https://doi.org/10.1016/s0040-4039(00)98548-4

43) Miyake, K. (2006). Invited review: Roles for accessory molecules in microbial recognition by Toll-like receptors. *Journal of Endotoxin Research*, *12*(4), 195–204. https://doi.org/10.1177/09680519060120040101

44) Aurell, C. A., & Wistrom, A. O. (1998). Critical Aggregation Concentrations of Gram-Negative Bacterial Lipopolysaccharides (LPS). *Biochemical and Biophysical Research Communications*, *253*(1), 119–123. https://doi.org/10.1006/bbrc.1998.9773

45) Ryu, J.-K., Kim, S. J., Rah, S.-H., Kang, J. I., Jung, H. E., Lee, D., Lee, H. K., Lee, J.-O., Park, B. S., Yoon, T.-Y., & Kim, H. M. (2017). Reconstruction of LPS Transfer Cascade Reveals Structural Determinants within LBP, CD14, and TLR4-MD2 for Efficient LPS Recognition and Transfer. *Immunity*, *46*(1), 38–50. https://doi.org/10.1016/j.immuni.2016.11.007

46) Kim, H. M., Park, B. S., Kim, J.-I., Kim, S. E., Lee, J., Oh, S. C., Enkhbayar, P., Matsushima, N., Lee, H., Yoo, O. J., & Lee, J.-O. (2007). Crystal Structure of the TLR4-MD-2 Complex with Bound Endotoxin Antagonist Eritoran. *Cell*, *130*(5), 906–917. https://doi.org/10.1016/j.cell.2007.08.002

47) Ohto, U., Fukase, K., Miyake, K., & Satow, Y. (2007). Crystal structures of human MD-2 and its complex with antiendotoxic lipid IVa. *Science (New York, N.Y.)*, *316*(5831), 1632–1634. https://doi.org/10.1126/science.1139111

48) Kim, H. M., Park, B. S., Kim, J.-I., Kim, S. E., Lee, J., Oh, S. C., Enkhbayar, P., Matsushima, N., Lee, H., Yoo, O. J., & Lee, J.-O. (2007b). Crystal Structure of the TLR4-MD-2 Complex with Bound Endotoxin Antagonist Eritoran. *Cell*, *130*(5), 906–917. https://doi.org/10.1016/j.cell.2007.08.002

49) Park, B. S., Song, D. H., Kim, H. M., Choi, B.-S., Lee, H., & Lee, J.-O. (2009). The structural basis of lipopolysaccharide recognition by the TLR4–MD-2 complex. *Nature*, *458*(7242), 1191–1195. https://doi.org/10.1038/nature07830

50) Kawasaki, T., & Kawai, T. (2014). Toll-Like Receptor Signaling Pathways. *Frontiers in Immunology*, *5*(461). https://doi.org/10.3389/fimmu.2014.00461

51) Roh, J. S., & Sohn, D. H. (2018). Damage-Associated Molecular Patterns in Inflammatory Diseases. *Immune Network*, *18*(4). https://doi.org/10.4110/in.2018.18.e27

52) Land WG. The Role of Damage-Associated Molecular Patterns (DAMPs) in Human Diseases: Part II: DAMPs as diagnostics, prognostics and therapeutics in clinical medicine. Sultan Qaboos Univ Med J. 2015 May;15(2):e157-70. Epub 2015 May 28. PMID: 26052447; PMCID: PMC4450777

53) Klune, J. R., Dhupar, R., Cardinal, J., Billiar, T. R., & Tsung, A. (2008). HMGB1: endogenous danger signaling. *Molecular Medicine (Cambridge, Mass.)*, *14*(7-8), 476–484. https://doi.org/10.2119/2008-00034.Klune

54) Zhang, X., & Mosser, D. (2008). Macrophage activation by endogenous danger signals. *The Journal of Pathology*, *214*(2), 161–178. https://doi.org/10.1002/path.2284

55) Mueller, M., Lindner, B., Kusumoto, S., Fukase, K., Schromm, A. B., & Seydel, U. (2004). Aggregates are the biologically active units of endotoxin. *The Journal of Biological Chemistry*, *279*(25), 26307–26313. https://doi.org/10.1074/jbc.M401231200

56) Pizzuto, M., & Pelegrin, P. (2020). Cardiolipin in Immune Signaling and Cell Death. *Trends in Cell Biology*, *30*(11), 892–903. https://doi.org/10.1016/j.tcb.2020.09.004

57) Saitoh, S., Akashi, S., Yamada, T., Tanimura, N., Kobayashi, M., Konno, K., Matsumoto, F., Fukase, K., Kusumoto, S., Nagai, Y., Kusumoto, Y., Kosugi, A., & Miyake, K. (2004). Lipid A antagonist, lipid IVa, is distinct from lipid A in interaction with Toll-like receptor 4 (TLR4)-MD-2 and ligand-induced TLR4 oligomerization. *International Immunology*, *16*(7), 961–969. https://doi.org/10.1093/intimm/dxh097

58) Hirotaka Kanoh, Nitta, T., Go, S., Kei-ichiro Inamori, Veillon, L., Nihei, W., Fujii, M., Kazuya Kabayama, Atsushi Shimoyama, Koichi Fukase, Umeharu Ohto, Shimizu, T., Watanabe, T., Shindo, H., Aoki, S., Sato, K., Nagasaki, M., Yutaka Yatomi, Naoko Komura, & Ando, H. (2020). Homeostatic and pathogenic roles of GM 3 ganglioside molecular species in TLR 4 signaling in obesity. *The EMBO Journal*, *39*(12). https://doi.org/10.15252/embj.2019101732

59) Chan, R. B., Perotte, A. J., Zhou, B., Liong, C., Shorr, E. J., Marder, K. S., Kang, U. J., Waters, C. H., Levy, O. A., Xu, Y., Shim, H. B., Pe'er, I., Di Paolo, G., & Alcalay, R. N. (2017). Elevated GM3 plasma concentration in idiopathic Parkinson's disease: A lipidomic analysis. *PLOS ONE*, *12*(2), e0172348. https://doi.org/10.1371/journal.pone.0172348

60) Wakil, S. J., & Abu-Elheiga, L. A. (2008). Fatty acid metabolism: target for metabolic syndrome. *Journal of Lipid Research*, *50*(Supplement), S138–S143. https://doi.org/10.1194/jlr.r800079-jlr200

61) Calder, P. C. (2015). Functional Roles of Fatty Acids and Their Effects on Human Health. *JPEN. Journal of Parenteral and Enteral Nutrition*, *39*(1 Suppl), 18S32S. https://doi.org/10.1177/0148607115595980

62) Sobocińska, J., Roszczenko-Jasińska, P., Ciesielska, A., & Kwiatkowska, K. (2018). Protein Palmitoylation and Its Role in Bacterial and Viral Infections. *Frontiers in Immunology*, *8*. https://doi.org/10.3389/fimmu.2017.02003

63) Lopez-Huertas, E. (2010). Health effects of oleic acid and long chain omega-3 fatty acids (EPA and DHA) enriched milks. A review of intervention studies. *Pharmacological Research*, *61*(3), 200–207. https://doi.org/10.1016/j.phrs.2009.10.007

64) Spector, A. A. (2001). Plasma Free Fatty Acid and Lipoproteins as Sources of Polyunsaturated Fatty Acid for the Brain. *Journal of Molecular Neuroscience*, *16*(2-3), 159–166. https://doi.org/10.1385/jmn:16:2-3:159

65) Rabionet, M., Gorgas, K., & Sandhoff, R. (2014). Ceramide synthesis in the epidermis. *Biochimica et Biophysica Acta (BBA) - Molecular and Cell Biology of Lipids*, *1841*(3), 422–434. https://doi.org/10.1016/j.bbalip.2013.08.011

66) Skinner, E. R., Watt, C., Besson, J. A. O., & Best, P. V. (1993). Differences in the fatty acid composition of the grey and white matter of different regions of the brains of patients with Alzheimer's disease and control subjects. *Brain*, *116*(3), 717–725. https://doi.org/10.1093/brain/116.3.717

67) Zock, P. L., Katan, M. B., & Mensink, R. P. (1995). Dietary trans fatty acids and lipoprotein cholesterol. *The American Journal of Clinical Nutrition*, *61*(3), 617–617. https://doi.org/10.1093/ajcn/61.3.617

68) Wong, S. W., Kwon, M.-J., Choi, A. M. K., Kim, H.-P., Nakahira, K., & Hwang, D. H. (2009). Fatty Acids Modulate Toll-like Receptor 4 Activation through Regulation of Receptor Dimerization and Recruitment into Lipid Rafts in a Reactive Oxygen Species-dependent Manner. *Journal of Biological Chemistry*, *284*(40), 27384–27392. https://doi.org/10.1074/jbc.m109.044065

69) Erridge, C., & Samani, N. J. (2009). Saturated Fatty Acids Do Not Directly Stimulate Toll-Like Receptor Signaling. *Arteriosclerosis, Thrombosis, and Vascular Biology*, *29*(11), 1944–1949. https://doi.org/10.1161/atvbaha.109.194050

70) Novak, T. E., Babcock, T. A., Jho, D. H., Helton, W. S., & Espat, N. J. (2003). NF-κB inhibition by ω-3 fatty acids modulates LPS-stimulated macrophage TNF-α transcription. *American Journal of Physiology-Lung Cellular and Molecular Physiology*, *284*(1), L84–L89. https://doi.org/10.1152/ajplung.00077.2002

71) Pollard, A. J., & Bijker, E. M. (2020). A guide to vaccinology: from basic principles to new developments. *Nature Reviews Immunology*, *21*(21), 1–18. https://doi.org/10.1038/s41577-020-00479-7

72) Abbas, A. K., Lichtman, A. H., Pillai, S., L, D., & Baker, A. (2021). *Cellular and molecular immunology*. Elsevier.

73) Shearer, W. T., Fleisher, T. A., Buckley, R. H., Ballas, Z., Ballow, M., Blaese, R. M., Bonilla, F. A., Conley, M. E., Cunningham-Rundles, C., Filipovich, A. H., Fuleihan, R., Gelfand, E. W., Hernandez-Trujillo, V., Holland, S. M., Hong, R., Lederman, H. M., Malech, H. L., Miles, S., Notarangelo, L. D., & Ochs, H. D. (2014). Recommendations for live viral and bacterial vaccines in immunodeficient patients and their close contacts. *Journal of Allergy and Clinical Immunology*, *133*(4), 961–966. https://doi.org/10.1016/j.jaci.2013.11.043

74) Christensen, D. (2016). Vaccine adjuvants: Why and how. *Human Vaccines & Immunotherapeutics*, *12*(10), 2709–2711. https://doi.org/10.1080/21645515.2016.1219003

75) Reed, S. G., Bertholet, S., Coler, R. N., & Friede, M. (2009). New horizons in adjuvants for vaccine development. *Trends in Immunology*, *30*(1), 23–32. https://doi.org/10.1016/j.it.2008.09.006

76) Pulendran, B., S. Arunachalam, P., & O'Hagan, D. T. (2021). Emerging concepts in the science of vaccine adjuvants. *Nature Reviews Drug Discovery*, *20*(6), 454–475. https://doi.org/10.1038/s41573-021-00163-y

77) Brewer, J. M., Conacher, M., Hunter, C. A., Mohrs, M., Brombacher, F., & Alexander, J. (1999). Aluminium Hydroxide Adjuvant Initiates Strong Antigen-Specific Th2 Responses in the Absence of IL-4- or IL-13-Mediated Signaling. *The Journal of Immunology*, *163*(12), 6448–6454. https://doi.org/10.4049/jimmunol.163.12.6448

78) Eisenbarth, S. C., Colegio, O. R., O'Connor, W., Sutterwala, F. S., & Flavell, R. A. (2008). Crucial role for the Nalp3 inflammasome in the immunostimulatory properties of aluminium adjuvants. *Nature*, *453*(7198), 1122–1126. https://doi.org/10.1038/nature06939

79) Oleszycka, E., McCluskey, S., Sharp, F. A., Muñoz-Wolf, N., Hams, E., Gorman, A. L., Fallon, P. G., & Lavelle, E. C. (2018). The vaccine adjuvant alum promotes IL-10 production that suppresses Th1 responses. *European Journal of Immunology*, *48*(4), 705–715. https://doi.org/10.1002/eji.201747150

80) Gavin, A. L., Hoebe, K., Duong, B., Ota, T., Martin, C., Beutler, B., & Nemazee, D. (2006). Adjuvant-Enhanced Antibody Responses in the Absence of Toll-Like Receptor Signaling. *Science*, *314*(5807), 1936–1938. https://doi.org/10.1126/science.1135299

81) O'Hagan, D. T., Ott, G. S., De Gregorio, E., & Seubert, A. (2012). The mechanism of action of MF59 – An innately attractive adjuvant formulation. *Vaccine*, *30*(29), 4341–4348. https://doi.org/10.1016/j.vaccine.2011.09.061

82) Ko, E.-J., & Kang, S.-M. (2018). Immunology and efficacy of MF59-adjuvanted vaccines. *Human Vaccines & Immunotherapeutics*, *14*(12), 3041–3045. https://doi.org/10.1080/21645515.2018.1495301

83) Zhao, T., Cai, Y., Jiang, Y., He, X., Wei, Y., Yu, Y., & Tian, X. (2023). Vaccine adjuvants: mechanisms and platforms. *Signal Transduction and Targeted Therapy*, *8*(1), 1–24. https://doi.org/10.1038/s41392-023-01557-7

84) Lacaille-Dubois, M.-A. (2019). Updated insights into the mechanism of action and clinical profile of the immunoadjuvant QS-21: A review. *Phytomedicine: International Journal of Phytotherapy and Phytopharmacology*, *60*, 152905. https://doi.org/10.1016/j.phymed.2019.152905

85) Coccia, M., Collignon, C., Hervé, C., Chalon, A., Welsby, I., Detienne, S., van Helden, M. J., Dutta, S., Genito, C. J., Waters, N. C., Van Deun, K., Smilde, A. K., van den Berg, R. A., Franco, D., Bourguignon, P., Morel, S., Garçon, N., Lambrecht, B. N., Goriely, S., & van der Most, R. (2017). Cellular and molecular synergy in AS01-adjuvanted vaccines results in an early IFNγ response promoting vaccine immunogenicity. *Npj Vaccines*, *2*(1), 1–14. https://doi.org/10.1038/s41541-017-0027-3

86) Lal, H., Cunningham, A. L., Godeaux, O., Chlibek, R., Diez-Domingo, J., Hwang, S.-J., Levin, M. J., McElhaney, J. E., Poder, A., Puig-Barberà, J., Vesikari, T., Watanabe, D., Weckx, L., Zahaf, T., & Heineman, T. C. (2015). Efficacy of an Adjuvanted Herpes Zoster Subunit Vaccine in Older Adults. *New England Journal of Medicine*, *372*(22), 2087–2096. https://doi.org/10.1056/nejmoa1501184

87) Olotu, A., Fegan, G., Wambua, J., Nyangweso, G., Leach, A., Lievens, M., Kaslow, D. C., Njuguna, P., Marsh, K., & Bejon, P. (2016). Seven-Year Efficacy of RTS,S/AS01 Malaria Vaccine among Young African Children. *New England Journal of Medicine*, *374*(26), 2519–2529. https://doi.org/10.1056/nejmoa1515257

88) Apostólico, J. de S., Lunardelli, V. A. S., Coirada, F. C., Boscardin, S. B., & Rosa, D. S. (2016). Adjuvants: Classification,Modus Operandi, and Licensing. *Journal of Immunology Research*, *2016*, 1–16. https://doi.org/10.1155/2016/1459394

89) Morel, S., Didierlaurent, A., Bourguignon, P., Delhaye, S., Baras, B., Jacob, V., Planty, C., Elouahabi, A., Harvengt, P., & Carlsen, H. (2011). Adjuvant System AS03 containing α-tocopherol modulates innate immune response and leads to improved adaptive immunity. *Vaccine*, *29*(13), 2461–2473. https://doi.org/10.1016/j.vaccine.2011.01.011

90) Goll, J. B., Jain, A., Jensen, T. L., Assis, R., Nakajima, R., Jasinskas, A., Coughlan, L., Cherikh, S. R., Gelber, C. E., Khan, S., Huw Davies, D., Meade, P., Stadlbauer, D., Strohmeier, S., Krammer, F., Chen, W. H., & Felgner, P. L. (2022). The antibody landscapes following AS03 and MF59 adjuvanted H5N1 vaccination. *Npj Vaccines*, *7*(1), 1–11.

91) Sridhar, S., Joaquin, A., Bonaparte, M. I., Bueso, A., Chabanon, A.-L., Chen, A., Chicz, R. M., Diemert, D., Essink, B. J., Fu, B., Grunenberg, N. A., Janosczyk, H., Keefer, M. C., Rivera M, D. M., Meng, Y., Michael, N. L., Munsiff, S. S., Ogbuagu, O., Raabe, V. N., & Severance, R. (2022). Safety and immunogenicity of an AS03-adjuvanted SARS-CoV-2 recombinant protein vaccine (CoV2 preS dTM) in healthy adults: interim findings from a phase 2, randomised, dose-finding, multicentre study. *The Lancet Infectious Diseases*. https://doi.org/10.1016/s1473-3099(21)00764-7

92) Annalaura Brai, Federica Poggialini, Pasqualini, C., Claudia Immacolata Trivisani, Chiara Vagaggini, & Dreassi, E. (2023). Progress towards Adjuvant Development: Focus on Antiviral Therapy. *International Journal of Molecular Sciences*, *24*(11), 9225–9225. https://doi.org/10.3390/ijms24119225

90-Parrón-Carreño, T., & Alarcón-Rodríguez, R. (2021). Fendrix® Vaccine Effectiveness in Healthcare Workers Who Are Non-Responsive to Engerix B® Vaccination. *Vaccines*, *9*(3), 279. https://doi.org/10.3390/vaccines9030279

94) Szarewski, A. (2010). HPV vaccine: Cervarix. *Expert Opinion on Biological Therapy*, *10*(3), 477–487. https://doi.org/10.1517/14712591003601944

95) Rossetti, C., & Peri, F. (2021). *The role of toll-like receptor 4 in infectious and non infectious inflammation*. Springer.

96) Shimoyama, A., & Fukase, K. (2021). Lipid A-Mediated Bacterial–Host Chemical Ecology: Synthetic Research of Bacterial Lipid As and Their Development as Adjuvants. *Molecules*, *26*(20), 6294. https://doi.org/10.3390/molecules26206294

97) Wang, Y.-Q., Bazin-Lee, H., Evans, J. T., Casella, C. R., & Mitchell, T. C. (2020). MPL Adjuvant Contains Competitive Antagonists of Human TLR4. *Frontiers in Immunology*, *11*. https://doi.org/10.3389/fimmu.2020.577823

98) Mata-Haro, V., Cekic, C., Martin, M., Chilton, P. M., Casella, C. R., & Mitchell, T. C. (2007). The Vaccine Adjuvant Monophosphoryl Lipid A as a TRIF-Biased Agonist of TLR4. *Science*, *316*(5831), 1628–1632. https://doi.org/10.1126/science.1138963

99) Obata, T., Goto, Y., Kunisawa, J., Sato, S., Sakamoto, M., Setoyama, H., Matsuki, T., Nonaka, K., Shibata, N., Gohda, M., Kagiyama, Y., Nochi, T., Yuki, Y., Fukuyama, Y., Mukai, A., Shinzaki, S., Fujihashi, K., Sasakawa, C., Iijima, H., & Goto, M. (2010). Indigenous opportunistic bacteria inhabit mammalian gut-associated lymphoid tissues and share a mucosal antibody-mediated symbiosis. *Proceedings of the National Academy of Sciences*, *107*(16), 7419–7424. https://doi.org/10.1073/pnas.1001061107

100) Shibata, N., Kunisawa, J., Hosomi, K., Fujimoto, Y., Mizote, K., Kitayama, N., Shimoyama, A., Mimuro, H., Sato, S., Kishishita, N., Ishii, K. J., Fukase, K., & Kiyono, H. (2018). Lymphoid tissue-resident Alcaligenes LPS induces IgA production without excessive inflammatory responses via weak TLR4 agonist activity. *Mucosal Immunology*, *11*(3), 693–702. https://doi.org/10.1038/mi.2017.103

101) Koji Hosomi, Shibata, N., Atsushi Shimoyama, Uto, T., Takahiro Nagatake, Tojima, Y., Nishino, T., Takeyama, H., Koichi Fukase, Hiroshi Kiyono, & Jun Kunisawa. (2020). Lymphoid Tissue–Resident Alcaligenes Establish an Intracellular Symbiotic Environment by Creating a Unique Energy Shift in Dendritic Cells. *Frontiers in Microbiology*, *11*. https://doi.org/10.3389/fmicb.2020.561005

102) Atsushi Shimoyama, Flaviana Di Lorenzo, Haruki Yamaura, Keisuke Mizote, Palmigiano, A., Pither, M. D., Speciale, I., Uto, T., Masui, S., Sturiale, L., Garozzo, D., Koji Hosomi, Shibata, N., Kazuya Kabayama, Fujimoto, Y., Silipo, A., Jun Kunisawa, Hiroshi Kiyono, Molinaro, A., & Koichi Fukase. (2021). Lipopolysaccharide from Gut-Associated Lymphoid-Tissue-Resident *Alcaligenes faecalis*: Complete Structure Determination and Chemical Synthesis of Its Lipid A. *Angewandte Chemie International Edition*, *60*(18), 10023–10031. https://doi.org/10.1002/anie.202012374

103) Wang, Y., Hosomi, K., Shimoyama, A., Yoshii, K., Yamaura, H., Nagatake, T., Nishino, T., Kiyono, H., Fukase, K., & Kunisawa, J. (2020). Adjuvant Activity of Synthetic Lipid A of Alcaligenes, a Gut-Associated Lymphoid Tissue-Resident Commensal Bacterium, to Augment

Antigen-Specific IgG and Th17 Responses in Systemic Vaccine. *Vaccines*, *8*(3), 395. https://doi.org/10.3390/vaccines8030395

104) Yoshii, K., Hosomi, K., Shimoyama, A., Wang, Y., Yamaura, H., Nagatake, T., Suzuki, H., Lan, H., Kiyono, H., Fukase, K., & Kunisawa, J. (2020). Chemically Synthesized Alcaligenes Lipid A Shows a Potent and Safe Nasal Vaccine Adjuvant Activity for the Induction of Streptococcus pneumoniae-Specific IgA and Th17 Mediated Protective Immunity. *Microorganisms*, *8*(8), 1102. https://doi.org/10.3390/microorganisms8081102

105) Elson, C. O., & Ealding, W. (1984). Generalized systemic and mucosal immunity in mice after mucosal stimulation with cholera toxin. *The Journal of Immunology*, *132*(6), 2736–2741. https://doi.org/10.4049/jimmunol.132.6.2736

106) Sun, X., Koji Hosomi, Atsushi Shimoyama, Yoshii, K., Azusa Saika, Haruki Yamaura, Takahiro Nagatake, Hiroshi Kiyono, Koichi Fukase, & Jun Kunisawa. (2023). *Alcaligene*s lipid A functions as a superior mucosal adjuvant to monophosphoryl lipid A via the recruitment and activation of CD11b+ dendritic cells in nasal tissue. *International Immunology*, *36*(1), 33–43. https://doi.org/10.1093/intimm/dxad045

107) Wang, Y.-Q., Bazin-Lee, H., Evans, J. T., Casella, C. R., & Mitchell, T. C. (2020b). MPL Adjuvant Contains Competitive Antagonists of Human TLR4. *Frontiers in Immunology*, *11*. https://doi.org/10.3389/fimmu.2020.577823

108) Fukuyama, Y., Okada, K., Yamaguchi, M., Kiyono, H., Mori, K., & Yuki, Y. (2015). Nasal Administration of Cholera Toxin as a Mucosal Adjuvant Damages the Olfactory System in Mice. *PLOS ONE*, *10*(9), e0139368. https://doi.org/10.1371/journal.pone.0139368

109) Mutsch, M., Zhou, W., Rhodes, P., Bopp, M., Chen, R. T., Linder, T., Spyr, C., & Steffen, R. (2004). Use of the Inactivated Intranasal Influenza Vaccine and the Risk of Bell's Palsy in Switzerland. *New England Journal of Medicine*, *350*(9), 896–903. https://doi.org/10.1056/nejmoa030595

110) Lavelle, E. C., & Ward, R. W. (2021). Mucosal vaccines — fortifying the frontiers. *Nature Reviews Immunology*, 1–15. https://doi.org/10.1038/s41577-021-00583-2

111) Mehta, M., Bui, T. A., Yang, X., Aksoy, Y. A., Goldys, E. M., & Deng, W. (2023). Lipid-Based Nanoparticles for Drug/Gene Delivery: An Overview of the Production Techniques and Difficulties Encountered in Their Industrial Development. *ACS Materials Science Au*, *3*(6). https://doi.org/10.1021/acsmaterialsau.3c00032

112) Roman, F., Burny, W., Ceregido, M. A., Laupèze, B., Temmerman, S. T., Warter, L., & Coccia, M. (2024). Adjuvant system AS01: from mode of action to effective vaccines. *Expert Review of Vaccines*, *23*(1), 715–729. https://doi.org/10.1080/14760584.2024.2382725

113) Narvekar, M., Xue, H. Y., Eoh, J. Y., & Wong, H. L. (2014). Nanocarrier for Poorly Water-Soluble Anticancer Drugs—Barriers of Translation and Solutions. *AAPS PharmSciTech*, *15*(4), 822–833. https://doi.org/10.1208/s12249-014-0107-x

114) Schoenmaker, L., Witzigmann, D., Kulkarni, J. A., Verbeke, R., Kersten, G., Jiskoot, W., & Crommelin, D. (2021). mRNA-lipid nanoparticle COVID-19 vaccines: structure and stability. *International Journal of Pharmaceutics*, *601*(120586), 120586. https://doi.org/10.1016/j.ijpharm.2021.120586

115) Hald Albertsen, C., Kulkarni, J. A., Witzigmann, D., Lind, M., Petersson, K., & Simonsen, J. B. (2022). The role of lipid components in lipid nanoparticles for vaccines and gene therapy. *Advanced Drug Delivery Reviews*, *188*, 114416. https://doi.org/10.1016/j.addr.2022.114416

116) Shi, R., Liu, X., Wang, Y., Pan, M., Wang, S., Shi, L., & Ni, B. (2024). Long-term stability and immunogenicity of lipid nanoparticle COVID-19 mRNA vaccine is affected by particle size. *Human Vaccines & Immunotherapeutics*, *20*(1), 2342592. https://doi.org/10.1080/21645515.2024.2342592

117) Tenchov, R., Bird, R., Curtze, A. E., & Zhou, Q. (2021). Lipid Nanoparticles—From Liposomes to mRNA Vaccine Delivery, a Landscape of Research Diversity and Advancement. *ACS Nano*, *15*(11). https://doi.org/10.1021/acsnano.1c04996

118) Smith, M. C., Crist, R. M., Clogston, J. D., & McNeil, S. E. (2017). Zeta potential: a case study of cationic, anionic, and neutral liposomes. *Analytical and Bioanalytical Chemistry*, *409*(24), 5779–5787. https://doi.org/10.1007/s00216-017-0527-z

119) Zhong, Z., Shi, S., Han, J., Zhang, Z., & Sun, X. (2009). Anionic Liposomes Increase the Efficiency of Adenovirus-Mediated Gene Transfer to Coxsackie-Adenovirus Receptor Deficient Cells. *Molecular Pharmaceutics*, *7*(1), 105–115. https://doi.org/10.1021/mp900151k

120) Barauskas, J., Johnsson, M., & Tiberg, F. (2005). Self-Assembled Lipid Superstructures: Beyond Vesicles and Liposomes. *Nano Letters*, *5*(8), 1615–1619. https://doi.org/10.1021/nl050678i

121) Neves, L. F., Duan, J., Voelker, A., Khanal, A., McNally, L., Steinbach-Rankins, J., & Ceresa, B. P. (2016). Preparation and optimisation of anionic liposomes for delivery of small peptides and cDNA to human corneal epithelial cells. *Journal of Microencapsulation*, *33*(4), 391–399. https://doi.org/10.1080/02652048.2016.1202343

122) Klibanov, A. L., Maruyama, K., Torchilin, V. P., & Huang, L. (1990). Amphipathic polyethyleneglycols effectively prolong the circulation time of liposomes. *FEBS Letters*, *268*(1), 235–237. https://doi.org/10.1016/0014-5793(90)81016-H

123) Padín-González, E., Lancaster, P., Bottini, M., Gasco, P., Tran, L., Fadeel, B., Wilkins, T., & Monopoli, M. P. (2022). Understanding the Role and Impact of Poly (Ethylene Glycol)

124) Ichinoo, T. (2020). *自然免疫活性化因子リピドA の機能制御を行う内因性リガンドの解析*.

125) Liu, T., Zhang, L., Joo, D., & Sun, S.-C. (2017). NF-κB signaling in inflammation. *Signal Transduction and Targeted Therapy*, *2*(17023). https://doi.org/10.1038/sigtrans.2017.23

126) Wright, S. S., Vasudevan, S. O., & Rathinam, V. A. (2022). Mechanisms and Consequences of Noncanonical Inflammasome-Mediated Pyroptosis. *Journal of Molecular Biology*, *434*(4), 167245. https://doi.org/10.1016/j.jmb.2021.167245

127) Huang, S., Rutkowsky, J. M., Snodgrass, R. G., Ono-Moore, K. D., Schneider, D. A., Newman, J. W., Adams, S. H., & Hwang, D. H. (2012). Saturated fatty acids activate TLR-mediated proinflammatory signaling pathways. *Journal of Lipid Research*, *53*(9), 2002–2013. https://doi.org/10.1194/jlr.d029546

128) Arouri, A., Kira Emilie Lauritsen, Nielsen, H. L., & Mouritsen, O. G. (2016). Effect of fatty acids on the permeability barrier of model and biological membranes. *Chemistry and Physics of Lipids*, *200*, 139–146. https://doi.org/10.1016/j.chemphyslip.2016.10.001

129) Rim Baccouch, Shi, Y., Vernay, E., Mathelié-Guinlet, M., Taib-Maamar, N., Sandrine Villette, Cécile Feuillie, Rascol, E., Nuss, P., Lecomte, S., Molinari, M., Galya Staneva, & Alves, I. D. (2023). The impact of lipid polyunsaturation on the physical and mechanical properties of lipid membranes. *Biochimica et Biophysica Acta (BBA) - Biomembranes*, *1865*(2), 184084–184084. https://doi.org/10.1016/j.bbamem.2022.184084

130) Shimoyama, A. (2018). Development of Chemically Synthesized Self-Adjuvanting Vaccines. *Trends in Glycoscience and Glycotechnology*, *30*(173), E41–E43. https://doi.org/10.4052/tigg.1747.6e

131) Manabe, Y., Chang, T., & Fukase, K. (2020). Recent advances in self-adjuvanting glycoconjugate vaccines. *Drug Discovery Today: Technologies*, *37*. https://doi.org/10.1016/j.ddtec.2020.11.006

132) Manabe, Y., & Koichi Fukase. (2023). Innovative Vaccine Strategy: Self-Adjuvanting Conjugate Vaccines. *Methods in Molecular Biology*, 55–72. https://doi.org/10.1007/978-1-0716-2910-9_5

133) Taku Aiga, Manabe, Y., Ito, K., Chang, T., Kazuya Kabayama, Shino Ohshima, Kametani, Y., Miura, A., Furukawa, H., Inaba, H., Matsuura, K., & Koichi Fukase. (2020). Immunological Evaluation of Co-Assembling a Lipidated Peptide Antigen and Lipophilic Adjuvants: Self-

Adjuvanting Anti-Breast-Cancer Vaccine Candidates. *Angewandte Chemie International Edition*, *59*(40), 17705–17711. https://doi.org/10.1002/anie.202007999

134) Verbeke, R., Lentacker, I., De Smedt, S. C., & Dewitte, H. (2019). Three decades of messenger RNA vaccine development. *Nano Today*, *28*, 100766. https://doi.org/10.1016/j.nantod.2019.100766

135) Kis, Z., Kontoravdi, C., Dey, A. K., Shattock, R., & Shah, N. (2020). Rapid development and deployment of high-volume vaccines for pandemic response. *Journal of Advanced Manufacturing and Processing*, *2*(3). https://doi.org/10.1002/amp2.10060

136) Freyn, A. W., Ramos da Silva, J., Rosado, V. C., Bliss, C. M., Pine, M., Mui, B. L., Tam, Y. K., Madden, T. D., de Souza Ferreira, L. C., Weissman, D., Krammer, F., Coughlan, L., Palese, P., Pardi, N., & Nachbagauer, R. (2020). A Multi-Targeting, Nucleoside-Modified mRNA Influenza Virus Vaccine Provides Broad Protection in Mice. *Molecular Therapy*, *28*(7), 1569–1584. https://doi.org/10.1016/j.ymthe.2020.04.018

137) Wu, K., Choi, A., Koch, M., Elbashir, S., Ma, L., Lee, D., Woods, A., Henry, C., Palandjian, C., Hill, A., Jani, H., Quinones, J., Nunna, N., O'Connell, S., McDermott, A. B., Falcone, S., Narayanan, E., Colpitts, T., Bennett, H., & Corbett, K. S. (2021). Variant SARS-CoV-2 mRNA vaccines confer broad neutralization as primary or booster series in mice. *Vaccine*, *39*(51), 7394–7400. https://doi.org/10.1016/j.vaccine.2021.11.001

138) Chaudhary, N., Weissman, D., & Whitehead, K. A. (2021). mRNA vaccines for infectious diseases: principles, delivery and clinical translation. *Nature Reviews Drug Discovery*, *20*(11). https://doi.org/10.1038/s41573-021-00283-5

139) Alving, C. R., Peachman, K. K., Matyas, G. R., Rao, M., & Beck, Z. (2020). Army Liposome Formulation (ALF) family of vaccine adjuvants. *Expert Review of Vaccines*, *19*(3), 279–292. https://doi.org/10.1080/14760584.2020.1745636

140) Lombardo, D., & Kiselev, M. A. (2022b). Methods of Liposomes Preparation: Formation and Control Factors of Versatile Nanocarriers for Biomedical and Nanomedicine Application. *Pharmaceutics*, *14*(3), 543. https://doi.org/10.3390/pharmaceutics14030543

141) Kimura, N., Maeki, M., Sato, Y., Note, Y., Ishida, A., Tani, H., Harashima, H., & Tokeshi, M. (2018). Development of the iLiNP Device: Fine Tuning the Lipid Nanoparticle Size within 10 nm for Drug Delivery. *ACS Omega*, *3*(5), 5044–5051. https://doi.org/10.1021/acsomega.8b00341

142) Akita, H. (2020). Development of an SS-Cleavable pH-Activated Lipid-Like Material (ssPalm) as a Nucleic Acid Delivery Device. *Biological & Pharmaceutical Bulletin*, *43*(11), 1617–1625. https://doi.org/10.1248/bpb.b20-00534

143) Gao, J., Ochyl, L., Yang, E., & Moon, J. (2017). Cationic liposomes promote antigen cross-presentation in dendritic cells by alkalizing the lysosomal pH and limiting the degradation of antigens. *International Journal of Nanomedicine*, *Volume 12*, 1251–1264. https://doi.org/10.2147/ijn.s125866

144) Kim, S., & Chang, R. (2016). Structure, Dynamics, and Phase Behavior of DOPC/DSPC Mixture Membrane Systems: Molecular Dynamics Simulation Studies. *Bulletin of the Korean Chemical Society*, *37*(7), 1076–1085. https://doi.org/10.1002/bkcs.10827

145) Liang, F., Lindgren, G., Lin, A., Thompson, E. A., Ols, S., Röhss, J., John, S., Hassett, K., Yuzhakov, O., Bahl, K., Brito, L. A., Salter, H., Ciaramella, G., & Loré, K. (2017). Efficient Targeting and Activation of Antigen-Presenting Cells In Vivo after Modified mRNA Vaccine Administration in Rhesus Macaques. *Molecular Therapy*, *25*(12), 2635–2647. https://doi.org/10.1016/j.ymthe.2017.08.006

146) Hou, Y., Liu, R., Hong, X., Zhang, Y., Bai, S., Luo, X., Zhang, Y., Gong, T., Zhang, Z., & Sun, X. (2021b). Engineering a sustained release vaccine with a pathogen-mimicking manner for robust and durable immune responses. *Journal of Controlled Release*, *333*, 162–175. https://doi.org/10.1016/j.jconrel.2021.03.037

147) Kehagia, E., Paraskevi Papakyriakopoulou, & Valsami, G. (2023). Advances in intranasal vaccine delivery: A promising non-invasive route of immunization. *Vaccine*, *41*(24), 3589–3603. https://doi.org/10.1016/j.vaccine.2023.05.011

148) Ding, Y., Li, Z., Jaklenec, A., & Hu, Q. (2021). Vaccine delivery systems toward lymph nodes. *Advanced Drug Delivery Reviews*, *179*, 113914. https://doi.org/10.1016/j.addr.2021.113914

149) Zhao, T., Cai, Y., Jiang, Y., He, X., Wei, Y., Yu, Y., & Tian, X. (2023b). Vaccine adjuvants: mechanisms and platforms. *Signal Transduction*

Supporting Information

Table S1: DLS and TEM results of HMM samples containing palmitic acid (C16:0) **6** or linolenic acid (C18:2) **11**

Concentration Ratio (Fatty acid : lipid A)	10:1	0.1:1	10:1	0.1:1
Fatty acid	Palmetic acid (C16:0)		Linolenic acid (C18:3)	
Sample preparation method	HMM	HMM	HMM	HMM
Effect on lipid A immune function *in vitro*	Attenuation effect	Attenuation effect	Attenuation effect	Boosting effect
DLS	**Peak**: 475.6 ± 32.7 **PI**: 0.449 ± 0.0238	**Peak**: 262.9 ± 20.4 **PI**: 0.495 ± 0.0224	**Peak**: 147.9 ± 17.1 **PI**: 0.365 ± 0.0153	**Peak**: 44.3 ± 15.6 **PI**: 0.403 ± 0.0299
TEM	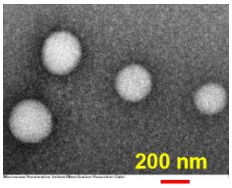 Aggregates size 100~500 nm	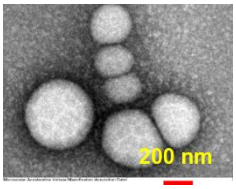 Aggregates size 100~300 nm	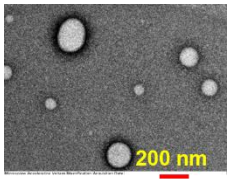 Aggregates size 100~200 nm	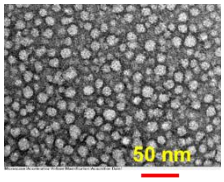 Aggregates size <50 nm 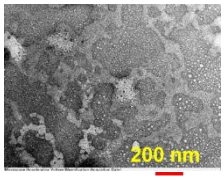 Amorphous aggregates 300~1000 nm

DLS of HMM and SMM samples

SMM stearic acid (C18:0) **5** : lipid A **1** (10:1)

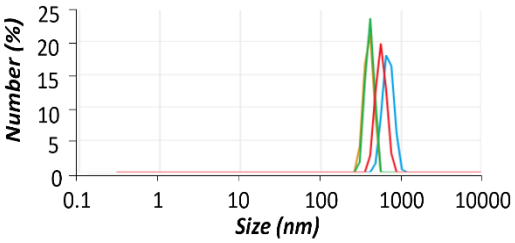

SMM linoleic acid (C18:2) **9** : lipid A **1** (10:1)

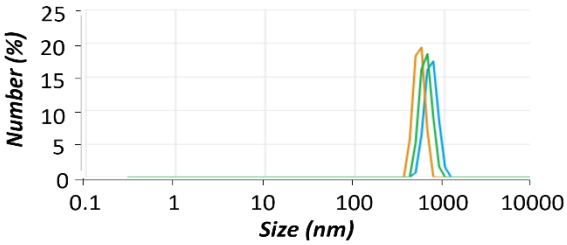

HMM stearic acid (C18:0) **5** : lipid A **1** (10:1)

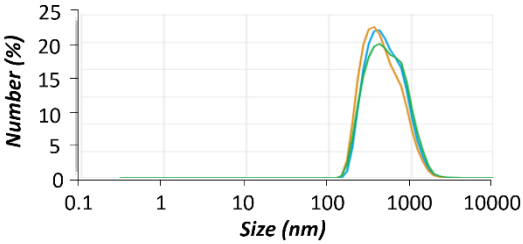

HMM stearic acid (C18:0) **5** : lipid A **1** (0.1:1)

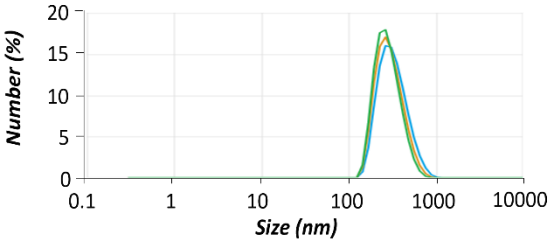

HMM linoleic acid (C18:2) **9** : lipid A **1** (10:1)

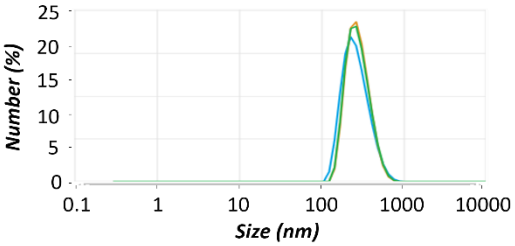

HMM linoleic acid (C18:2) **9** : lipid A **1** (0.1:1)

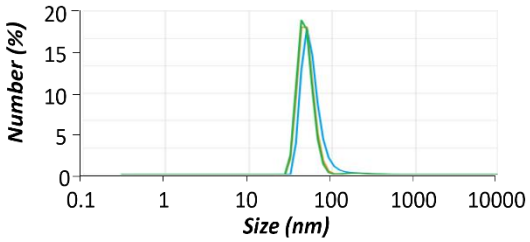

HMM palmitic acid (C16:0) **6** : lipid A **1** (10:1)

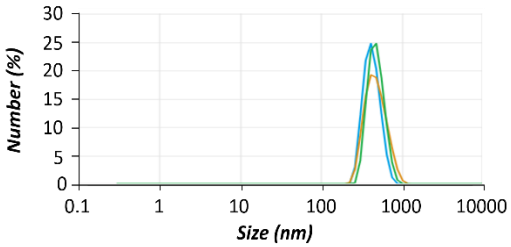

HMM palmitic acid (C16:0) **6** : lipid A **1** (10:1)

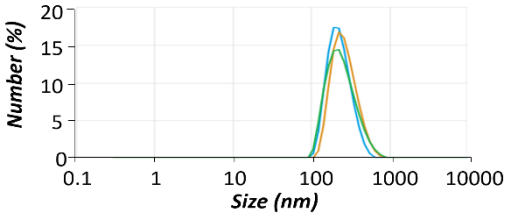

HMM linolenic acid (C18:3) **10** : lipid A **1** (10:1)

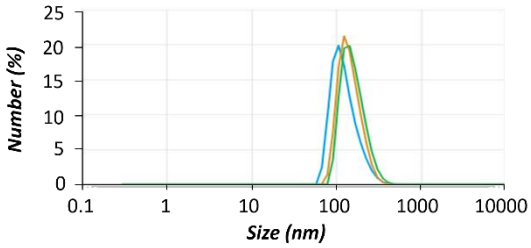

HMM linolenic acid (C18:3) **10** : lipid A **1** (0.1:1)

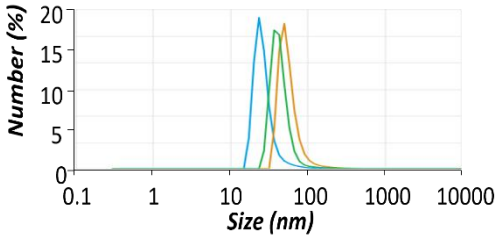

DLS of LNPs for immunization

AfLA **4**/ Cholesterol **15**/ DMG-PEG **16**/ DSPC **13**/ DOTAP **17** = 1/38/1.5/10/49.5 mol%

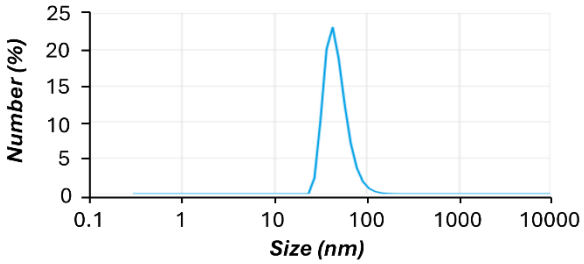

AfLA **4**/ Cholesterol **15**/ DMG-PEG **16**/ DSPC **13**/ DOTAP **17** = 1/38/1.5/10/49.5 mol%

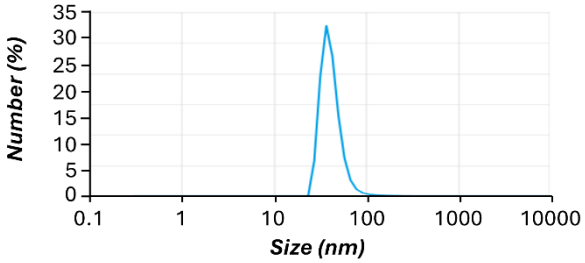

AfLA **4**/ Cholesterol **15**/ DMG-PEG **16**/ DOPC **14**/ DOTAP **17** = 1/38/1.5/29.7/29.7 mol%

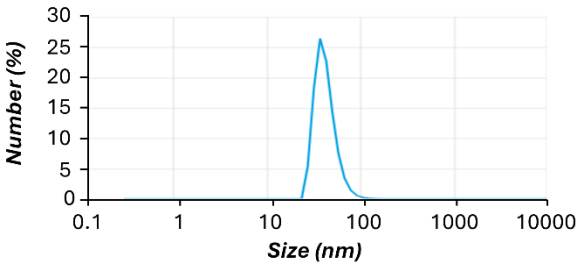

AfLA **4**/ Cholesterol **15**/ DMG-PEG **16**/ DOPC **14**/ DOTAP **17** = 1/38/1.5/59.5/0 mol%

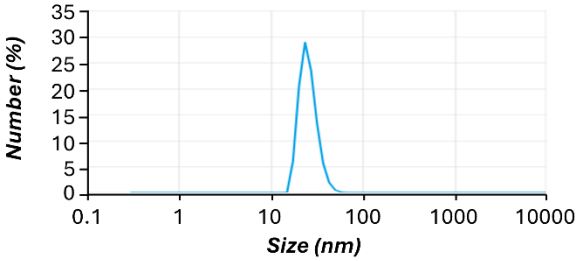

AfLA **4**/ Cholesterol **15**/ DMG-PEG **16**/ DOPC **14**/ DOPG **19** = 1/38/1.5/10/49.5 mol%

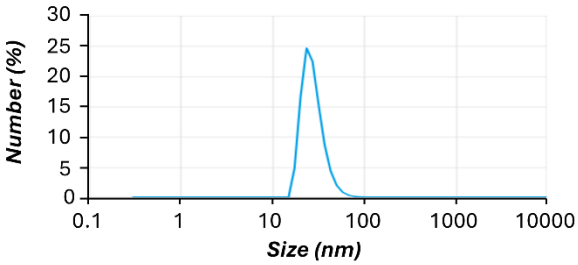

AfLA **4**/ Cholesterol **15**/ DMG-PEG **16**/ DOPC **14**/ ss-OP **20** = 1/38/1.5/10/49.5 mol%

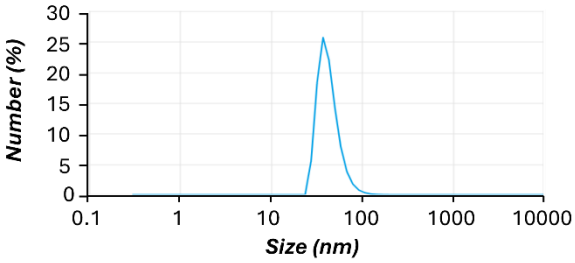

LC/MS of AfLA **4** in lipid nanoparticles

LC/MS was performed using column UHPLC PEEK Column InertSustain C18 3µm, 2.1×100mm. Solvent A was 10 mM ammonia in methanol/water (8/2) and solvent B was 10 mM ammonia in isopropanol. The eluent was collected at a flow rate of 0.2 mL/min and a linear gradient of 0% to 95% solvent B over 33 minutes.

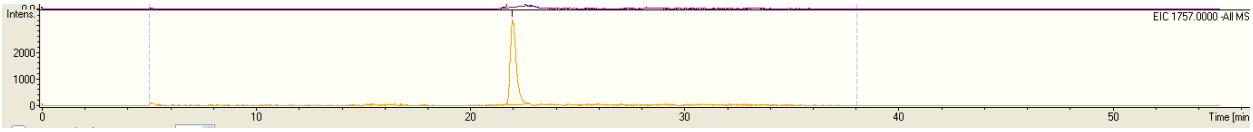

Experimental Section

Chemical synthesis

E. coli lipid A **1** was chemically synthesized as previously described [42]. *A. faecalis* lipid A **4** was chemically synthesized as previously described [102]

Materials

These chemicals were purchased from the following companies. CL (C18:2) **2** (C563), Stearic acid **5** (NS4-10505) was purchased from Kishida Chemical Co. Ltd. Palmitic acid **6** (76119-5G), myristic acid **7** (70079-5G), lauric acid **8** (167280050), linoleic acid **10** (L1376-1G), linolenic acid **11** (L2376-500MG) were purchased from Sigma-Aldrich. Oleic acid **9** (151781) and docosahexaenoic acid **12** (159097) were purchased from MP Biomedicals. CL (C18:1) **18** (710335) was purchased from Avanti Polar Lipids, Inc. *E. coli* LPS was purchased from FUJIFILM Wako Pure Chemical Co. 1,2-dioleoyl-3-trimethylammonium-propane (DOTAP **17**, COATSOME CL-8181TA), 1,2-Dioleoyl-sn-glycero-3-phosphoglycerol, sodium salt (DOPG-Na

19, COATSOME MG-8181LS), 1,2-Dioleoyl-sn-glycero-3-phosphocholine (DOPC **14**, COATSOME MC-8181), SS-OP **20** (COATSOME SS-OP), 1,2-Distearoyl-sn-glycero-3-phosphocholine (DSPC **13**, COATSOME MC-8080), and 1,2-Dimyristoyl-rac-glycero-methoxypolyethylene-glycol-2000 (DMG-PEG 2000 **16**, SUNBRIGHT GM-020) was purchased from NOF CORPORATION (Tokyo, Japan). Cholesterol **15** was purchased from Sigma-Aldrich Co. LLC (C8667-500MG, St. Louis, US).

Sample Preparation

SMM (Simple mixing method)

E. coli lipid A **1** and fatty acids **5-12** were measured and kept in separate test tube, then dissolved in DMSO to make stock solutions. During the 2nd day of SEAP reporter assay, lipid A **1** and fatty acids **5-12** stock solutions were sonicated for 1 minute at room temperature, before they were separatedly diluted by saline to make 5 % DMSO in saline solution. All samples were diluted continuously using 5% DMSO solution until the appropriate concentration. Then 12.5 uL of fatty acids **5-12** and 12.5 uL of lipid A **1** were added to each well, which already contained HEK-Blue hTLR4^{TM} cells cultured in 100 uL of D(-/+) medium with 0.1% FBS (DMEM high-glucose medium supplemented with FBS (0.1%), glutamine (2 mM), penicillin (100 units/ mL) and streptomycin (100 ug/mL)). Final DMSO concentration in each well is 1%.

HMM (Homogenous mixing method)

E. coli lipid A **1** and fatty acids **5-12** were measured and kept in separate test tube, then dissolve in tert-butyl alcohol (^{t}BuOH). All samples were diluted separately by ^{t}BuOH until reaching the appropriate concentration. Then, lipid A **1** and fatty acids **5-12** were added together and lyophilizing overnight. The next day, 200 µL of chloroform (CHCl3) was added to each tube containing LPS/lipid A mixed with endogenous components. The tubes were sonicated for 3 minutes at room temperature, before the $CHCl_3$ were evaporated. ^{t}BuOH was added to each tube and the solutions were lyophilized overnight. All the samples were then dissolved in DMSO as stock solutions. On the 2nd day of SEAP reporter assay, the samples sonicated for 3 minutes at room temperature before being diluted by saline to make 5% DMSO in saline solution. All samples were diluted continuously using 5% DMSO solution until the appropriate concentration. Then, 25 uL of each sample was added to each well, which already contained HEK-Blue hTLR4^{TM} cells cultured in 100 uL of D(-/+) medium with 0.1% FBS (DMEM high-glucose medium supplemented with FBS (0.1%), glutamine (2 mM), penicillin (100 units/ mL) and streptomycin (100 ug/mL)). Final DMSO concentration in each well is 1%.

DLS

For each measurement, 25 µL of sample solution was transferred into ZEN2112 quartz cell and measured by Zetasizer Ultra. The measurement method is “Back”, the analysis model is “General

Purpose", the material is "Liposome" and the dispersant is "Water". After each measurement, the quartz cell was washed with chloroform:methanol (1:1), and then with distilled water multiple times. The data was then analyzed using Zetasizer software.

For zeta potential measurement, 25 μL of sample solution was mixed with 830 μL of 10 mM HEPES (pH 7.4). 730 μL of solution was then transferred into DTS1070 cell and measured by Zetasizer Ultra. The measurement method is "Zeta Potential", the analysis model is "General Purpose", the material is "Liposome" and the dispersant is "Water". After each measurement, the DTS1070 cell was washed distilled water multiple times. The data was analyzed using Zetasizer software.

TEM

The droplet of sample was placed on carbon-film grids. After incubation for 30 seconds, excess liquid was blotted off by touching the one end of the grid with the filter paper. After the grid was partially dried, a drop of the staining solution (gadolinium acetate in water) was added on. After 90 seconds, excess staining solution was blotted off, and the grid was dried at room temperature. The grid was then observed by JEM 2100 electron microscopy (Osaka University) at an accelerating voltage of 200 kV.

Biological Experiments

Materials and Reagents

HEK-Blue hTLR4^{TM} cells were purchased from Invivogen. THP-1 cells were purchased from JCRB Cell Bank. Dulbecco's modified Eagle's medium (D-MEM), antibiotic/antimycotic supplement were purchased from FUJIFILM Wako Pure Chemical Co. Roswell Park Memorial Institute (RPMI)-1640 was purchased from American Type Culture Collection. Phorbol 12-myristate 13-acetate (PMA) was purchased from Focus Biomolecules. Fetal bovine serum (FBS) was purchased from Corning. Bovine serum albumin (BSA), Tween 20 and 0.5 N aqueous HCl were purchased from Nacalai Tesque Inc. Ovalbumin (OVA) was purchased from Sigma-Aldrich. Horseradish peroxidaseconjugated goat anti-mouse IgG, IgG1, IgG2a, IgG2b, IgG3 and IgA was purchased from Southern Biotech, Inc. Tetramethylbenzidine peroxidase substrate was purchased from SeraCare Life Sciences Inc. ELISA kit for human IL-6 and MCP-1 were purchased from Invitrogen, Thermofisher.

Mice

Female BALB/c mice (4 weeks old) were purchased from CLEA Japan, Inc. (Tokyo, Japan) and housed under specific pathogen-free conditions at the National Institute of Biomedical Innovation, Health, and Nutrition (Osaka, Japan). All experiments were approved by the Animal Care and Use

Committee of the National Institute of Biomedical Innovation, Health and Nutrition, and were conducted according to their guidelines.

Cell Culture

HEK-Blue hTLR4™ cells were cultured in D-MEM high-glucose medium supplemented with FBS (10%) and penicillin-streptomycin (1%). THP-1 cells were cultured in RPMI-1640 medium supplemented with FBS (10%) and penicillin-streptomycin (1%). All cells were incubated in a humidified 5% CO_2 atmosphere at 37 °C.

SEAP Reporter Assay

HEK-Blue hTLR4™ cells (InvivoGen) were cultured in Dulbecco's modified Eagle's medium (DMEM) supplemented with high glucose, fetal bovine serum (FBS, 10%), glutamine (2 mM), penicillin (100 units/mL) and streptomycin (100 µg/mL) in a petri dish. After three days of incubation at 37 °C in 5% CO_2 atmosphere, the cells were detached using 0.25% Trypsin-EDTA solution, and the cell concentration was estimated using an automatic cell counter. Then the cells were diluted in DMEM high-glucose medium supplemented with glutamine (2 mM), penicillin (100 units/mL) and streptomycin in the absence of FBS, and the cells were seeded in a 96-well plate at a density of 2 x 10^4 cells/well and incubated for 20 h at 37 °C in 5% CO_2 atmosphere. Thereafter, the supernatant was removed, and the cell monolayers were washed with saline. To each well was added D-MEM high-glucose medium (100 µL) supplemented with FBS (0.1%), L-glutamine (2 mM), penicillin (100 units/mL) and streptomycin (100 µg/mL) and treated with the appropriate concentration of samples (dissolved in 25 µL of 5% DMSO in saline, 25 µL of 5% DMSO in PBS, or 25 µL of PBS). After 20 h incubation in same conditions as above, supernatants were collected. 50 µL of each sample supernatant was added to p-NPP solution in PBS (0.8 mM, 100 µL) and incubated at room temperature in the dark for 4 h. Finally, the absorbance was measured at 405 nm spectrophotomically using plate reader.

Quantification of cytokines in THP-1 cells by ELISA

THP-1 cells were cultured in Roswell Park Memorial Institute (RPMI) medium supplemented with fetal bovine serum (FBS, 10 %), glutamine (2 mM), penicillin (100 units/mL) and streptomycin (100 µg/mL). After estimating the cell concentration using an automatic cell counter, cells were diluted in RPMI medium supplemented with the same ingredients as above plus phorbo myristate acetate (PMA, 0.5 µM) for differentiation. Then the cells were seeded in a 96-well plate at a density of 6 x 10^4 cells/well and differentiated for 72 h. at 37 °C in 5% CO_2 atmosphere. Supernatant was removed, and cell monolayers were washed with saline. To each well was added RPMI medium (100 µL) supplemented with fetal bovine serum (FBS, 10 %), glutamine (2 mM), penicillin (100 units/mL) and streptomycin (100 ug/mL) without PMA, and treated with the appropriate concentration of samples (dissolved in 25 µL of 5% DMSO in saline, 25 µL of 5% DMSO in PBS, or 25 µL of PBS). After 20 h of incubation at 37 °C in 5% CO_2 atmosphere,

supernatants were collected, and the induced quantities of cytokines in the supernatant were measured by the ELISA kit systems for IL-6 (Human IL-6 uncoated ELISA, Invitrogen), MCP-1 (Human MCP-1 uncoated ELISA, Invitrogen) in Nunc Maxisorp^{TM} 96-well plates as provided, by following the protocol indicated by the manufacturer in each case.

Subcutaneous immunization of mice

The immunization procedure was according to the previously reported protocol. Mice were immunized around the thoracic area with 1 μg of ovalbumin (OVA), or 1 μg of OVA with 1 μg of AfLA **4** in LNPs, or 1 μg of OVA with 1 μg of non-iLiNP AfLA **4** in 200 μL of PBS on days 0 and 7. On day 14, serum was collected from mice and stored at -80 ºC for measurement of OVA-specific IgG, IgG1, IgG2a and IgG2b by ELISA.

Intranasal immunization of mice

The immunization procedure was according to the previously reported protocol. Mice were immunized with 5 μg of OVA with or 1 μg of OVA with 1 μg of AfLA **4** in LNPs, or 1 μg of OVA with 1 μg of non-iLiNP AfLA **4** in 30 μL of PBS on days 0, 7 and 14. Each mouse received 15 μL of the solution in each nose. On day 21, serum was collected followed by collection of nasal wash fluid and bronchoalveolar lavage fluid (BALF). Nasal wash was collected by creating an opening at the trachea and forcing 200 μL PBS through the opening and the nostrils using a pipette up to the nasal openings where the PBS is collected into an Eppendorf tube. The BALF is collected by inserting a pipette containing 1 mL PBS through the trachea pushing it in and out the bronchi for three times. The collected fluids were all stored at -80 ºC for measurement of OVA-specific IgA and IgG antibody responses.

Measurement of OVA-specific IgG or OVA-specific IgA by ELISA

Flat-bottom 96-well immunoplates (Thermo Fisher Scientific, Waltham, MA, USA) were coated with 1 mg/ml of OVA diluted in PBS at 4 °C overnight. After incubation, the plates were blocked with 1% (w/v) bovine serum albumin (BSA; Nacalai Tesque) in PBS for 2 h at room temperature. After blocking, the plates were washed three times with PBS containing 0.05% (v/v) Tween 20 (Nacalai Tesque). Samples were 2-fold serially diluted with PBS containing 1% (w/v) bovine serum albumin (BSA) and 0.05% (v/v) Tween 20, added to the plates, and incubated for 2 h at room temperature. Plates were washed three times with PBS containing 0.05% and then incubated for 1 h at room temperature with horseradish peroxidase conjugated goat anti-mouse IgG or IgA (Southern Biotech, Birmingham, AL, USA) diluted in PBS containing 1% (w/v) BSA and 0.05% (v/v) Tween 20. Plates were washed three times with PBS containing 0.05% Tween 20 and then incubated for 2 min at room temperature with tetramethylbenzidine peroxidase substrate (SeraCare Life Sciences, Milford, MA, USA); reactions were stopped by adding 0.5 N HCl (NacalaiTesque). Absorbance at 450 nm was measured by using an iMark Microplate Absorbance Reader (Bio-Rad Laboratories, Hercules, CA, USA).

Acknowledgements

All samples preparations and in vitro biological experiments in this research were conducted at the Natural Products Organic Chemistry Laboratory, Department of Chemistry, Graduate School of Science, Osaka University. I am deeply grateful to Professor Koichi Fukase for his invaluable insights, guidance, and for fostering an exceptional research environment that not only enabled scientific discovery but also nurtured intellectual growth. My heartfelt thanks also go to Associate Professor Atsushi Shimoyama, whose daily guidance and unwavering support extended beyond research, demonstrating genuine care and encouragement throughout my journey.

I extend my sincere appreciation to Professor Kazuya Kabayama, Associate Professor Yoshiyuki Manabe and Assistant Professor Masayuki Takamatsu of the Natural Products Organic Chemistry Laboratory for their invaluable assistance and encouragement during my time in the lab.

The in vivo evaluations of lipid nanoparticles biological activity were conducted at the Laboratory of Vaccine Materials, National Institute of Biomedical Innovation, Health and Nutrition (NIBIOHN). I am profoundly thankful for the opportunity to be part of the collaborative research led by Professor Jun Kunisawa, and for the invaluable support and guidance of Dr. Ken Yoshii in the animal experiments.

I also owe special thanks to Professor Manabu Tokeshi and Professor Masatoshi Maeki, Graduate School of Engineering, Hokkaido University, for providing the iLiNP device, which was essential for the synthesis of lipid nanoparticles. My gratitude also extends to Dr. Akihiro Ito, Graduate School of Science, Osaka University, for his assistance with TEM instruments.

I am immensely thankful to the Japanese government for granting me the MEXT scholarship during my undergraduate studies at Osaka University, and to Mitsubishi Corporation for their generous scholarship support during my PhD studies.

My deepest gratitude goes to the laboratory secretaries, Marika Yamauchi, Yukie Terashi, Michiyo Nakamoto, and Madoka Miyazaki, whose administrative support ensured smooth daily operations in the lab. I am also grateful to all the current members and alumni of the Natural Products Organic Chemistry Laboratory—not only for their research assistance but for the cherished memories we shared. To my friends and colleagues from my 9.5 years at Osaka University, I deeply value the bonds and experiences that enriched this journey.

Finally, I want to express my utmost gratitude to my family – especially my mom, dad, cousin (sister) and grandparents – who have been my unwavering source of inspiration. Their love, encouragement, and belief in me gave me the strength to persevere and overcome challenges throughout my studies.